

# Sample Complexity of Neural Policy Mirror Descent for Policy Optimization on Low-Dimensional Manifolds

Zhenghao Xu<sup>\*</sup>   Xiang Ji<sup>†</sup>   Minshuo Chen<sup>†</sup>   Mengdi Wang<sup>†</sup>   Tuo Zhao<sup>\*</sup>

## Abstract

Policy-based algorithms equipped with deep neural networks have achieved great success in solving high-dimensional policy optimization problems in reinforcement learning. However, current analyses cannot explain why they are resistant to the curse of dimensionality. In this work, we study the sample complexity of the neural policy mirror descent (NPMD) algorithm with convolutional neural networks (CNN) as function approximators. Motivated by the empirical observation that many high-dimensional environments have state spaces possessing low-dimensional structures, such as those taking images as states, we consider the state space to be a  $d$ -dimensional manifold embedded in the  $D$ -dimensional Euclidean space with intrinsic dimension  $d \ll D$ . We show that in each iteration of NPMD, both the value function and the policy can be well approximated by CNNs. The approximation errors are controlled by the size of the networks, and the smoothness of the previous networks can be inherited. As a result, by properly choosing the network size and hyperparameters, NPMD can find an  $\epsilon$ -optimal policy with  $\tilde{O}(\epsilon^{-\frac{d}{\alpha}-2})$  samples in expectation, where  $\alpha \in (0, 1]$  indicates the smoothness of environment. Compared to previous work, our result exhibits that NPMD can leverage the low-dimensional structure of state space to escape from the curse of dimensionality, providing an explanation for the efficacy of deep policy-based algorithms.

## 1 Introduction

Deep Reinforcement Learning (DRL) is a popular approach for solving complex decision-making problems in various domains. DRL methods, especially policy-based ones including DDPG (Lillicrap et al., 2015), TRPO (Schulman et al., 2015), and PPO (Schulman et al., 2017), are able to handle high-dimensional state space efficiently by leveraging function approximation with neural networks. For instance, in Atari games (Brockman et al., 2016), the states are images of size  $210 \times 160$  with RGB color channels, resulting in a continuous state space of dimension 100,800, to which tabular algorithms such as policy iteration (Puterman, 1994) and policy mirror descent (PMD, Lan 2023) are not applicable. Surprisingly, such a high dimension does not seem to significantly impact the efficacy of the aforementioned DRL algorithms.

---

<sup>\*</sup>School of Industrial and Systems Engineering, Georgia Tech, Atlanta, USA. Email: [zhenghaoxu@gatech.edu](mailto:zhenghaoxu@gatech.edu), [tourzhao@gatech.edu](mailto:tourzhao@gatech.edu).

<sup>†</sup>Department of Electrical and Computer Engineering, Princeton University, Princeton, USA

Despite the empirical success of these DRL methods in high dimensions, there currently exist no satisfactory results in theory that can explain the reason behind them. Most of the existing works about function approximation in RL focus on linear function class (Agarwal et al., 2021; Alfano and Rebeschini, 2022; Yuan et al., 2023). They assume the value function and the policy can be well approximated by linear functions of features representing states and actions (Jin et al., 2020), which is restrictive and requires feature engineering. One way to relax such a linearity assumption is to consider the reproducing kernel Hilbert space (RKHS) which allows nonlinear function approximation (Agarwal et al., 2020; Yang et al., 2020) through random features (Rahimi and Recht, 2007). However, the commonly used reproducing kernels such as the Gaussian radial basis function and randomized ReLU kernel suffer from the curse of dimensionality in sample complexity without additional smoothness assumptions (Bach, 2017; Yehudai and Shamir, 2019; Hsu et al., 2021).

Moreover, some researchers study neural network approximation in the neural tangent kernel (NTK) regime, which is equivalent to an RKHS (Jacot et al., 2018; Liu et al., 2019; Wang et al., 2019). As a consequence, these results inherit the curse of dimensionality from general RKHS. Some other works investigate neural network approximation from a non-parametric perspective (Fan et al., 2020; Nguyen-Tang et al., 2022), but they consider value-based methods where only value function is approximated and also suffer from the curse of dimensionality. There are alternative lines of work on policy optimization with general function approximation, but they either assume the functions can be well approximated without any further verification (Xie et al., 2021; Lan, 2022; Alfano et al., 2023), or require some strong assumptions such as third-time differentiability (Yin et al., 2022).

One possible explanation for the empirical effectiveness of DRL algorithms is the adaptivity of neural networks to the intrinsic low-dimensional structure of the state space. In the Atari games example, the images share common textures and are rendered using just a small number of internal states, such as the type, position, and angle of each object, thus the intrinsic dimension of the state space is in fact very small compared to the data dimension of 100,800. However, the extent of this adaptivity is yet to be explored in DRL literature.

To bridge this gap between theory and practice, we propose to investigate neural policy optimization within environments possessing low-dimensional state space structures. Specifically, we consider the infinite-horizon discounted Markov decision process (MDP) with continuous state space  $\mathcal{S}$ , finite action space  $\mathcal{A}$ , and discount factor  $\gamma$ . We focus on the sample complexity of the neural policy mirror descent (NPMD) method. NPMD is based on the actor-critic framework (Konda and Tsitsiklis, 1999; Grondman et al., 2012) where both the policy (actor) and value function (critic) are approximated by neural networks. It can be viewed as an extension to the PMD method (Lan, 2023) with neural network approximation. The NPMD-type methods including TRPO (Schulman et al., 2015) and PPO (Schulman et al., 2017) are widely used in applications like game AI (Berner et al., 2019) and fine-tuning large language models (Ziegler et al., 2019; Ouyang et al., 2022). Moreover, instead of working on general Euclidean space, we assume the state space to be a  $d$ -dimensional manifold embedded in the  $D$ -dimensional Euclidean space where  $d \ll D$ .

Algorithm	Approximation	Regularity	Complexity	Remark
NPG (P) (Yuan et al., 2023)	Linear	Linear (D)	$\tilde{O}(\epsilon^{-2})$	strong regularity
NPPO (P) (Liu et al., 2019)	NTK (2-layer ReLU)	RKHS (D)	$\tilde{O}(\epsilon^{-4})$ <sup>1</sup>	strong regularity
FQI (V) (Fan et al., 2020)	FNN (Deep ReLU)	Hölder (I)	$\tilde{O}(\epsilon^{-\frac{D}{\alpha}-2})$	curse of dimension
FQI (V) (Nguyen-Tang et al., 2022)	FNN (Deep ReLU)	Besov (I)	$\tilde{O}(\epsilon^{-\frac{2D}{\alpha}-2})$	curse of dimension
NPMD (P) (This paper)	CNN (Deep ReLU)	Lipschitz (I) <sup>2</sup>	$\tilde{O}(\epsilon^{-\frac{d}{\alpha}-2})$	$d \ll D$

Table 1: Comparison with existing results. The algorithms are classified as value-based (V) or policy-based (P). NPG refers to the natural policy gradient (Kakade, 2001). FQI is analogous to deep Q-learning (Mnih et al., 2013). NPPO and NPMD are analogous to the PPO algorithm (Schulman et al., 2017). The regularity assumptions are made on value functions to be approximated, which can be algorithm-dependent (D) or algorithm-independent (I). The complexity is the expected number of samples required to find an  $\epsilon$ -optimal policy whose value function is at most  $\epsilon$  to the global optimal in expectation.

We summarize our main contributions as follows:

- (1) We first investigate the universal approximation of the convolutional neural network (CNN), which is a popular architecture for image data. We show that under the Lipschitz MDP condition (Assumption 4), CNN can well approximate both the value function and the policy (Theorem 2, Corollary 1). Compared to the results in Liu et al. (2019) and Yuan et al. (2023), our analysis decouples the regularity conditions from algorithmic specifications. For example, in Liu et al. (2019), the value functions are assumed to be in a network width-dependent set that approximates the NTK-induced RKHS, while our regularity assumptions are not based on the network architecture in advance. In Yuan et al. (2023), the approximation error is highly related to the design of the feature map.
- (2) Based on CNN function approximation, we then derive  $\tilde{O}(|\mathcal{A}|^{\frac{d}{2\alpha}+2}(1-\gamma)^{-\frac{4d}{\alpha}-10}\epsilon^{-\frac{d}{\alpha}-2})$  sample complexity bound for NPMD with CNN approximation to find a policy whose value function is at most  $\epsilon$  to the global optimal in expectation (Corollary 2). Here,  $\alpha \in (0, 1]$  is the exponent of the Lipschitz condition and  $\tilde{O}(\cdot)$  hides the logarithmic terms and some coefficients related to distribution mismatch and concentrability (see Assumptions 2 and 3). Compared to the results in Fan et al. (2020) and Nguyen-Tang et al. (2022), the curse of dimensionality (exponential dependence on  $D$ ) is avoided by exploiting the intrinsic  $d$ -dimensional structure. To the best of

<sup>1</sup>The complexity in Liu et al. (2019) implicitly suffers from the curse of dimensionality due to hidden constants related to NTK, including the width of the network and the radius of the RKHS norm ball. These constants can have exponential dependence on  $D$  (Yehudai and Shamir, 2019).

<sup>2</sup>We define Lipschitz continuity for all  $\alpha \in (0, 1]$ , which reduces to the normally defined Lipschitz condition when  $\alpha = 1$  and reduces to the normally defined Hölder continuity when  $\alpha \in (0, 1)$ .

our knowledge, this is the first sample complexity result for policy gradient methods with deep neural network function approximation.

The rest of this paper is organized as follows. In Section 2, we introduce the background and preliminaries including MDP, CNN, and Riemannian manifold. In Section 3, we present the NPMD algorithm with a detailed formulation. We provide our main results in Section 4, and we make some concluding remarks in Section 5. Proof details are provided in the appendix. Some preliminary results for this paper have been presented in Ji et al. (2022) which focuses on policy evaluation only. We extend the scope to policy optimization.

## 1.1 Related Work

Our work is based on previous studies on policy gradient methods with function approximation as well as deep supervised learning on manifolds.

**Policy gradient methods.** The policy gradient method (Williams, 1992; Sutton et al., 1999) is first developed under the compatible function approximation framework. The natural policy gradient (NPG) method (Kakade, 2001) extends the policy gradient method by incorporating the geometry of the parameter space to improve convergence properties. Trust region policy optimization (TRPO, Schulman et al. 2015) and proximal policy optimization (PPO, Schulman et al. 2017) are modern variants of policy gradient methods with neural network function approximation that use constraints or penalties to prevent aggressive updates, resulting in more stable and efficient learning. Other notable methods include deep deterministic policy gradient (DDPG, Lillicrap et al. 2015), asynchronous advantage actor-critic (A3C, Mnih et al. 2016), and mirror descent policy optimization (MDPO, Tomar et al. 2020) algorithms. These modern methods are often used to handle high-dimensional state spaces and have been shown to achieve state-of-the-art results in a variety of RL domains. For example, the PPO algorithm and its variants are used in training some of the most advanced artificial intelligence, such as OpenAI Five (Berner et al., 2019) and GPT-4 (OpenAI, 2023). From a theoretical perspective, policy gradient methods such as NPG and PPO can be unified under the generalized PMD framework (Geist et al., 2019; Shani et al., 2020; Xiao, 2022; Lan, 2023).

**Linear function approximation.** The majority of existing research on function approximation considers the linear function class (Agarwal et al., 2021; Alfano and Rebeschini, 2022; Yuan et al., 2023), which is the only known option for the compatible function approximation framework by far (Sutton et al., 1999). However, these linear function approximation methods are restrictive. Only in simple environments, such as linear MDP (Jin et al., 2020), can high approximation quality be guaranteed, which necessitates carefully designed features. Regrettably, the task of crafting such features is either infeasible or demands substantial effort from domain experts, and any misspecification of features could lead to exponential error (Du et al., 2020).

**Reproducing kernel approach.** The reproducing kernel Hilbert space (RKHS) has been adopted to relax the limitation of the linear function class and to enable more expressive nonlinear function approximation (Agarwal et al., 2020; Yang et al., 2020). To achieve efficient computation, random features are employed (Rahimi and Recht, 2007). Nevertheless, the RKHS suffers from the curse of dimensionality, which hinders its performance on high-dimensional problems.

**Neural tangent kernel.** One approach to investigating the function approximation capabilities of neural networks is through the use of the neural tangent kernel (NTK, Jacot et al. 2018; Liu et al. 2019; Wang et al. 2019; Yang et al. 2020). The NTK approach can be viewed as training a neural network with gradient descent under a specific regime, and as the width of the neural network approaches infinity, it converges to an RKHS. As a consequence, like other RKHS approaches, the NTK approach suffers from the curse of dimensionality, limiting its performance on high-dimensional problems. Additionally, some literature has pointed out that the NTK is susceptible to the kernel degeneracy problem (Chen and Xu, 2020; Huang et al., 2020), which may impact its overall learnability.

**Non-parametric neural network approximation.** The non-parametric approach has been adopted to study the sample complexity of neural function approximation in RL under mild smoothness assumptions, such as Fan et al. (2020) and Nguyen-Tang et al. (2022). These analyses are mainly focused on value-based methods and are not applicable to policy gradient methods due to the lack of smoothness in neural policies.

**Deep supervised learning on manifolds.** Parallel to DRL, existing work on deep supervised learning extensively studies the adaptivity of neural networks to the intrinsic low-dimensional data manifold embedded in high-dimensional ambient space, and how this adaptivity helps neural networks escape from the curse of dimensionality. In deep supervised learning, it has been shown that the sample complexity’s exponential dependence on the ambient dimension  $D$  can be replaced by the dependence on the manifold dimension  $d$  (Chen et al., 2019; Schmidt-Hieber, 2019; Liu et al., 2021). These analyses focus on fitting a single target function whose smoothness is predetermined by the nature of the learning task, while in our setting, the target functions are policies and their associated value functions, whose smoothness can get worse in each iteration.

## 1.2 Notation

For  $n \in \mathbb{N}$ ,  $[n] := \{i \mid 1 \leq i \leq n\}$ . For  $a \in \mathbb{R}$ ,  $\lceil a \rceil$  denotes the smallest integer no less than  $a$ . For  $a, b \in \mathbb{R}$ ,  $a \vee b := \max(a, b)$ . For a vector,  $\|\cdot\|_p$  denotes the  $p$ -norm for any  $1 \leq p \leq +\infty$ . For a matrix,  $\|\cdot\|_0$  denotes the number of nonzero entries and  $\|\cdot\|_\infty$  denotes the maximum magnitude of entries. For a finite set,  $|\cdot|$  denotes its number of elements. For a function  $f: \mathcal{X} \rightarrow \mathbb{R}$ ,  $\|f\|_\infty$  denotes the maximal value of  $|f|$  over  $\mathcal{X}$ . Given distribution  $\rho$  on  $\mathcal{X}$ , we use  $f(\rho) := \mathbb{E}_{x \sim \rho}[f(x)]$  to denote the expected value of  $f(x)$  where  $x \sim \rho$ . Given distributions  $\mu$  and  $\nu$  on  $\mathcal{X}$ , the total variation distance is defined

as  $d_{\text{TV}}(\mu, \nu) := \sup_{A \in \Sigma} |\mu(A) - \nu(A)|$ , where  $\Sigma$  is the measurable sets on  $\mathcal{X}$ . When  $\mu$  is absolutely continuous with respect to  $\nu$ , the Pearson  $\chi^2$ -divergence is defined as  $\chi^2(\mu, \nu) := \mathbb{E}_\nu[(\frac{d\mu}{d\nu} - 1)^2]$ , where  $\frac{d\mu}{d\nu}$  denotes the Radon-Nikodym derivative.

Let  $\mathcal{A}$  be a finite set, we denote  $P^{|\mathcal{A}|} := \{(p_a)_{a \in \mathcal{A}} \mid p_a \in P\}$  as the Cartesian product of  $P$ 's indexed by  $\mathcal{A}$ ,  $\mathbf{1} := (1)_{a \in \mathcal{A}} \in \mathbb{R}^{|\mathcal{A}|}$  as the vector with all entries being 1,  $\Delta_{\mathcal{A}} := \{p \in \mathbb{R}^{|\mathcal{A}|} \mid \sum_{a \in \mathcal{A}} p_a = 1, p_a \geq 0\}$  as the probability simplex over  $\mathcal{A}$ , and define the inner product  $\langle \cdot, \cdot \rangle : \mathbb{R}^{|\mathcal{A}|} \times \mathbb{R}^{|\mathcal{A}|} \rightarrow \mathbb{R}$  as  $\langle p, q \rangle := \sum_{a \in \mathcal{A}} p_a q_a$ . Let  $\pi : \mathcal{S} \rightarrow \Delta_{\mathcal{A}}$  be a map, we use  $h^\pi(s) := \langle \log \pi(s), \pi(s) \rangle$  to denote the negative entropy of  $\pi$  at  $s \in \mathcal{S}$  where  $\log(\cdot)$  is performed entrywise and denote the Kullback-Leibler (KL) divergence between two distributions  $\pi'(s)$  and  $\pi(s)$  by  $D_\pi^{\pi'}(s) := \langle \log \pi'(s) - \log \pi(s), \pi'(s) \rangle \geq 0$ .

## 2 Background

We introduce the problem setting and briefly review the Markov decision process, Riemannian manifold, and convolutional neural networks.

### 2.1 Markov Decision Process

We consider an infinite-horizon discounted Markov decision process (MDP) denoted as  $\mathcal{M} = (\mathcal{S}, \mathcal{A}, \mathcal{P}, c, \gamma)$ , where  $\mathcal{S} \subseteq \mathbb{R}^D$  is a continuous state space in  $\mathbb{R}^D$ ,  $\mathcal{A}$  is a finite action space,  $\mathcal{P}$  is the transition kernel that describes the next state distribution  $s' \sim \mathcal{P}(\cdot | s, a)$  at state  $s \in \mathcal{S}$  when action  $a \in \mathcal{A}$  is taken,  $c : \mathcal{S} \times \mathcal{A} \rightarrow [0, C]$  is a cost function bounded by some constant  $C > 0$ , and  $\gamma \in (0, 1)$  is a discount factor.

A *stochastic policy*  $\pi : \mathcal{S} \rightarrow \Delta_{\mathcal{A}}$  describes the behavior of an agent. For any state  $s \in \mathcal{S}$ ,  $\pi(\cdot | s) \in \Delta_{\mathcal{A}}$  gives a conditional probability distribution over the action space  $\mathcal{A}$ , where  $\pi(a | s)$  is the probability of taking action  $a$  at state  $s$ .

Given a policy  $\pi$ , the expected cost starting from state  $s$  is given by the *state value function*

$$V^\pi(s) = \mathbb{E}_{\substack{a_t \sim \pi(\cdot | s_t), \\ s_{t+1} \sim \mathcal{P}(\cdot | s_t, a_t)}} \left[ \sum_{t=0}^{\infty} \gamma^t c(s_t, a_t) \mid s_0 = s \right].$$

The goal of policy optimization is to learn an optimal policy  $\pi^*$  by solving a stochastic optimization problem, where the objective function is the expected value function for a given initial state distribution  $\rho$ .<sup>3</sup>

$$V^*(\rho) := V^{\pi^*}(\rho) = \underset{\pi}{\text{minimize}} \mathbb{E}_{s \sim \rho} [V^\pi(s)]. \quad (1)$$

A policy  $\pi$  is called  $\epsilon$ -*optimal*, if

$$V^\pi(\rho) - V^*(\rho) \leq \epsilon.$$

---

<sup>3</sup>The optimal policy  $\pi^*$  does not depend on the choice of  $\rho$ .

In our *generative model* setting, the algorithm cannot directly access the transition kernel  $\mathcal{P}$  and the cost function  $c$ . Instead, the algorithm can provide any state-action pair to the environment and get  $s' \sim \mathcal{P}(\cdot|s, a)$  and  $c_{s,a} = c(s, a)$  by invoking a sample oracle. We also assume a sample oracle that can output  $s \sim \rho$ . The (expected) number of sample oracle calls required to obtain an  $\epsilon$ -optimal policy is referred to as the *sample complexity* of the algorithm.

The state value function is closely related to the *state-action value function*, which is the expected cost starting from state  $s$  and taking action  $a$ :

$$Q^\pi(s, a) = \mathbb{E}_{\substack{s_{t+1} \sim \mathcal{P}(\cdot|s_t, a_t), \\ a_{t+1} \sim \pi(\cdot|s_{t+1})}} \left[ \sum_{t=0}^{\infty} \gamma^t c(s_t, a_t) \mid s_0 = s, a_0 = a \right].$$

By definition, the value functions are bounded:

$$0 \leq V^\pi(s) \leq \frac{C}{1-\gamma}, \quad 0 \leq Q^\pi(s, a) \leq \frac{C}{1-\gamma}. \quad (2)$$

The value functions satisfy the following relations:

$$V^\pi(s) = \langle Q^\pi(s, \cdot), \pi(\cdot|s) \rangle = \mathbb{E}_{a \sim \pi(\cdot|s)} [Q^\pi(s, a)], \quad (3)$$

$$Q^\pi(s, a) = c(s, a) + \gamma \mathbb{E}_{s' \sim \mathcal{P}(\cdot|s, a)} [V^\pi(s')]. \quad (4)$$

For the convenience of analysis, we define recursively

$$\mathcal{P}_0^\pi = \rho, \quad \mathcal{P}_{t+1}^\pi = \mathbb{E}_{s \sim \mathcal{P}_t^\pi, a \sim \pi(\cdot|s)} [\mathcal{P}(\cdot|s, a)], \quad (5)$$

and define the *state visitation distribution* and the *state-action visitation distribution* respectively:

$$\nu_\rho^\pi = (1-\gamma) \sum_{t=0}^{\infty} \gamma^t \mathcal{P}_t^\pi, \quad (6)$$

$$\bar{\nu}_\rho^\pi(s, a) = \nu_\rho^\pi(s) \times \pi(a|s), \quad \forall s \in \mathcal{S}, a \in \mathcal{A}. \quad (7)$$

The prefactor  $1-\gamma$  in (6) makes  $\nu_\rho^\pi$  be a distribution. The visitation distributions reflect the frequency of visiting state  $s$  or state-action pair  $(s, a)$  along the trajectories starting from  $s_0 \sim \rho$  and taking actions according to policy  $\pi$ . It follows immediately from the definition that the state visitation distribution is lower bounded by the initial distribution (in terms of Radon-Nikodym derivative) with factor  $1-\gamma$ :

$$\frac{d\nu_\rho^\pi}{d\rho} = (1-\gamma) \sum_{t=0}^{\infty} \gamma^t \frac{d\mathcal{P}_t^\pi}{d\rho} \geq (1-\gamma) \frac{d\mathcal{P}_0^\pi}{d\rho} = 1-\gamma. \quad (8)$$

We can rewrite the value functions using the visitation distributions:

$$V^\pi(\rho) = \sum_{t=0}^{\infty} \gamma^t \int_{\mathcal{S}} \sum_{a \in \mathcal{A}} c(s, a) \pi(a|s) d\mathcal{P}_t^\pi(s) = \frac{1}{1-\gamma} \mathbb{E}_{(s,a) \sim \bar{\nu}_\rho^\pi} [c(s, a)], \quad (9)$$

$$Q^\pi(s, a) = c(s, a) + \gamma V^\pi(\mathcal{P}(\cdot|s, a)) = c(s, a) + \frac{\gamma}{1-\gamma} \mathbb{E}_{(s', a') \sim \bar{\nu}_{\mathcal{P}(\cdot|s, a)}^\pi} [c(s', a')], \quad (10)$$

where (10) is from (9) and (4).

## 2.2 Riemannian Manifold

We consider the state space  $\mathcal{S}$  to be a  $d$ -dimensional Riemannian manifold isometrically embedded in  $\mathbb{R}^D$ . A *chart* for  $\mathcal{S}$  is a pair  $(U, \phi)$  such that  $U \subset \mathcal{S}$  is open and  $\phi : U \rightarrow \mathbb{R}^d$  is a homeomorphism, i.e.,  $\phi$  is a bijection; its inverse and itself are continuous. Two charts  $(U, \phi)$  and  $(V, \psi)$  are called  *$C^k$  compatible* if and only if

$$\phi \circ \psi^{-1} : \psi(U \cap V) \rightarrow \phi(U \cap V) \quad \text{and} \quad \psi \circ \phi^{-1} : \phi(U \cap V) \rightarrow \psi(U \cap V)$$

are both  $C^k$  functions ( $k$  times continuously differentiable). A  *$C^k$  atlas* of  $\mathcal{S}$  is a collection of  $C^k$  compatible charts  $\{(U_i, \phi_i)\}_{i \in I}$  such that  $\bigcup_{i \in I} U_i = \mathcal{S}$ . An atlas of  $\mathcal{S}$  contains an open cover of  $\mathcal{S}$  and mappings from each open cover to  $\mathbb{R}^d$ .

**Definition 1** (Smooth manifold). *A manifold  $\mathcal{S}$  is smooth if it has a  $C^\infty$  atlas.*

We introduce the *reach* (Federer, 1959; Niyogi et al., 2008) of a manifold to characterize the curvature of  $\mathcal{S}$ .

**Definition 2** (Reach). *The medial axis of  $\mathcal{S}$  is defined as  $\bar{\mathcal{T}}(\mathcal{S})$ , which is the closure of*

$$\mathcal{T}(\mathcal{S}) = \{x \in \mathbb{R}^D \mid \exists x_1 \neq x_2 \in \mathcal{S}, \|x - x_1\|_2 = \|x - x_2\|_2 = \inf_{y \in \mathcal{S}} \|x - y\|_2\}.$$

*The reach  $\omega$  of  $\mathcal{S}$  is the minimum distance between  $\mathcal{S}$  and  $\bar{\mathcal{T}}(\mathcal{S})$ , that is,*

$$\omega = \inf_{x \in \bar{\mathcal{T}}(\mathcal{S}), y \in \mathcal{S}} \|x - y\|_2.$$

Roughly speaking, reach measures how fast a manifold “bends”. A manifold with a large reach “bends” relatively slowly. On the contrary, a small  $\omega$  signifies more complicated local geometric structures, which are possibly hard to fully capture.

## 2.3 Convolutional Neural Networks

We consider one-sided stride-one convolutional neural networks (CNNs) with the rectified linear unit (ReLU) activation function  $\text{ReLU}(z) = \max(z, 0)$ . Specifically, a CNN we consider consists of a padding layer, several convolutional blocks, and finally a fully connected output layer.



Given an input vector  $x \in \mathbb{R}^D$ , the network first applies a padding operator  $P : \mathbb{R}^D \rightarrow \mathbb{R}^{D \times C}$  for some integer  $C \geq 1$  such that

$$Z = P(x) = \begin{bmatrix} x & 0 & \cdots & 0 \end{bmatrix} \in \mathbb{R}^{D \times C}.$$

Then the matrix  $Z$  is passed through  $M$  convolutional blocks. We will denote the input matrix to the  $m$ -th block as  $Z_m$  and its output as  $Z_{m+1}$  (so that  $Z_1 = Z$ ).

We now define convolution as illustrated in Figure 1. Let  $\mathcal{W} = (\mathcal{W}_{j,i,l})_{j,i,l} \in \mathbb{R}^{C' \times I \times C}$  be a filter where  $C'$  is the output channel size,  $I$  is the filter size and  $C$  is the input channel size. For  $Z \in \mathbb{R}^{D \times C}$ , the convolution of  $Z$  with  $\mathcal{W}$ , denoted with  $\mathcal{W} * Z$ , results in  $Y \in \mathbb{R}^{D \times C'}$  with

$$Y_{k,j} = \sum_{i=1}^I \sum_{l=1}^C \mathcal{W}_{j,i,l} Z_{k+i-1,l},$$

where we set  $Z_{k+i-1,l} = 0$  for  $k+i-1 > D$ .

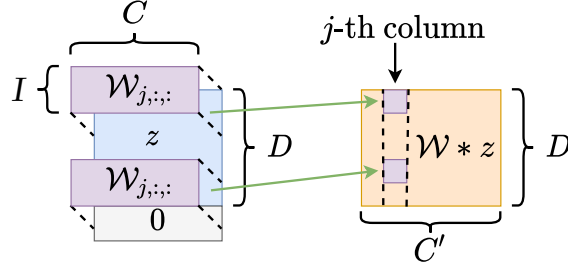


Figure 1: Convolution of  $\mathcal{W} * Z$ .  $\mathcal{W}_{j,:}$  is a  $I \times C$  matrix for the  $j$ -th output channel.

In the  $m$ -th convolutional block, let  $\mathcal{W}_m = \{\mathcal{W}_m^{(1)}, \dots, \mathcal{W}_m^{(L_m)}\}$  be a collection of filters and  $\mathcal{B}_m = \{\mathcal{B}_m^{(1)}, \dots, \mathcal{B}_m^{(L_m)}\}$  be a collection of biases of proper sizes. The  $m$ -th block maps its input matrix  $Z_m \in \mathbb{R}^{D \times C}$  to  $Z_{m+1} \in \mathbb{R}^{D \times C}$  by

$$Z_{m+1} = \text{ReLU} \left( \mathcal{W}_m^{(L_m)} * \cdots * \text{ReLU} \left( \mathcal{W}_m^{(1)} * Z_m + \mathcal{B}_m^{(1)} \right) \cdots + \mathcal{B}_m^{(L_m)} \right) \quad (11)$$

with ReLU applied entrywise. For notational simplicity, we denote this series of operations in the  $m$ -th block with a single operator from  $\mathbb{R}^{D \times C}$  to  $\mathbb{R}^{D \times C}$  with  $\text{Conv}_{\mathcal{W}_m, \mathcal{B}_m}$ , so (11) can be abbreviated as

$$Z_{m+1} = \text{Conv}_{\mathcal{W}_m, \mathcal{B}_m}(Z_m).$$

Overall, we denote the mapping from input  $x$  to the output of the  $M$ -th convolutional block as

$$G(x) = (\text{Conv}_{\mathcal{W}_M, \mathcal{B}_M}) \circ \cdots \circ (\text{Conv}_{\mathcal{W}_1, \mathcal{B}_1}) \circ P(x). \quad (12)$$

Given (12), a CNN applies an additional fully connected layer to  $G$  and outputs

$$f(x) = W \otimes G(x) + b,$$

where  $W \in \mathbb{R}^{D \times C}$  and  $b \in \mathbb{R}$  are a weight matrix and a bias, respectively, and  $\otimes$  denotes the sum of entrywise product, that is,  $W \otimes G(x) = \sum_{i,j} W_{i,j} [G(x)]_{i,j}$ . Thus, we define a class of CNNs of the same architecture as

$$\begin{aligned} \mathcal{F}(M, L, J, I, R_1, R_2) = \\ \{f \mid f(x) = W \otimes G(x) + b, \|W\|_\infty \vee |b| \leq R_2, \text{ where } G(x) \text{ is in (12) with } M \text{ blocks.} \\ \mathcal{W}_m^{(l)} \in \mathbb{R}^{C_m^{(l+1)} \times I_m^{(l)} \times C_m^{(l)}}, \mathcal{B}_m^{(l)} \in \mathbb{R}^{D \times C_m^{(l+1)}}, \text{ where } C_m^{(l)} \leq J, I_m^{(l)} \leq I, \forall l \in [L], m \in [M]; \\ \max_{m,l} \|\mathcal{W}_m^{(l)}\|_\infty \vee \|\mathcal{B}_m^{(l)}\|_\infty \leq R_1\}. \end{aligned} \quad (13)$$

### 3 Neural Policy Mirror Descent

In this section, we present our neural policy mirror descent (NPMD) algorithm. It is an extension of the policy mirror descent (PMD) method with a *critic network*  $Q_w$  parameterized by  $w$  to approximate the state-action value function, and an *actor network*  $f_\theta$  parameterized by  $\theta$  to determine the policy. Both networks belong to a neural network function class  $\mathcal{F}$ , which we will specify later in Section 4.

The NPMD algorithm starts from a uniform policy  $\pi_0$ . At the  $k$ -th iteration (indexed from 0), the policy  $\pi_k$  is determined by the actor network  $f_{\theta_k}$  along with a hyperparameter  $\lambda_k$ . The NPMD algorithm first performs a critic update, training the critic network  $Q_{w_k}$  to fit the state-action value function of the current policy. Then, the NPMD algorithm performs an actor update, indirectly obtaining an improved policy  $\pi_{k+1}$  by updating the actor network to  $f_{\theta_{k+1}}$ .

#### 3.1 Critic Update

For the critic update at the  $k$ -th iteration, the goal is to approximate the exact state-action value function  $Q^{\pi_k}$  with the critic network  $Q_{w_k}$ . The component of  $Q_{w_k}$  corresponding to each action  $a \in \mathcal{A}$  is a neural network  $Q_{w_k}(\cdot, a) \in \mathcal{F}$  parameterized by  $w_{k,a}$ , which takes  $s \in \mathcal{S}$  as input and outputs a scalar. For simplicity, we let all  $|\mathcal{A}|$  networks share the same architecture and denote  $w_k := (w_{k,a})_{a \in \mathcal{A}} \in \mathcal{W}_k$ . We define the critic loss as

$$\mathcal{L}_{\text{critic}}(w_k; \pi_k) = \mathbb{E}_{s \sim \nu_\rho^{\pi_k}} \|Q_{w_k}(s, \cdot) - Q^{\pi_k}(s, \cdot)\|_2^2, \quad (14)$$

where  $Q_{w_k}(s, \cdot)$  and  $Q^{\pi_k}(s, \cdot)$  are  $|\mathcal{A}|$ -dimensional vectors and  $\nu_\rho^{\pi_k}$  is the state visitation distribution defined as (6).

Directly minimizing the critic loss (14) is difficult since  $Q^{\pi_k}$  is unknown in advance. Instead, we sample  $N$  points  $\{s_i\}_{i=1}^N$  independently from the distribution  $\nu_\rho^{\pi_k}$  and use the empirical risk on these

samples to approximate (14). For notation simplicity, we omit the iteration index  $k$  of samples. The empirical risk  $\widehat{\mathcal{L}}_{\text{critic}}$  is defined as

$$\widehat{\mathcal{L}}_{\text{critic}}(w_k; \Xi_k) = \frac{1}{N} \sum_{i=1}^N \sum_{a \in \mathcal{A}} \left| Q_{w_k}(s_i, a) - c(s_i, a) - \frac{\gamma}{1-\gamma} c(s'_{i,a}, a'_{i,a}) \right|^2, \quad (15)$$

where  $N$  is sufficiently large, each pair  $(s'_{i,a}, a'_{i,a})$  is sampled from distribution  $\bar{\nu}_{\mathcal{P}(\cdot|s_i,a)}^{\pi_k}$ , and  $\Xi_k$  denotes the collection of samples. We let  $w_k$  be the solution to the empirical risk minimization (ERM) problem, namely

$$w_k = \underset{w \in \mathcal{W}_k}{\operatorname{argmin}} \widehat{\mathcal{L}}_{\text{critic}}(w; \Xi_k). \quad (16)$$

### 3.2 Actor Update

For the actor update, the goal is to learn an improved policy. If no function approximation is considered, an ideal PMD update is given by Lan (2023):

$$\pi_{k+1}^*(s) = \underset{\pi(\cdot|s) \in \Delta_{\mathcal{A}}}{\operatorname{argmin}} \langle Q_{w_k}(s, \cdot) + \tau_k \nabla h^{\pi_k}(s, \cdot), \pi(\cdot|s) \rangle + \frac{1}{\eta_k} D_{\pi_k}^{\pi}(s), \quad \forall s \in \mathcal{S}, \quad (17)$$

where  $h^{\pi_k}(s)$  is the entropy regularizer, the gradient is taken with respect to  $\pi_k(\cdot|s)$ ,  $D_{\pi_k}^{\pi}(s)$  is the Kullback-Leibler (KL) divergence between  $\pi$  and  $\pi_k$ ,  $\tau_k$  is a decreasing regularization parameter, and  $\eta_k$  is the step size.

With neural function approximation, we train a neural policy  $\pi_{k+1}$  to approximate the ideal policy  $\pi_{k+1}^*$ . For any  $k \geq 0$ , the neural policy  $\pi_k$  takes the form

$$\pi_k(a|s) = \frac{\exp(\lambda_k^{-1} f_{\theta_k}(s, a))}{\sum_{a' \in \mathcal{A}} \exp(\lambda_k^{-1} f_{\theta_k}(s, a'))}, \quad (18)$$

where  $\theta_k := (\theta_{k,a})_{a \in \mathcal{A}}$  is the collection of neural network parameters and  $\lambda_k > 0$  is a temperature parameter (will be discussed later). For any  $a \in \mathcal{A}$ ,  $f_{\theta_k}(\cdot, a) \in \mathcal{F}$  is a neural network parameterized by  $\theta_{k,a}$ , which takes  $s \in \mathcal{S}$  as input and outputs a scalar. Again, we let all  $|\mathcal{A}|$  neural networks share the same parameter space and denote  $\theta_k := (\theta_{k,a})_{a \in \mathcal{A}} \in \Theta_k$ . With definition (18), the ideal PMD update (17) admits a closed-form solution.

**Lemma 1.** *The exact solution of (17) with neural policy  $\pi_k$  defined as (18) is given by*

$$\pi_{k+1}^*(a|s) = \frac{\exp(g_{k+1}^*(s, a))}{\sum_{a' \in \mathcal{A}} \exp(g_{k+1}^*(s, a'))}, \quad (19)$$

where  $g_{k+1}^* = (1 - \eta_k \tau_k) \lambda_k^{-1} f_{\theta_k} - \eta_k Q_{w_k}$ .

The proof of Lemma 1 is given in Appendix B.1. In view of Lemma 1, approximating  $\pi_{k+1}^*$  with

---

**Algorithm 1:** Neural Policy Mirror Descent
 

---

**Input:** Iteration number  $K$ , initial distribution  $\rho$ , sample size per iteration  $N$ , step size  $\eta_k > 0$ , regularization factor  $\tau_k > 0$ , temperature parameter  $\lambda_k > 0$ , discount factor  $\gamma \in (0, 1)$ , neural network parameter space  $\mathcal{W}, \Theta$

Initialize  $\theta_0 = 0$  ;

**for**  $k = 0$  **to**  $K - 1$  **do**

Sample  $\{s_i\}_{i=1}^N$  with  $s_i \sim \nu_\rho^{\pi_k}$ ;

**for**  $a \in \mathcal{A}$  **do**

Sample  $\{(s'_{i,a}, a'_{i,a})\}_{i=1}^N$  with  $(s'_{i,a}, a'_{i,a}) \sim \bar{\nu}_{\mathcal{P}(\cdot|s_i,a)}^{\pi_k}$ ;

Update  $\Xi_k \leftarrow \Xi_k \cup \{(s_i, s'_{i,a}, a'_{i,a})\}_{i=1}^N$ ;

**end**

Update  $w_k \leftarrow \operatorname{argmin}_{w \in \mathcal{W}_k} \widehat{\mathcal{L}}_{\text{critic}}(w; \pi_k, \Xi_k)$  as (16) ; // Critic update

Update  $\theta_{k+1} \leftarrow \operatorname{argmin}_{\theta \in \Theta_{k+1}} \widehat{\mathcal{L}}_{\text{actor}}(\theta; \theta_k, w_k, \Xi_k)$  as (22) ; // Actor update

**end**

**Output:**  $\theta_K$  as the policy parameter

---

$\pi_{k+1}$  is equivalent to approximating  $g_{k+1}^*$  with the scaled actor network  $\lambda_{k+1}^{-1} f_{\theta_{k+1}}$ . We define the actor loss to be minimized as

$$\begin{aligned} & \mathcal{L}_{\text{actor}}(\theta_{k+1}; \theta_k, w_k) \\ &= \mathbb{E}_{s \sim \nu_\rho^{\pi_k}} \left\| \lambda_{k+1}^{-1} f_{\theta_{k+1}}(s, \cdot) - (1 - \eta_k \tau_k) \lambda_k^{-1} f_{\theta_k}(s, \cdot) + \eta_k Q_{w_k}(s, \cdot) \right\|_2^2, \end{aligned} \quad (20)$$

where  $\lambda_k$  is the current temperature,  $\lambda_{k+1}$  is the next temperature,  $\tau_k$  is the regularization factor, and  $\eta_k$  is the step size. For notation simplicity, we omit the hyperparameters  $\tau_k, \eta_k, \lambda_{k+1}$  and  $\lambda_k$  in  $\mathcal{L}_{\text{actor}}$ . Similar to the critic update, instead of minimizing (20) directly, we minimize the empirical risk defined as

$$\begin{aligned} & \widehat{\mathcal{L}}_{\text{actor}}(\theta_{k+1}; \theta_k, w_k, \Xi_k) \\ &= \frac{1}{N} \sum_{i=1}^N \sum_{a \in \mathcal{A}} \left| \lambda_{k+1}^{-1} f_{\theta_{k+1}}(s_i, a) - (1 - \eta_k \tau_k) \lambda_k^{-1} f_{\theta_k}(s_i, a) + \eta_k Q_{w_k}(s_i, a) \right|^2, \end{aligned} \quad (21)$$

where  $\Xi_k$  contains the same sampled states  $\{s_i\}_{i=1}^N$  as used in the critic update from  $\nu_\rho^{\pi_k}$ . The improved actor parameter  $\theta_{k+1}$  is given by the solution to the ERM problem:

$$\theta_{k+1} = \operatorname{argmin}_{\theta \in \Theta_{k+1}} \widehat{\mathcal{L}}_{\text{actor}}(\theta; \theta_k, w_k, \Xi_k). \quad (22)$$

When the sample size  $N$  is sufficiently large, we have  $\lambda_{k+1}^{-1} f_{\theta_{k+1}} \approx g_{k+1}^*$  and hence  $\pi_{k+1} \approx \pi_{k+1}^*$ .

**Remark 1.** *The temperature parameter  $\lambda_k$  is introduced mainly for technical reasons. For any infinite-horizon discounted MDP, there always exists a deterministic optimal policy  $\pi^*$  (Puterman, 1994), while*

the neural policy  $\pi_k$  adopted to approximate  $\pi^*$  is fully stochastic in the sense that  $\pi_k(a|s) > 0$  for any  $(s, a) \in \mathcal{S} \times \mathcal{A}$ . Using the temperature parameter  $\lambda_k$  allows us to control the spikiness of  $\pi_k$ . As  $\lambda_k$  approaches zero,  $\pi_k$  is prone to the action with the maximal value of  $f_{\theta_k}$ . This makes stochastic policy  $\pi_k$  closer to the deterministic policy  $\pi^*$ .

**Remark 2.** Our algorithm uses neural policy  $\pi_{k+1}$  to approximate the ideal policy  $\pi_{k+1}^*$  at each iteration. This allows us to keep the most up-to-date policy with only one actor network. If no actor is used to approximate  $\pi_{k+1}^*$ , ideally, we can obtain an implicitly defined policy by iteratively calling (17). However, this requires us to store all the  $k + 1$  critic networks to calculate  $\pi_{k+1}^*$ , which is not scalable.

We summarize NPMD in Algorithm 1. Note that Algorithm 1 requires samples from the visitation distributions. We provide a sampling algorithm in Appendix A.

## 4 Main Results

In this section, we present our main results on the sample complexity of Algorithm 1. As mentioned in Section 1, we focus on RL environments with low-dimensional structures, for which we make the following smooth manifold assumption on the state space.

**Assumption 1** (State space manifold). *The state space  $\mathcal{S}$  is a  $d$ -dimensional compact Riemannian manifold isometrically embedded in  $\mathbb{R}^D$  where  $d \ll D$ . There exists  $B > 0$  such that  $\|x\|_\infty \leq B$  for any  $x \in \mathcal{S}$ . The surface area of  $\mathcal{S}$  is  $\text{Area}(\mathcal{S}) < \infty$ , and the reach of  $\mathcal{S}$  is  $\omega > 0$ .*

We first derive the iteration complexity with well-approximated value functions and neural policies, then derive the number of samples to meet the requirement for approximation. Combining the results together, we establish the overall sample complexity for Algorithm 1.

### 4.1 Iteration Complexity

We make the following assumptions on the initial and visitation distributions for iteration complexity.

**Assumption 2** (Full support). *The initial distribution  $\rho$  has full support on  $\mathcal{S}$ , that is, for any measurable subset  $S \subseteq \mathcal{S}$ ,  $\rho(S) > 0$ .*

Assumption 2 requires that every state can be visited when doing sampling. In view of (8), as long as  $\rho$  has full support, the visitation distribution also has full support even if the policy itself is deterministic. We measure the distribution mismatch between the optimal visitation distribution  $\nu_\rho^{\pi^*}$  and the initial distribution  $\rho$  by a mismatch coefficient denoted as  $\kappa$ :

$$\kappa := \left\| \frac{d\nu_\rho^{\pi^*}}{d\rho} \right\|_\infty. \quad (23)$$

Under Assumption 2, the Radon-Nikodym derivative  $\frac{d\nu_\rho^{\pi^*}}{d\rho}$  is well-defined. We assume  $\kappa < \infty$ . Accordingly, we define the shifted discount factor as

$$\gamma_\rho := 1 - (1 - \gamma)/\kappa. \quad (24)$$

**Assumption 3** (Concentrability). *There exists  $C_\nu < \infty$  such that for all  $k \geq 0$  iterations of Algorithm 1,*

$$\chi^2(\nu_\rho^\pi, \nu_\rho^{\pi_k}) + 1 \leq C_\nu,$$

where  $\pi$  takes  $\pi_{k+1}$  or  $\pi^*$ ,  $\chi^2(\nu_\rho^\pi, \nu_\rho^{\pi_k}) = \mathbb{E}_{\nu_\rho^{\pi_k}}[(\frac{d\nu_\rho^\pi}{d\nu_\rho^{\pi_k}} - 1)^2]$  is the  $\chi^2$ -divergence.

Assumption 3 requires the concentrability of the visitation distributions. The distance between visitation distributions is measured by the  $\chi^2$ -divergence, which is well-defined under Assumption 2 since the absolute continuity holds for fully supported distributions. This type of concentrability assumption is commonly adopted in the RL literature (Agarwal et al., 2021; Yuan et al., 2023) and is tighter than the absolute density ratio  $\left\| \frac{d\nu_\rho^\pi}{d\nu_\rho^{\pi_k}} \right\|_\infty$ . Assumptions 2 and 3 together forms the *optimism* in RL, that is, the initial distribution is not too far away from the optimal visitation distribution in terms of  $\chi^2$ -divergence, and the policy  $\pi_k$  at each iteration is sufficiently exploratory to find out the optimal policy.

With Assumptions 2 and 3, we have the following one-step improvement lemma for Algorithm 1. The proof is provided in Appendix C.2.

**Lemma 2.** *Suppose Assumptions 2 and 3 hold. If  $1 - \eta_k \tau_k \geq 0$ , then Algorithm 1 yields*

$$\begin{aligned} (V^{\pi_{k+1}}(\rho) - V^*(\rho)) &+ \frac{1}{\kappa \eta_k} \mathbb{E}_{s \sim \nu_\rho^{\pi^*}} [D_{\pi_{k+1}}^{\pi^*}(s)] \\ &\leq \gamma_\rho (V^{\pi_k}(\rho) - V^*(\rho)) + \frac{1 - \eta_k \tau_k}{\kappa \eta_k} \mathbb{E}_{s \sim \nu_\rho^{\pi^*}} [D_{\pi_k}^{\pi^*}(s)] + \frac{2\tau_k \log |\mathcal{A}|}{\kappa(1 - \gamma_\rho)} \\ &\quad + \frac{4\sqrt{C_\nu}}{\kappa(1 - \gamma_\rho)} \left( \sqrt{\mathcal{L}_{\text{critic}}(w_k; \pi_k)} + \frac{1}{\eta_k} \sqrt{\mathcal{L}_{\text{actor}}(\theta_{k+1}; \theta_k, w_k)} \right). \end{aligned}$$

Lemma 2 demonstrates that the optimality gap in value function decreases at rate  $\gamma_\rho$  up to approximation errors introduced by the critic and actor updates, plus an additional regularization term. When these errors are properly controlled, we can establish iteration complexity for Algorithm 1.

**Theorem 1.** *Suppose Assumptions 2 and 3 hold. If  $\eta_k = \frac{1 - \gamma_\rho}{\tau_k}$ ,  $\tau_k = C\gamma_\rho^{k+1}$  for all  $k \geq 0$ , the critic loss and the actor loss satisfy respectively*

$$\mathbb{E}[\mathcal{L}_{\text{critic}}(w_k; \pi_k)] \leq C^2 \gamma_\rho^{2(k+1)}, \quad \mathbb{E}[\mathcal{L}_{\text{actor}}(\theta_{k+1}; \theta_k, w_k)] \leq (1 - \gamma_\rho)^2,$$

then after  $k \geq 1$  iterations, the expected optimality gap of  $\pi_k$  given by Algorithm 1 is

$$\mathbb{E}[V^{\pi_k}(\rho) - V^*(\rho)] \leq \gamma_\rho^k (C_1 + C_2(k+1)) \cdot \frac{C}{1 - \gamma},$$

where  $C_1 = 1 + \log |\mathcal{A}|$ ,  $C_2 = 8\sqrt{C_\nu} + 2\log |\mathcal{A}|$ .

Moreover, for any  $\epsilon > 0$ , the number of iterations required for  $\mathbb{E}[V^{\pi_k}(\rho) - V^*(\rho)] \leq \epsilon$  is

$$\tilde{O} \left( \log_{\frac{1}{\gamma_\rho}} \left( \frac{C(\sqrt{C_\nu} + \log |\mathcal{A}|)}{\kappa(1 - \gamma_\rho)^2 \epsilon} \right) \right).$$

The proof of Theorem 1 is provided in Appendix C.3. The regularization term is controlled by exponentially decreasing the regularization parameter  $\tau_k$  and using an exponentially increasing step size  $\eta_k$  accordingly. The critic loss should be exponentially decreasing, while the actor loss should be small for any consecutive temperatures  $\lambda_k$  and  $\lambda_{k+1}$ . We show in the following subsections that these requirements can be met by properly designing the CNN architecture and using sufficiently many training samples. As long as the conditions are satisfied, Theorem 1 guarantees to find an  $\epsilon$ -optimal policy (in expectation) after  $\tilde{O}(\log \frac{1}{\epsilon})$  iterations.

## 4.2 Function Approximation on Lipschitz MDP with CNN

The iteration complexity in Theorem 1 is valid if the state-action value function  $Q^{\pi_k}$  and the policy  $\pi_{k+1}^*$  are well approximated by the critic and actor networks at each iteration. However, we have not yet specified the CNN architecture that can meet these requirements. In this section, we study the function approximation on *Lipschitz MDP*, which possesses Lipschitz transition kernel  $\mathcal{P}$  and Lipschitz cost function  $c$ . Here, the Lipschitzness is defined with respect to the *geodesic distance* on the state space  $\mathcal{S}$ , which is a  $d$ -dimensional Riemannian manifold (Assumption 1). Recall the definition of geodesic distance:

**Definition 3** (Geodesic distance). *The geodesic distance between two points  $x, y \in \mathcal{S}$  is defined as*

$$d_{\mathcal{S}}(x, y) := \inf_{\Gamma: [0,1] \rightarrow \mathcal{S}} \int_0^1 \|\Gamma'(t)\|_2 dt \quad (25)$$

*s.t.*  $\Gamma(0) = x, \Gamma(1) = y, \Gamma$  is piecewise  $C^1$ .

One can show the existence of a solution to the minimization problem (25) under mild conditions and that  $d_{\mathcal{S}}(\cdot, \cdot)$  is indeed a distance. More references can be found in [Do Carmo and Flaherty Francis \(1992\)](#). With geodesic distance, we define Lipschitz functions on the Riemannian manifold  $\mathcal{S}$ .

**Definition 4** (Lipschitz function). *Let  $L \geq 0$  and  $\alpha \in (0, 1]$  be constants. A function  $f: \mathcal{S} \rightarrow \mathbb{R}$  is called  $(L, \alpha)$ -Lipschitz if for any  $x, y \in \mathcal{S}$ ,*

$$|f(x) - f(y)| \leq L \cdot d_{\mathcal{S}}^\alpha(x, y).$$

For any fixed  $\alpha$ , the Lipschitz constant  $L$  in Definition 4 measures the smoothness of the function. A function is considered smooth if it possesses a small Lipschitz constant, whereas a non-smooth function will exhibit a large Lipschitz constant. Throughout the remainder of this paper, when we

mention Lipschitzness, we specifically mean the property of being Lipschitz continuous with a moderate constant.

**Remark 3.** *The geodesic distance (Definition 3) in Definition 4 is a global distance rather than a local one. This makes our definition of Lipschitz functions different from those based on local Euclidean distance and partition of unity as in Chen et al. (2019) and Liu et al. (2021). The two ways of defining Lipschitzness have some technical differences, but they agree with each other in our setting up to constant factors.*

*When the atlas  $\{(U_i, \phi_i)\}_{i \in I}$  are local projections onto tangent spaces as in Chen et al. (2019), the local Euclidean distance between two points in the same open set  $U_i$  is no greater than their Euclidean distance in  $\mathbb{R}^D$ , which is further less than their geodesic distance, hence the Lipschitzness defined with local distances implies Definition 4.*

*On the other hand, when the curvature of manifold  $\mathcal{S}$  is not too large compared to the radius of the open set  $U_i$ , then Definition 4 also implies Lipschitzness in the Euclidean sense on each local coordinate  $\phi_i(U_i) \subset [0, 1]^d$  (Lemma 12). Here, we adopt the global definition for simplicity.*

We now formally define the Lipschitz MDP condition, which ensures the Lipschitzness of the state-action value function  $Q^\pi$  for any policy  $\pi$ .

**Assumption 4** (Lipschitz MDP). *There exist constants  $L_{\mathcal{P}}, L_c \geq 0$  and  $\alpha \in (0, 1]$  such that for any tuple  $(s, s', a) \in \mathcal{S} \times \mathcal{S} \times \mathcal{A}$ , the cost function  $c(\cdot, a): \mathcal{S} \rightarrow \mathbb{R}$  is  $(L_c, \alpha)$ -Lipschitz and the transition kernel  $\mathcal{P}$  satisfies*

$$d_{\text{TV}}(\mathcal{P}(\cdot|s, a), \mathcal{P}(\cdot|s', a)) \leq L_{\mathcal{P}} \cdot d_{\mathcal{S}}^\alpha(s, s'),$$

where  $d_{\text{TV}}(\cdot, \cdot)$  is the total variation distance.

Assumption 4 requires that when two states are close to each other, taking the same action would admit similar transition distributions and corresponding costs. This assumption holds for many spatially smooth environments, especially those driven by physical simulations such as MuJuCo (Todorov et al., 2012) and classic control environments (Brockman et al., 2016). Under Assumption 4, we show in Lemma 3 that the state-action value function  $Q^\pi$  is Lipschitz regardless of the evaluated policy  $\pi$ . The proof of Lemma 3 is provided in Appendix E.3.

**Lemma 3.** *If Assumption 4 holds, then for any policy  $\pi$  and any action  $a \in \mathcal{A}$ , the state-action value function  $Q^\pi(\cdot, a): \mathcal{S} \rightarrow \mathbb{R}$  is  $(L_Q, \alpha)$ -Lipschitz with  $L_Q = L_c + \frac{\gamma C}{1-\gamma} L_{\mathcal{P}}$  being the Lipschitz constant. That is, for any policy  $\pi$  and any tuple  $(s, s', a) \in \mathcal{S} \times \mathcal{S} \times \mathcal{A}$ , we have*

$$|Q^\pi(s, a) - Q^\pi(s', a)| \leq L_Q \cdot d_{\mathcal{S}}^\alpha(s, s').$$

The Lipschitz constant  $L_Q = L_c + \frac{\gamma C}{1-\gamma} L_{\mathcal{P}}$  scales linearly with the magnitude of the cost function  $c$  as  $L_c$  does. In view of this property, we define a normalized Lipschitz constant which is invariant to



the scaling of the cost:

$$\bar{L}_Q := (1 - \gamma)L_c/C + \gamma L_{\mathcal{P}}. \quad (26)$$

This normalized Lipschitz constant is a convex combination of  $L_c/C$  and  $L_{\mathcal{P}}$ , so it will not exceed the larger one for any  $\gamma$ .

We make a few remarks on the Lipschitz condition.

**Remark 4.** *Assumption 4 is a sufficient condition for the Lipschitzness of  $Q^{\pi_k}$ , regardless of the smoothness of  $\pi_k$ . The Lipschitzness of the target function is a minimal requirement for approximation theory and it is almost essential even for simple regression problems. However, even if Assumption 4 does not hold,  $Q^{\pi_k}$  being Lipschitz is still possible. An extreme example is when state space  $\mathcal{S} = \mathbb{S}^1$  is a circle and the transition is a fixed rotation whichever action is taken. In this case, the transition kernel is not Lipschitz since the total variation distance between transitions is always 1. Meanwhile,  $Q^{\pi_k}$  is Lipschitz for any  $\pi_k$  provided that  $c$  is Lipschitz. Similar arguments can be found in [Fan et al. \(2020\)](#) and [Nguyen-Tang et al. \(2022\)](#) for non-smooth MDP having smooth Bellman operator, but they implicitly involve the smoothness of neural policy  $\pi_k$ .*

**Remark 5.** *In practice, many environments adhere to the Lipschitz condition, with only an extremely small portion of states being exceptions. For example, in the Box2D Car Racing environment ([Brockman et al., 2016](#)), the cost remains constant for each frame until a tile is reached, for which the agent will be given a huge reward. Even though this type of partially smooth environment does not fulfill the Lipschitz condition on a global scale, it is reasonable to expect the existence of an environment that is globally smooth and satisfies Assumption 4. Such a globally smooth environment could serve as a regularization of the original non-smooth environment, which inevitably introduces bias to the problem. When this bias is negligible compared to the extent of smoothness, we can study the smooth approximation under Assumption 4 without loss of generality.*

With Lemma 3 established, we show that a CNN of the form (13) can uniformly approximate  $Q^{\pi_k}(\cdot, a)$  for any  $a \in \mathcal{A}$ . The approximation error depends on the specified CNN architecture.

**Theorem 2** (Critic approximation). *Suppose Assumptions 1 and 4 hold. For any integers  $I \in [2, D]$  and  $\tilde{M}, \tilde{J} > 0$ , we let*

$$\begin{aligned} M &= O(\tilde{M}), \quad L = O(\log(\tilde{M}\tilde{J}) + D + \log D), \quad J = O(D\tilde{J}), \\ R_1 &= (8ID)^{-1}\tilde{M}^{-\frac{1}{I}} = O(1), \quad \log R_2 = O(\log^2(\tilde{M}\tilde{J}) + D \log(\tilde{M}\tilde{J})), \end{aligned}$$

where  $O(\cdot)$  hides a constant depending on  $\log L_Q$ ,  $\log \frac{C}{1-\gamma}$ ,  $d$ ,  $\alpha$ ,  $\omega$ ,  $B$ , and the surface area  $\text{Area}(\mathcal{S})$ . Then for any policy  $\pi$  and any action  $a \in \mathcal{A}$ , there exists a CNN  $Q_w(\cdot, a) \in \mathcal{F}(M, L, J, I, R_1, R_2)$  such

that

$$\|Q_w(\cdot, a) - Q^\pi(\cdot, a)\|_\infty \leq \frac{C}{1-\gamma}(\bar{L}_Q + 1)(\widetilde{M}\widetilde{J})^{-\frac{\alpha}{d}}.$$

Here,  $L_Q$  and  $\bar{L}_Q$  are defined as in Lemma 3 and (26).

We provide a proof overview for Theorem 2 in Appendix E.1 and the detailed proof in Appendix E.2. Compared to our preliminary work (Theorem 1 in Ji et al. (2022)) that deals with a larger class of Besov functions by using cardinal B-spline approximation as a crucial step, we simplify the proof for Lipschitz functions where first-order spline approximation is sufficient.

To bound the approximation error by  $\epsilon$ , we require the number of parameters in  $Q_w(\cdot, a)$  to be  $O(MLJ^2I) = \tilde{O}(D^3I\epsilon^{-\frac{d}{\alpha}})$ . Note that the exponent over  $\epsilon$  is the intrinsic dimension  $d$  rather than the data dimension  $D$ , and the hidden terms in  $\tilde{O}(\cdot)$  also have no exponential dependence on  $D$ . This implies that CNN approximation does not suffer from the curse of dimensionality when the data support has a low-dimensional manifold structure.

Next, we consider function approximation for policy  $\pi_{k+1}^*$  in the actor update. As mentioned in Section 3.2, our goal is to learn a deterministic optimal policy, which is equivalent to a discrete mapping from  $\mathcal{S}$  to  $\mathcal{A}$ . Such a mapping is not continuous given the discrete nature of  $\mathcal{A}$ , so it is difficult to be approximated directly. Instead, we iteratively update a temperature-controlled neural policy  $\pi_k$  in the form of (18) to approximate the deterministic optimal policy  $\pi^*$ . Although  $\pi_k$  is a stochastic policy by construction, it can approximate the deterministic policy that chooses the action  $a \in \mathcal{A}$  with the maximal value of  $f_{\theta_k}(s, a)$  by using a sufficiently small temperature  $\lambda_k > 0$ . Therefore, as long as the actor network  $f_{\theta_k}(s, \cdot)$  is learned to admit a maximizer  $a \in \text{supp}(\pi^*(\cdot|s))$  for any state  $s \in \mathcal{S}$ , it can serve as a good approximation of the optimal policy  $\pi^*$ .

To learn such an actor network, we iteratively train a new actor network  $f_{\theta_{k+1}}$  based on the current critic and actor networks  $Q_{w_k}$  and  $f_{\theta_k}$ . According to Lemma 1, the target function for the next actor network  $f_{\theta_{k+1}}$  is given by

$$\lambda_{k+1}g_{k+1}^* = (1 - \eta_k\tau_k)\lambda_k^{-1}\lambda_{k+1}f_{\theta_k} - \eta_k\lambda_{k+1}Q_{w_k},$$

which is a weighted sum of the current critic and actor networks. This approximation target is not Lipschitz, since  $Q_{w_k}$  is just an approximation of the Lipschitz function  $Q^{\pi_k}$ , not a Lipschitz function in itself. Consequently, Theorem 2 cannot be directly transferred to actor approximation. To address the issue, we introduce the *approximately Lipschitz* condition to describe the smoothness inherited from approximating a Lipschitz function.

**Definition 5** (Approximate Lipschitzness). *Let  $L, \epsilon \geq 0$  and  $\alpha \in (0, 1]$  be constants. A function  $f: \mathcal{S} \rightarrow \mathbb{R}$  is called  $(L, \alpha, \epsilon)$ -approximately Lipschitz if for any  $x, y \in \mathcal{S}$ ,*

$$|f(x) - f(y)| \leq L \cdot d_{\mathcal{S}}^\alpha(x, y) + 2\epsilon.$$

Here,  $L$  is called the Lipschitz constant, and  $\epsilon$  is called the proximity constant. When  $\epsilon = 0$ ,  $f$  is  $(L, \alpha)$ -Lipschitz as defined in Definition 4.

Definition 5 relaxes the Lipschitz condition by allowing a proximity constant  $\epsilon$ . When  $\epsilon = 0$ , the condition reduces to the Lipschitz continuity, and the Lipschitz constant is exactly the one in Definition 4. When  $\epsilon \geq \|f\|_\infty$ , the condition is vacuously true for all  $L \geq 0$ . When  $\epsilon$  is somewhere between 0 and  $\|f\|_\infty$ , a larger  $\epsilon$  allows a potentially smaller Lipschitz constant  $L$ . As Lemma 4 shows, the approximate Lipschitzness is a property of any uniform approximation of a Lipschitz function.

**Lemma 4.** *If  $\bar{f}_0: \mathcal{S} \rightarrow \mathbb{R}$  is  $(L, \alpha)$ -Lipschitz,  $f: \mathcal{S} \rightarrow \mathbb{R}$  satisfies  $\|f - \bar{f}_0\|_\infty \leq \epsilon$  for some  $\epsilon > 0$ , then  $f$  is  $(L, \alpha, \epsilon)$ -approximately Lipschitz.*

*Proof.* For any  $x, y \in \mathcal{X}$ ,

$$\begin{aligned} |f(x) - f(y)| &= |\bar{f}_0(x) - \bar{f}_0(y) + f(x) - \bar{f}_0(x) - f(y) + \bar{f}_0(y)| \\ &\leq |\bar{f}_0(x) - \bar{f}_0(y)| + |f(x) - \bar{f}_0(x)| + |-f(y) + \bar{f}_0(y)| \\ &\leq L \cdot d_{\mathcal{S}}^\alpha(x, y) + 2\epsilon. \end{aligned}$$

The first inequality comes from the triangle inequality. The second inequality is from  $L$ -Lipschitz continuity of  $\bar{f}_0$  and that  $\|f - \bar{f}_0\|_\infty \leq \epsilon$ .  $\square$

It follows immediately from Theorem 2 and Lemma 4 that there exists an  $(L_Q, \epsilon, \epsilon_Q)$ -approximately Lipschitz  $Q_{w_k}$  that can uniformly approximate  $Q^{\pi_k}$  up to  $\epsilon_Q$  error. Therefore, we can impose (approximately) Lipschitz restrictions on the CNN function class without damaging its approximation power for the state-action value function. To be more precise, for any CNN class  $\mathcal{F} = \mathcal{F}(M, L, J, I, R_1, R_2)$ , we define its Lipschitz-restricted version  $\mathcal{F}_{\text{Lip}}(A, L_f, \alpha, \epsilon_f)$  as

$$\mathcal{F}_{\text{Lip}}(A, L_f, \alpha, \epsilon_f) = \{f \in \mathcal{F} \mid \|f\|_\infty \leq A, f \text{ is } (L_f, \alpha, \epsilon_f)\text{-approximately Lipschitz}\}. \quad (27)$$

Moreover, we denote the parameter space of the Lipschitz-restricted critic and actor network classes as  $\mathcal{W}_{\text{Lip}}$  and  $\Theta_{\text{Lip}}$  respectively:

$$\mathcal{W}_{\text{Lip}}(A, L_Q, \alpha, \epsilon_Q) = \{w \mid Q_w(\cdot, a) \in \mathcal{F}_{\text{Lip}}(A, L_Q, \alpha, \epsilon_Q), \forall a \in \mathcal{A}\}, \quad (28)$$

$$\Theta_{\text{Lip}}(A, L_f, \alpha, \epsilon_f) = \{\theta \mid f_\theta(\cdot, a) \in \mathcal{F}_{\text{Lip}}(A, L_f, \alpha, \epsilon_f), \forall a \in \mathcal{A}\}. \quad (29)$$

Then by setting  $\mathcal{W}_k = \mathcal{W}_{\text{Lip}}$  and  $\Theta_k = \Theta_{\text{Lip}}$  in Algorithm 1, we ensure the  $k$ -th critic network  $Q_{w_k}$  and actor network  $f_{\theta_k}$  are both approximately Lipschitz, and such a restriction on  $\mathcal{W}_k$  will not affect the approximation power of  $Q_{w_k}$  for  $Q^{\pi_k}$ . In addition, the target function  $\lambda_{k+1}g_{k+1}^*$  for the next actor is also approximately Lipschitz since it is a weighted sum of two approximately Lipschitz functions. By carefully selecting the temperature parameters to match the configuration of  $\eta_k$  and  $\tau_k$  in Theorem 1, the approximate Lipschitzness of target functions for actor updates in all iterations can be uniformly controlled.

**Lemma 5.** For  $k \geq 0$ , we let  $\eta_k = \frac{1-\gamma\rho}{\tau_k}$ ,  $\tau_k = C\gamma_\rho^{k+1}$ ,  $\lambda_k = \frac{C\gamma_\rho^k}{1-\gamma_\rho}$ ,  $\mathcal{W}_k = \mathcal{W}_{\text{Lip}}(\frac{C}{1-\gamma}, L_Q, \alpha, \epsilon_Q)$  and  $\Theta_k = \Theta_{\text{Lip}}(\frac{C}{(1-\gamma_\rho^2)(1-\gamma)}, \frac{L_Q}{1-\gamma_\rho^2}, \alpha, \frac{\epsilon_Q}{1-\gamma_\rho^2})$  with some  $\epsilon_Q \geq 0$ . Then the target actor  $\lambda_{k+1}g_{k+1}^*$  defined in Lemma 1 is  $(\frac{L_Q}{1-\gamma_\rho^2}, \alpha, \frac{\epsilon_Q}{1-\gamma_\rho^2})$ -approximately Lipschitz and is uniformly bounded by  $\frac{C}{(1-\gamma_\rho^2)(1-\gamma)}$ .

*Proof.* By Lemma 1 and our choice of  $\eta_k$ ,  $\tau_k$  and  $\lambda_k$ , the target function of the  $k$ -th critic update is

$$\begin{aligned}\lambda_{k+1}g_{k+1}^* &= (1 - \eta_k\tau_k)\lambda_{k+1}\lambda_k^{-1}f_{\theta_k} - \eta_k\lambda_{k+1}Q_{w_k} \\ &= \gamma_\rho^2 f_{\theta_k} - Q_{w_k}.\end{aligned}$$

We initialize  $\theta_0 = 0$  in Algorithm 1, thus  $\theta_0 \in \Theta_{\text{Lip}}(0, 0, \alpha, 0) \subseteq \Theta_0$ . It is easy to verify that if  $f: \mathcal{S} \rightarrow \mathbb{R}$  is  $(L_f, \alpha, \epsilon_f)$ -approximately Lipschitz and  $g: \mathcal{S} \rightarrow \mathbb{R}$  is  $(L_g, \alpha, \epsilon_g)$ -approximately Lipschitz,  $c \in \mathbb{R}$ , then  $f+g$  is  $(L_f+L_g, \alpha, \epsilon_f+\epsilon_g)$ -approximately Lipschitz, and  $c \cdot f$  is  $(|c|L_f, \alpha, |c|\epsilon_f)$ -approximately Lipschitz. Combining this fact and our choice of  $\mathcal{W}_k$  and  $\Theta_k$ , we have that  $\lambda_1g_1^*$  is  $(\frac{L_Q}{1-\gamma_\rho^2}, \alpha, \frac{\epsilon_Q}{1-\gamma_\rho^2})$ -approximately Lipschitz and is uniformly bounded by  $\frac{C}{(1-\gamma_\rho^2)(1-\gamma)}$ .  $\square$

Lemma 5 shows the target actor is approximately Lipschitz in each iteration with  $\mathcal{W}_k$  and  $\Theta_k$  inserted. It remains to derive the approximation error for actor update with Lipschitz-restricted class  $\Theta_{k+1} = \Theta_{\text{Lip}}$ . We first show in Theorem 3 that any bounded and approximately Lipschitz function on  $\mathcal{S}$  can be well approximated by a CNN with enough parameters, and this CNN is also bounded and approximately Lipschitz.

**Theorem 3.** Suppose Assumption 1 holds, the target function  $f_0: \mathcal{S} \rightarrow \mathbb{R}$  is bounded and  $(L_f, \alpha, \epsilon_f)$ -approximately Lipschitz. For any integers  $I \in [2, D]$  and  $\widetilde{M}, \widetilde{J} > 0$ , we let

$$\begin{aligned}M &= O(\widetilde{M}), \quad L = O(\log(\widetilde{M}\widetilde{J}) + D + \log D), \quad J = O(D\widetilde{J}), \\ R_1 &= (8ID)^{-1}\widetilde{M}^{-\frac{1}{I}} = O(1), \quad \log R_2 = O(\log^2(\widetilde{M}\widetilde{J}) + D \log(\widetilde{M}\widetilde{J})),\end{aligned}$$

where  $O(\cdot)$  hides a constant depending on  $\log L_f$ ,  $\log \|f_0\|_\infty$ ,  $\alpha$ ,  $\omega$ ,  $B$ , and the surface area  $\text{Area}(\mathcal{S})$ . Then there exists a CNN  $f \in \mathcal{F}(M, L, J, I, R_1, R_2)$  such that

$$\|f - f_0\|_\infty \leq (L_f + \|f_0\|_\infty)(\widetilde{M}\widetilde{J})^{-\frac{\alpha}{I}} + 2\epsilon_f.$$

Moreover,  $f$  is  $(L_f, \alpha, \widehat{\epsilon}_f)$ -approximately Lipschitz with  $\widehat{\epsilon}_f = (L_f + \|f_0\|_\infty)(\widetilde{M}\widetilde{J})^{-\frac{\alpha}{I}}$  and is uniformly bounded by  $\|f_0\|_\infty$ .

The proof of Theorem 3 is provided in Appendix E.4. Theorem 3 shows the existence of an approximately Lipschitz CNN that is close under  $L^\infty$  norm to any approximately Lipschitz target function on  $\mathcal{S}$ . As a corollary, we obtain the approximation error for the actor update.

**Corollary 1** (Actor approximation). Suppose Assumptions 1 and 4 hold. For any integers  $I \in [2, D]$

and  $\widetilde{M}, \widetilde{J} > 0$ , we let

$$\begin{aligned} M &= O(\widetilde{M}), \quad L = O(\log(\widetilde{M}\widetilde{J}) + D + \log D), \quad J = O(D\widetilde{J}), \\ R_1 &= (8ID)^{-1}\widetilde{M}^{-\frac{1}{L}} = O(1), \quad \log R_2 = O(\log^2(\widetilde{M}\widetilde{J}) + D \log(\widetilde{M}\widetilde{J})), \end{aligned}$$

where  $O(\cdot)$  hides a constant depending on  $\log L_Q$ ,  $\log \frac{C}{1-\gamma}$ ,  $d$ ,  $\alpha$ ,  $\omega$ ,  $B$ , and the surface area  $\text{Area}(\mathcal{S})$ . If  $\eta_k$ ,  $\tau_k$ ,  $\lambda_k$ ,  $\mathcal{W}_k$  and  $\Theta_k$  are as specified in Lemma 5 for all  $k \geq 0$ ,  $\epsilon_Q = \frac{C}{1-\gamma}(\bar{L}_Q + 1)(\widetilde{M}\widetilde{J})^{-\frac{\alpha}{d}}$ , then for any  $w_k \in \mathcal{W}_k$  and  $\theta_k \in \Theta_k$ , there exists  $\theta \in \Theta_{k+1}$  such that

$$\|f_\theta(\cdot, a) - \lambda_{k+1}g_{k+1}^*(\cdot, a)\|_\infty \leq \frac{3\epsilon_Q}{1 - \gamma_\rho^2}.$$

Here,  $g_{k+1}^*$ ,  $L_Q$  and  $\bar{L}_Q$  are defined as in Lemmas 1 and 3 and (26).

We note that the requirement for proximity constant  $\epsilon_Q$  in Corollary 1 is the same as the approximation error in Theorem 2. This alignment maintains the consistency of the Lipschitz constraints imposed on  $\mathcal{W}_k$ ,  $\Theta_k$ , and  $\Theta_{k+1}$ . In this case, the actor approximation error is comparable to the critic approximation error, and they both depend on the CNN architecture. Therefore, a large CNN class  $\mathcal{F} = \mathcal{F}(M, L, J, I, R_1, R_2)$  guarantees the existence of good approximations to both the state-action value function and the policy.

### 4.3 Sample Complexity

We have demonstrated that CNN approximation can be applied to both the state-action value function and the policy. To make sure that the solutions to the ERM subproblems (16) and (22) indeed provide good approximations for  $Q^{\pi_k}$  and  $\pi_{k+1}^*$ , the number of samples must be sufficient. In this section, we derive the sample complexity for Algorithm 1. To be more precise, we consider the expected number of oracle accesses to the transition kernel  $\mathcal{P}$  and the cost function  $c$  for Algorithm 1 to find a policy  $\pi_K$  that satisfies  $\mathbb{E}[V^{\pi_K}(\rho) - V^*(\rho)] \leq \epsilon$ .

We keep using the same notation for CNN class  $\mathcal{F} = \mathcal{F}(M, L, J, I, R_1, R_2)$  and its Lipschitz-restricted version  $\mathcal{F}_{\text{Lip}}$  as defined in (27), as well as the parameter spaces  $\mathcal{W}_{\text{Lip}}$  and  $\Theta_{\text{Lip}}$  as denoted in (28) and (29). We show the following lemma that characterizes the number of samples  $N$  sufficient for accurate critic update at the  $k$ -th iteration.

**Theorem 4** (Critic sample size). *Suppose Assumptions 1 and 4 hold. For  $k \geq 0$ , we let  $\eta_k$  and  $\tau_k$  be the same as in Theorem 1 and  $\mathcal{W}_k = \mathcal{W}_{\text{Lip}}(\frac{C}{1-\gamma}, L_Q, \alpha, \epsilon_Q)$  with*

$$\begin{aligned} M &= O(N^{\frac{d}{d+2\alpha}}), \quad L = O(\log N + D + \log D), \quad J = O(D), \quad I \in [2, D], \quad R_1 = O(1), \\ \log R_2 &= O(\log^2 N + D \log N), \quad \epsilon_Q = (L_Q^2 + C^2/(1-\gamma)^2)D^{\frac{3\alpha}{2\alpha+d}}N^{-\frac{\alpha}{2\alpha+d}}. \end{aligned}$$

If we take sample size  $N = \widetilde{O}(\frac{\sqrt{|A|}}{1-\gamma}\gamma_\rho^{-(K+1)})^{\frac{d}{\alpha}+2}$ , then  $\mathbb{E}[\mathcal{L}_{\text{critic}}(w_k; \pi_k)] \leq C^2\gamma_\rho^{2(k+1)}$  holds for all

$k \leq K$  in Algorithm 1.

Moreover, if Assumptions 2 and 3 hold, then for any  $\epsilon > 0$ , it suffices to let

$$N = \tilde{O} \left( \frac{\kappa C (\sqrt{C_\nu} + \log |\mathcal{A}|) \sqrt{|\mathcal{A}|}}{(1-\gamma)^3 \epsilon} \right)^{\frac{d}{\alpha} + 2}$$

so that  $\mathbb{E}[\mathcal{L}_{\text{critic}}(w_k; \pi_k)] \leq C^2 \gamma_\rho^{2(k+1)}$  for all  $k \leq K$ , where  $K$  is the iteration number given in Theorem 1 that guarantees  $\mathbb{E}[V^{\pi_k}(\rho) - V^*(\rho)] \leq \epsilon$ . Here,  $O(\cdot)$  and  $\tilde{O}(\cdot)$  hide the constant depending on  $D^{\frac{6\alpha}{2\alpha+d}}$ ,  $\bar{L}_Q$ ,  $\log L_Q$ ,  $\log \frac{C}{1-\gamma}$ ,  $d$ ,  $\alpha$ ,  $\omega$ ,  $B$ , and the surface area  $\text{Area}(\mathcal{S})$ .

The proof of Theorem 4 is provided in Appendix D.1. As shown in Theorem 4, when the iteration number  $k$  increases, the required number of samples  $N$  grows exponentially at rate  $\tilde{O}(\gamma^{-\frac{d}{\alpha}-2})$ . By Theorem 1, the total number of iterations is  $\tilde{O}(\log \frac{1}{\epsilon})$ , so the growing procedure will not continue for too long. As a result, the number of samples for the last iteration is  $\tilde{O}(\epsilon^{-\frac{d}{\alpha}-2})$ , and the overall sample complexity for critic updates is in the same order up to logarithm terms. Moreover, the exponent over  $\epsilon$  is again the intrinsic dimension  $d$  instead of the data dimension  $D$ , which implies avoidance from the curse of dimensionality.

We now turn to derive a similar bound for actor updates. As shown in Lemma 5, with adequately chosen temperature parameters, we can restrict the actor network class with constant parameters for all iterations, and the resulting target actor will have the same approximate Lipschitzness guarantee as the subsequent actor network. Hence we have the following Theorem 5 characterizing the sufficient sample size for accurate actor updates.

**Theorem 5** (Actor sample size). *Suppose Assumptions 1 and 4 hold. For  $k \geq 0$ , we let  $\eta_k$  and  $\tau_k$  be the same as in Theorem 1,  $\lambda_k = \frac{C \gamma_\rho^{k+1}}{1-\gamma_\rho}$ ,  $\mathcal{W}_k = \mathcal{W}_{\text{Lip}}(\frac{C}{1-\gamma}, L_Q, \alpha, \epsilon_Q)$  and  $\Theta_k = \Theta_{\text{Lip}}(\frac{C}{(1-\gamma_\rho^2)(1-\gamma)}, \frac{L_Q}{1-\gamma_\rho^2}, \alpha, \frac{\epsilon_Q}{1-\gamma_\rho^2})$  with*

$$M = O(N^{\frac{d}{d+2\alpha}}), \quad L = O(\log N + D + \log D), \quad J = O(D), \quad I \in [2, D], \quad R_1 = O(1),$$

$$\log R_2 = O(\log^2 N + D \log N), \quad \epsilon_Q = (L_Q^2 + C^2 / (1-\gamma)^2) D^{\frac{3\alpha}{2\alpha+d}} N^{-\frac{\alpha}{2\alpha+d}},$$

If we take sample size  $N = \tilde{O} \left( \frac{\sqrt{|\mathcal{A}|} \gamma_\rho^{-(K+1)}}{(1-\gamma_\rho^2)(1-\gamma)} \right)^{\frac{d}{\alpha} + 2}$ , then  $\mathbb{E}[\mathcal{L}_{\text{actor}}(\theta_{k+1}; \theta_k, w_k)] \leq (1-\gamma_\rho)^2$  holds for all  $k \leq K$  in Algorithm 1.

Moreover, if Assumptions 2 and 3, then for any  $\epsilon > 0$ , it suffices to let

$$N = \tilde{O} \left( \frac{\kappa^2 C (\sqrt{C_\nu} + \log |\mathcal{A}|) \sqrt{|\mathcal{A}|}}{(1-\gamma)^4 \epsilon} \right)^{\frac{d}{\alpha} + 2}$$

so that  $\mathbb{E}[\mathcal{L}_{\text{actor}}(\theta_{k+1}; \theta_k, w_k)] \leq (1-\gamma_\rho)^2$  for all  $k \leq K$ , where  $K$  is the iteration number given in Theorem 1 that guarantees  $\mathbb{E}[V^{\pi_K}(\rho) - V^*(\rho)] \leq \epsilon$ . Here,  $O(\cdot)$  and  $\tilde{O}(\cdot)$  hide the constant depending on  $D^{\frac{6\alpha}{2\alpha+d}}$ ,  $\bar{L}_Q$ ,  $\log L_Q$ ,  $\log \frac{C}{1-\gamma}$ ,  $d$ ,  $\alpha$ ,  $\omega$ ,  $B$ , and the surface area  $\text{Area}(\mathcal{S})$ .

The proof of Theorem 5 is provided in Appendix D.2, which is similar to the proof of Theorem 4. Compared to Theorem 4, Theorem 5 requires a  $\tilde{O}((1 - \gamma_\rho^2)^{-\frac{d}{\alpha} - 2})$  times larger sample size because the target actor in each iteration has a worse approximate Lipschitzness than the target actor. Nevertheless, we can align the sample size to the larger one for actor updates so that both the actor and the critic will be accurate. Combining the results together, we establish the overall sample complexity for Algorithm 1.

**Corollary 2** (Overall sample complexity). *Suppose Assumptions 1 to 4 hold. For  $k \geq 0$ , we let  $\eta_k$  and  $\tau_k$  be the same as in Theorem 1,  $\lambda_k = \frac{C\gamma_\rho^{k+1}}{1-\gamma_\rho}$ ,  $\mathcal{W}_k = \mathcal{W}_{\text{Lip}}(\frac{C}{1-\gamma}, L_Q, \alpha, \epsilon_Q)$  and  $\Theta_k = \Theta_{\text{Lip}}(\frac{C}{(1-\gamma_\rho^2)(1-\gamma)}, \frac{L_Q}{1-\gamma_\rho^2}, \alpha, \frac{\epsilon_Q}{1-\gamma_\rho^2})$  with*

$$M = O(N^{\frac{d}{d+2\alpha}}), L = O(\log N + D + \log D), J = O(D), I \in [2, D], R_1 = O(1),$$

$$\log R_2 = O(\log^2 N + D \log N), \epsilon_Q^{(k)} = (L_Q^2 + C^2/(1-\gamma)^2)D^{\frac{3\alpha}{2\alpha+d}}N^{-\frac{\alpha}{2\alpha+d}}.$$

Then for  $\epsilon > 0$ , it suffices to set  $N = \tilde{O}\left(\frac{\kappa^2 C(\sqrt{C_\nu} + \log |\mathcal{A}|)\sqrt{|\mathcal{A}|}}{(1-\gamma)^4 \epsilon}\right)^{\frac{d}{\alpha} + 2}$ , and the expected number of oracle calls for Algorithm 1 to find a  $\pi_K$  satisfying  $\mathbb{E}[V^{\pi_K}(\rho) - V^*(\rho)] \leq \epsilon$  is

$$\tilde{O}\left(\kappa^{\frac{2d}{\alpha} + 5} C_\nu^{\frac{d}{2\alpha} + 1} |\mathcal{A}|^{\frac{d}{2\alpha} + 2} (1-\gamma)^{-\frac{4d}{\alpha} - 10} C_\alpha^{\frac{d}{\alpha} + 2} \epsilon^{-\frac{d}{\alpha} - 2}\right).$$

Here,  $O(\cdot)$  and  $\tilde{O}(\cdot)$  hide the constant depending on  $D^{\frac{6\alpha}{2\alpha+d}}$ ,  $\bar{L}_Q$ ,  $\log L_Q$ ,  $\log \frac{C}{1-\gamma}$ ,  $d$ ,  $\alpha$ ,  $\omega$ ,  $B$ , and the surface area  $\text{Area}(\mathcal{S})$ .

*Proof.* Let  $K$  be the iteration number in Theorem 1. By Theorems 4 and 5, our specification of  $N$  ensures that  $\mathbb{E}[\mathcal{L}_{\text{critic}}(w_k; \pi_k)] \leq C^2 \gamma_\rho^{2(k+1)}$  and  $\mathbb{E}[\mathcal{L}_{\text{actor}}(\theta_{k+1}; \theta_k, w_k)] \leq (1 - \gamma_\rho)^2$  for all  $k \leq K$ . Note that we have  $|\mathcal{A}|$  actions in total, and by Lemma 6, each sample requires  $O(\frac{1}{1-\gamma})$  oracle calls. As a result, the overall sample complexity is

$$O\left(\frac{KN|\mathcal{A}|}{1-\gamma}\right) = \tilde{O}\left(\frac{1}{\log \frac{1}{\gamma_\rho}} \kappa^{\frac{2d}{\alpha} + 4} C_\nu^{\frac{d}{2\alpha} + 1} |\mathcal{A}|^{\frac{d}{2\alpha} + 2} C_\alpha^{\frac{d}{\alpha} + 2} (1-\gamma)^{-\frac{4d}{\alpha} - 9} \epsilon^{-\frac{d}{\alpha} - 2}\right)$$

$$\leq \tilde{O}\left(\kappa^{\frac{2d}{\alpha} + 5} C_\nu^{\frac{d}{2\alpha} + 1} |\mathcal{A}|^{\frac{d}{2\alpha} + 2} C_\alpha^{\frac{d}{\alpha} + 2} (1-\gamma)^{-\frac{4d}{\alpha} - 10} \epsilon^{-\frac{d}{\alpha} - 2}\right),$$

where the inequality uses  $\frac{1}{\log \frac{1}{\gamma_\rho}} \leq \frac{1}{1-\gamma_\rho} = \frac{\kappa}{1-\gamma}$ .  $\square$

Corollary 2 characterizes the expected number of oracle access to the environment for finding an  $\epsilon$ -optimal (in the sense of expected value function) policy  $\pi_K$ . The resulting sample complexity  $\tilde{O}\left(\kappa^{\frac{2d}{\alpha} + 5} C_\nu^{\frac{d}{2\alpha} + 1} |\mathcal{A}|^{\frac{d}{2\alpha} + 2} (1-\gamma)^{-\frac{4d}{\alpha} - 10} C_\alpha^{\frac{d}{\alpha} + 2} \epsilon^{-\frac{d}{\alpha} - 2}\right)$  has no exponential dependence on the data dimension  $D$ . In our assumption,  $d \ll D$ , thus the sample complexity does not suffer from the curse of dimensionality.



## 5 Conclusion and Discussion

We have derived the overall sample complexity for NPMD (Algorithm 1) on Lipschitz MDP with intrinsically low-dimensional state space  $\mathcal{S}$ . Our result gives a concrete characterization of the expected number of samples required for an  $\epsilon$ -optimal policy under mild regularity assumptions and shows no curse of dimensionality. We make a few remarks about this result.

**Tightness in  $\epsilon$ .** The sample complexity  $\tilde{O}(\epsilon^{-\frac{d}{\alpha}-2})$  can be interpreted as two parts. The first part  $\tilde{O}(\epsilon^{-2})$  comes from iterations of the NPMD algorithm and is optimal up to logarithm terms. It matches the complexity of PMD in tabular case (Lan, 2023) and NPG on linear MDP (Yuan et al., 2023). The second part  $\tilde{O}(\epsilon^{-\frac{d}{\alpha}})$  comes from function approximation on  $d$ -dimensional state space manifold. Intuitively, it matches the number of states  $|\mathcal{S}_{\text{dis}}|$  appeared in the complexity of tabular PMD if we discretize the continuous state space into a finite set of points  $\mathcal{S}_{\text{dis}} \subset \mathcal{S}$ .<sup>4</sup> This part scales with the intrinsic dimension  $d$  of  $\mathcal{S}$  and can be interpreted as the result of neural networks adapting to the low-dimensional state space geometry. It is yet to be examined whether the overall complexity is tight in  $\epsilon$ .

**Dependence on the cost function scale.** The sample complexity reasonably depends on  $C^{-1}\epsilon$ , which can be viewed as the relative error. Therefore, as long as  $\epsilon$  scales with the cost function, the term  $C^{\frac{d}{\alpha}+2}\epsilon^{-\frac{d}{\alpha}-2}$  in the complexity bound remains the same. Although the scaling of the cost function can still affect the hidden constant depending on  $\log L_Q = \log(L_c + \frac{\gamma C}{1-\gamma}L_P)$  and  $\log \frac{C}{1-\gamma}$ , it will not have a major impact since the dominating term is the normalized Lipschitz constant  $\bar{L}_Q$ , which is invariant to the scaling of the cost function.

**Distribution mismatch and concentrability.** The distribution mismatch coefficient  $\kappa$  in (23) and concentrability coefficient  $C_\nu$  in Assumption 3 have been widely used in the analysis of PMD-type methods in both the tabular setting (Xiao, 2022) and linear function approximation (Agarwal et al., 2021; Alfano and Rebeschini, 2022; Yuan et al., 2023). The mismatch coefficient  $\kappa$  occurs when the initial distribution  $\rho$  is different from the optimal visitation distribution  $\nu_\rho^{\pi^*}$ . When Assumption 2 does not hold, that is,  $\rho$  has no full support,  $\kappa$  can possibly be infinity, leading to a vacuous complexity bound. This mismatch coefficient is unavoidable even for the analysis of tabular PMD (Xiao, 2022) and can affect the iteration complexity through  $\gamma_\rho$  as shown in Theorem 1.

The concentrability coefficient  $C_\nu$  comes from the change of error measures. In the  $k$ -th iteration of NPMD, we cannot directly sample states from  $\nu_\rho^{\pi_{k+1}}$  or  $\nu_\rho^{\pi^*}$  because the corresponding policies  $\pi_{k+1}$  and  $\pi^*$  are not available yet. Instead, we sample states from  $\nu_\rho^{\pi_k}$  and solve the ERM subproblems with these samples. As a result, the actor and critic errors are naturally measured in  $\nu_\rho^{\pi_k}$ , and  $C_\nu$  comes in when measuring the errors in  $\nu_\rho^{\pi_{k+1}}$  and  $\nu_\rho^{\pi^*}$ , which are related to the performance difference between consecutive policies. The concentrability coefficient is unavoidable when we have function

---

<sup>4</sup>We note that directly performing discretization is difficult when  $\mathcal{S}$  has a complicated geometric structure.



approximation errors measured in the  $L^2$  norm. To remove  $C_\nu$ , one has to consider the exact PMD case where there is no function approximation at all or derive  $L^\infty$  error bounds for critic and actor updates, both are intractable for continuous state space.

As suggested in Yuan et al. (2023) for finite state space, both coefficients can be potentially improved if we decouple the sampling distribution in Algorithm 1 and the evaluation distribution in the policy optimization problem (1). Indeed, one can replace  $\rho$  in (1) by another distribution  $\rho'$ , and replace the initial distribution in Algorithm 2 by  $\rho$ . In this case, we can choose  $\rho'$  with full support to satisfy Assumption 2 and  $\kappa$  becomes  $\kappa' = \left\| \frac{d\nu_{\rho'}^{\pi^*}}{d\rho'} \right\|_\infty$ . The optimality gap can be translated as

$$V^{\pi_k}(\rho) - V^*(\rho) \leq \left\| \frac{d\rho}{d\rho'} \right\|_\infty (V^{\pi_k}(\rho') - V^*(\rho')).$$

Similarly, Assumption 3 can be replaced by

$$\chi^2(\nu_{\rho'}^\pi, \nu_{\rho'}^{\pi_k}) + 1 \leq C'_\nu$$

for some  $C'_\nu$ . However, we note that the pathological behavior of distribution mismatch and concentrability in the continuous state space is not always removable as it requires the Radon-Nikodym derivatives to exist, and it is difficult to ensure  $\kappa' < \kappa$  and  $C'_\nu < C_\nu$  for a better complexity. To the best of our knowledge, it remains an open problem to study function approximation policy gradient methods in continuous state space without Assumptions 2 and 3.

**Computational concerns.** In each iteration of Algorithm 1, there are two ERM subproblems with approximately Lipschitz constraints, which are assumed to be solvable. However, solving such problems is non-trivial due to the non-convex objectives and the approximately Lipschitz constraints. In practice, one can use gradient-based methods such as gradient descent (GD) and its variants to minimize the objectives, but little is known about their theoretical convergence behavior. Recently there has been some work studying the GD dynamics in the NTK or mean-field regime (Jacot et al., 2018; Song et al., 2018), but the gap remains as they cannot fully explain the global convergence behavior of GD-like methods, and their results cannot adapt to the low-dimensional manifold structure.

Meanwhile, there is no existing result on optimization with approximate Lipschitzness constraints. One can apply Lipschitz regularization methods, such as spectral regularization (Yoshida and Miyato, 2017; Gogianu et al., 2021), gradient regularization (Gulrajani et al., 2017), projected gradient descent for Lipschitz constant constraint (Gouk et al., 2021), and adversarial training (Miyato et al., 2018). Most of these techniques are heuristic, so they cannot exactly control the Lipschitzness of networks. Nevertheless, they could result in approximately Lipschitz networks as it is a relaxed condition. We leave the study of approximately Lipschitz-constrained optimization of neural networks for future work.

**Overparameterization.** In modern deep learning practice, there exists a propensity to employ overparameterized models that have more parameters than the number of data. Our current analysis is based on the classical bias-variance trade-off argument and cannot handle the overparameterization case. Recently, [Zhang and Wang \(2022\)](#) have established deep non-parametric regression results that apply to overparameterized models, but their work does not exploit the low-dimensional structure. It is an interesting future direction to examine if their work can be extended to the manifold setting and fit into our analysis. We expect it to close the theory-practice gap in DRL further.

**Comparison with value-based methods.** The sample complexity we derive for NPMD matches the bound for the value-based FQI method in [Fan et al. \(2020\)](#) when  $d = D$ , while our result is significantly better when the intrinsic dimension  $d \ll D$ . This shows that policy-based methods can achieve as good performance as value-based methods in theory. From a technical perspective, value-based methods only have smooth value functions (under the Bellman closedness assumption ([Fan et al., 2020](#); [Nguyen-Tang et al., 2022](#))) to approximate. On the other hand, policy-based methods require repetitively approximating new policies, whose Lipschitz constant will accumulate. We address the issue by introducing the notion of approximate Lipschitzness, imposing approximately Lipschitz constraints on the neural networks, and establishing approximation theory for them. Our analysis framework can be applied to more general scenarios where there is iterative refitting of neural networks.

**Beyond Lipschitz MDP.** In this paper, we work on Lipschitz MDP (Assumption 4). In practice, the MDP can be either smoother or not as smooth as Lipschitz MDP. For the former case, one can have Hölder smooth MDP with higher exponent, namely  $\alpha > 1$ , and expect there is a better sample complexity. If we only consider the policy evaluation and value-based algorithms, where the target value function is smooth, then this is possible as suggested by the results from deep supervised learning ([Chen et al., 2022](#)). However, for policy-based methods, it is unclear whether neural networks that approximate Hölder function can have smoothness beyond approximate Lipschitzness. It is a future direction to examine the sample complexity of policy-based methods in smooth MDP. For the latter case, one can consider extending the Lipschitz condition to the more general Sobolev or Besov conditions to deal with spatial inhomogeneity in smoothness. Also, as mentioned in Remarks 4 and 5, one can use a smooth approximation of the non-smooth MDP as a surrogate in this case.

## Acknowledgement

We thank Yan Li for the discussion in the early stage of this work.

## References

- AGARWAL, A., HENAFF, M., KAKADE, S. and SUN, W. (2020). Pc-pg: Policy cover directed exploration for provable policy gradient learning. *Advances in Neural Information Processing Systems*, **33** 13399–13412.
- AGARWAL, A., KAKADE, S. M., LEE, J. D. and MAHAJAN, G. (2021). On the theory of policy gradient methods: Optimality, approximation, and distribution shift. *The Journal of Machine Learning Research*, **22** 4431–4506.
- ALFANO, C. and REBESCHINI, P. (2022). Linear convergence for natural policy gradient with log-linear policy parametrization. *arXiv preprint arXiv:2209.15382*.
- ALFANO, C., YUAN, R. and REBESCHINI, P. (2023). A novel framework for policy mirror descent with general parametrization and linear convergence. *arXiv preprint arXiv:2301.13139*.
- BACH, F. (2017). Breaking the curse of dimensionality with convex neural networks. *The Journal of Machine Learning Research*, **18** 629–681.
- BERNER, C., BROCKMAN, G., CHAN, B., CHEUNG, V., DEBIAK, P., DENNISON, C., FARHI, D., FISCHER, Q., HASHME, S., HESSE, C. ET AL. (2019). Dota 2 with large scale deep reinforcement learning. *arXiv preprint arXiv:1912.06680*.
- BROCKMAN, G., CHEUNG, V., PETTERSSON, L., SCHNEIDER, J., SCHULMAN, J., TANG, J. and ZAREMBA, W. (2016). Openai gym. *arXiv preprint arXiv:1606.01540*.
- CHEN, L. and XU, S. (2020). Deep neural tangent kernel and laplace kernel have the same rkhs. *arXiv preprint arXiv:2009.10683*.
- CHEN, M., JIANG, H., LIAO, W. and ZHAO, T. (2019). Efficient approximation of deep relu networks for functions on low dimensional manifolds. *Advances in Neural Information Processing Systems*, **32**.
- CHEN, M., JIANG, H., LIAO, W. and ZHAO, T. (2022). Nonparametric regression on low-dimensional manifolds using deep relu networks: Function approximation and statistical recovery. *Information and Inference: A Journal of the IMA*, **11** 1203–1253.
- CONWAY, J. H. and SLOANE, N. J. A. (1988). *Sphere Packings, Lattices and Groups*, vol. 290. Springer.
- DO CARMO, M. P. and FLAHERTY FRANCIS, J. (1992). *Riemannian Geometry*, vol. 6. Springer.
- DU, S. S., KAKADE, S. M., WANG, R. and YANG, L. F. (2020). Is a good representation sufficient for sample efficient reinforcement learning? In *International Conference on Learning Representations*.

- FAN, J., WANG, Z., XIE, Y. and YANG, Z. (2020). A theoretical analysis of deep q-learning. In *Learning for Dynamics and Control*. PMLR.
- FEDERER, H. (1959). Curvature measures. *Transactions of the American Mathematical Society*, **93** 418–491.
- GEIST, M., SCHERRER, B. and PIETQUIN, O. (2019). A theory of regularized markov decision processes. In *International Conference on Machine Learning*. PMLR.
- GOGIANU, F., BERARIU, T., ROSCA, M. C., CLOPATH, C., BUSONIU, L. and PASCANU, R. (2021). Spectral normalisation for deep reinforcement learning: an optimisation perspective. In *International Conference on Machine Learning*. PMLR.
- GOUK, H., FRANK, E., PFAHRINGER, B. and CREE, M. J. (2021). Regularisation of neural networks by enforcing lipschitz continuity. *Machine Learning*, **110** 393–416.
- GRONDMAN, I., BUSONIU, L., LOPES, G. A. and BABUSKA, R. (2012). A survey of actor-critic reinforcement learning: Standard and natural policy gradients. *IEEE Transactions on Systems, Man, and Cybernetics, Part C (Applications and Reviews)*, **42** 1291–1307.
- GULRAJANI, I., AHMED, F., ARJOVSKY, M., DUMOULIN, V. and COURVILLE, A. C. (2017). Improved training of wasserstein gans. *Advances in neural information processing systems*, **30**.
- HSU, D., SANFORD, C. H., SERVEDIO, R. and VLATAKIS-GKARAGKOUNIS, E. V. (2021). On the approximation power of two-layer networks of random relus. In *Conference on Learning Theory*. PMLR.
- HUANG, K., WANG, Y., TAO, M. and ZHAO, T. (2020). Why do deep residual networks generalize better than deep feedforward networks?—a neural tangent kernel perspective. *Advances in Neural Information Processing Systems*, **33** 2698–2709.
- JACOT, A., GABRIEL, F. and HONGLER, C. (2018). Neural tangent kernel: Convergence and generalization in neural networks. *Advances in Neural Information Processing Systems*, **31**.
- JI, X., CHEN, M., WANG, M. and ZHAO, T. (2022). Sample complexity of nonparametric off-policy evaluation on low-dimensional manifolds using deep networks. *arXiv preprint arXiv:2206.02887*.
- JIN, C., YANG, Z., WANG, Z. and JORDAN, M. I. (2020). Provably efficient reinforcement learning with linear function approximation. In *Conference on Learning Theory*. PMLR.
- KAKADE, S. M. (2001). A natural policy gradient. *Advances in Neural Information Processing Systems*, **14**.
- KONDA, V. and TSITSIKLIS, J. (1999). Actor-critic algorithms. *Advances in Neural Information Processing Systems*, **12**.

- LAN, G. (2022). Policy optimization over general state and action spaces. *arXiv preprint arXiv:2211.16715*.
- LAN, G. (2023). Policy mirror descent for reinforcement learning: Linear convergence, new sampling complexity, and generalized problem classes. *Mathematical programming*, **198** 1059–1106.
- LILICRAP, T. P., HUNT, J. J., PRITZEL, A., HEESS, N., EREZ, T., TASSA, Y., SILVER, D. and WIERSTRA, D. (2015). Continuous control with deep reinforcement learning. *arXiv preprint arXiv:1509.02971*.
- LIU, B., CAI, Q., YANG, Z. and WANG, Z. (2019). Neural proximal/trust region policy optimization attains globally optimal policy. *Advances in Neural Information Processing Systems*, **32**.
- LIU, H., CHEN, M., ER, S., LIAO, W., ZHANG, T. and ZHAO, T. (2022). Benefits of overparameterized convolutional residual networks: Function approximation under smoothness constraint. In *International Conference on Machine Learning*. PMLR.
- LIU, H., CHEN, M., ZHAO, T. and LIAO, W. (2021). Besov function approximation and binary classification on low-dimensional manifolds using convolutional residual networks. In *International Conference on Machine Learning*. PMLR.
- MİYATO, T., MAEDA, S.-I., KOYAMA, M. and ISHII, S. (2018). Virtual adversarial training: a regularization method for supervised and semi-supervised learning. *IEEE transactions on pattern analysis and machine intelligence*, **41** 1979–1993.
- MNIH, V., BADIA, A. P., MIRZA, M., GRAVES, A., LILICRAP, T., HARLEY, T., SILVER, D. and KAVUKCUOGLU, K. (2016). Asynchronous methods for deep reinforcement learning. In *International conference on machine learning*. PMLR.
- MNIH, V., KAVUKCUOGLU, K., SILVER, D., GRAVES, A., ANTONOGLU, I., WIERSTRA, D. and RIEDMILLER, M. (2013). Playing atari with deep reinforcement learning. *arXiv preprint arXiv:1312.5602*.
- NGUYEN-TANG, T., GUPTA, S., TRAN-THE, H. and VENKATESH, S. (2022). On sample complexity of offline reinforcement learning with deep reLU networks in besov spaces. *Transactions of Machine Learning Research*.  
<https://openreview.net/forum?id=LdEmOumNcv>
- NIYOGI, P., SMALE, S. and WEINBERGER, S. (2008). Finding the homology of submanifolds with high confidence from random samples. *Discrete & Computational Geometry*, **39** 419–441.
- ONO, K. and SUZUKI, T. (2019). Approximation and non-parametric estimation of resnet-type convolutional neural networks. In *International conference on machine learning*. PMLR.

- OPENAI (2023). Gpt-4 technical report. *arXiv preprint arXiv:2303.08774*.
- OUYANG, L., WU, J., JIANG, X., ALMEIDA, D., WAINWRIGHT, C., MISHKIN, P., ZHANG, C., AGARWAL, S., SLAMA, K., RAY, A. ET AL. (2022). Training language models to follow instructions with human feedback. *Advances in Neural Information Processing Systems*, **35** 27730–27744.
- PUTERMAN, M. L. (1994). *Markov Decision Processes: Discrete Stochastic Dynamic Programming*. John Wiley & Sons.
- RAHIMI, A. and RECHT, B. (2007). Random features for large-scale kernel machines. *Advances in Neural Information Processing Systems*, **20**.
- SCHMIDT-HIEBER, J. (2019). Deep relu network approximation of functions on a manifold. *arXiv preprint arXiv:1908.00695*.
- SCHULMAN, J., LEVINE, S., ABBEEL, P., JORDAN, M. and MORITZ, P. (2015). Trust region policy optimization. In *International conference on machine learning*. PMLR.
- SCHULMAN, J., WOLSKI, F., DHARIWAL, P., RADFORD, A. and KLIMOV, O. (2017). Proximal policy optimization algorithms. *arXiv preprint arXiv:1707.06347*.
- SHANI, L., EFRONI, Y. and MANNOR, S. (2020). Adaptive trust region policy optimization: Global convergence and faster rates for regularized mdps. In *Proceedings of the AAAI Conference on Artificial Intelligence*, vol. 34(04).
- SONG, M., MONTANARI, A. and NGUYEN, P. (2018). A mean field view of the landscape of two-layers neural networks. *Proceedings of the National Academy of Sciences*, **115** E7665–E7671.
- SUTTON, R. S., MCALLESTER, D., SINGH, S. and MANSOUR, Y. (1999). Policy gradient methods for reinforcement learning with function approximation. *Advances in Neural Information Processing Systems*, **12**.
- TODOROV, E., EREZ, T. and TASSA, Y. (2012). Mujoco: A physics engine for model-based control. In *IEEE/RSJ International Conference on Intelligent Robots and Systems*. IEEE.
- TOMAR, M., SHANI, L., EFRONI, Y. and GHAVAMZADEH, M. (2020). Mirror descent policy optimization. *arXiv preprint arXiv:2005.09814*.
- WANG, L., CAI, Q., YANG, Z. and WANG, Z. (2019). Neural policy gradient methods: Global optimality and rates of convergence. In *International Conference on Learning Representations*.
- WILLIAMS, R. J. (1992). Simple statistical gradient-following algorithms for connectionist reinforcement learning. *Reinforcement learning* 5–32.
- XIAO, L. (2022). On the convergence rates of policy gradient methods. *Journal of Machine Learning Research*, **23** 1–36.

- XIE, T., CHENG, C.-A., JIANG, N., MINEIRO, P. and AGARWAL, A. (2021). Bellman-consistent pessimism for offline reinforcement learning. *Advances in Neural Information Processing Systems*, **34** 6683–6694.
- YANG, Z., JIN, C., WANG, Z., WANG, M. and JORDAN, M. (2020). Provably efficient reinforcement learning with kernel and neural function approximations. *Advances in Neural Information Processing Systems*, **33** 13903–13916.
- YAROTSKY, D. (2017). Error bounds for approximations with deep relu networks. *Neural Networks*, **94** 103–114.
- YEHUDAI, G. and SHAMIR, O. (2019). On the power and limitations of random features for understanding neural networks. *Advances in Neural Information Processing Systems*, **32**.
- YIN, M., WANG, M. and WANG, Y.-X. (2022). Offline reinforcement learning with differentiable function approximation is provably efficient. *arXiv preprint arXiv:2210.00750*.
- YOSHIDA, Y. and MIYATO, T. (2017). Spectral norm regularization for improving the generalizability of deep learning. *arXiv preprint arXiv:1705.10941*.
- YUAN, R., DU, S. S., GOWER, R. M., LAZARIC, A. and XIAO, L. (2023). Linear convergence of natural policy gradient methods with log-linear policies. In *International Conference on Learning Representations*.
- ZHANG, K. and WANG, Y.-X. (2022). Deep learning meets nonparametric regression: Are weight-decayed dnns locally adaptive? In *International Conference on Learning Representations*.
- ZIEGLER, D. M., STIENNON, N., WU, J., BROWN, T. B., RADFORD, A., AMODEI, D., CHRISTIANO, P. and IRVING, G. (2019). Fine-tuning language models from human preferences. *arXiv preprint arXiv:1909.08593*.

## A Algorithms

This section presents the missing sampling algorithm (Algorithm 2) for Algorithm 1, along with some auxiliary results related to the algorithms.

---

**Algorithm 2:** Sampling  $s \sim \nu_\rho^\pi$  or  $(s, a) \sim \bar{\nu}_\rho^\pi$

---

**Input:** Distribution  $\rho$ , policy  $\pi$ , factor  $\gamma \in (0, 1)$   
Initialize  $flag = true$ ,  $t = 0$ ,  $s_0 \sim \rho$ ,  $a_0 \sim \pi(\cdot|s_0)$ ;  
**while**  $flag$  is true **do**  
    Sample  $p \sim \text{Unif}([0, 1])$ ;  
    **if**  $p \leq \gamma$  **then**  
        Sample  $s_{t+1} \sim \mathcal{P}(\cdot|s_t, a_t)$ ;  
        Sample  $a_{t+1} \sim \pi(\cdot|s_{t+1})$ ;  
         $t \leftarrow t + 1$ ;  
    **else**  
         $flag = false$ ;  
    **end**  
**end**  
**Output:**  $s_t$  as  $s$  or  $(s_t, a_t)$  as  $(s, a)$

---

### A.1 Sample Complexity of Algorithm 2

We compute the expected number of sample oracle calls of Algorithm 2.

**Lemma 6.** *Algorithm 2 returns  $(s, a) \sim \bar{\nu}_\rho^\pi$ , and the expected number of sample oracle calls for each pair of  $(s, a)$  is  $\frac{1}{1-\gamma}$ .*

*Proof.* Let  $T$  be the terminating time (trajectory length) of Algorithm 2, which has probability

$$\mathbb{P}(T = t) = \gamma^t(1 - \gamma).$$

The probability distribution of the output  $s_t$  is then given by

$$\mathcal{P}_{\text{out}} = \sum_{t=0}^{\infty} \mathcal{P}_t^\pi \cdot \mathbb{P}(T = t) = \sum_{t=0}^{\infty} \mathcal{P}_t^\pi \cdot \gamma^t(1 - \gamma),$$

which is exactly  $\nu_\rho^\pi$  according to (6). Since  $\mathbb{P}(a_t = a|s_t) = \pi(a|s_t)$ , we have  $(s, a) \sim \bar{\nu}_\rho^\pi$ . The expected number of sample oracle calls is  $\mathbb{E}[T + 1]$ , which is

$$\mathbb{E}[T + 1] = \sum_{t=0}^{\infty} (t + 1)\gamma^t(1 - \gamma) = \frac{1}{1 - \gamma}.$$

The expected trajectory length  $\frac{1}{1-\gamma}$  is also called the *effective horizon*. □



## A.2 Critic Loss Translation

The critic loss can be translated to the mean squared error (MSE) with respect to the Bayes estimator. Recall the state-action value function of the form (10):

$$Q^\pi(s, a) = c(s, a) + \frac{\gamma}{1 - \gamma} \mathbb{E}_{(s', a') \sim \bar{\nu}_{\mathcal{P}(\cdot|s, a)}^\pi} [c(s', a')].$$

For any fixed  $a \in \mathcal{A}$  and  $k \geq 0$ , let  $X \sim \nu_\rho^{\pi^k}$  be a random variable on  $\mathcal{S}$  and  $Z = (S, A)$  be another random variable with conditional distribution  $p_{Z|X} = \bar{\nu}_{\mathcal{P}(\cdot|X, a)}^{\pi^k}$ . We define

$$Y = c(X, a) + \frac{\gamma}{1 - \gamma} c(S, A)$$

as the target. Reformulating (10) gives

$$Y = Q^{\pi^k}(X, a) + \zeta,$$

where

$$\zeta = \frac{\gamma}{1 - \gamma} \left( c(S, A) - \mathbb{E}_{(s', a') \sim \bar{\nu}_{\mathcal{P}(\cdot|X, a)}^{\pi^k}} [c(s', a')] \right) \quad (30)$$

is a random variable. We can verify several properties of the noise term  $\zeta$ .

**Lemma 7.** *The noise term  $\zeta$  defined in (30) is a zero-mean sub-Gaussian random variable with variance proxy  $\sigma^2 = \frac{\gamma^2 C^2}{4(1-\gamma)^2}$  and is uncorrelated with  $X$ .*

*Proof.* By direct computation, we show that  $\zeta$  is zero-mean:

$$\begin{aligned} \mathbb{E}[\zeta] &= \frac{\gamma}{1 - \gamma} \mathbb{E}_{X, Z} \left[ c(S, A) - \mathbb{E}_{(s', a') \sim \bar{\nu}_{\mathcal{P}(\cdot|X, a)}^{\pi^k}} [c(s', a')] \right] \\ &= \frac{\gamma}{1 - \gamma} \mathbb{E}_X \left[ \mathbb{E}_{Z|X} [c(S, A)] - \mathbb{E}_{(s', a') \sim \bar{\nu}_{\mathcal{P}(\cdot|X, a)}^{\pi^k}} [c(s', a')] \right] \\ &= \frac{\gamma}{1 - \gamma} \mathbb{E}_X [0] \\ &= 0. \end{aligned}$$

By (2) we know that given any realization of  $X$ ,

$$\frac{-\gamma\mu}{1 - \gamma} \leq \zeta \leq \frac{\gamma(C - \mu)}{1 - \gamma},$$

where  $\mu = \mathbb{E}_{Z|X} [c(S, A)]$ , thus  $\zeta$  is sub-Gaussian with variance proxy  $\sigma^2 = \frac{\gamma^2 C^2}{4(1-\gamma)^2}$ . Since

$$\mathbb{E}[X \cdot \zeta] = \mathbb{E}[\mathbb{E}[X \cdot \zeta | X]] = \mathbb{E}[X \cdot \mathbb{E}[\zeta | X]] = \mathbb{E}[X \cdot 0] = 0 = \mathbb{E}[X] \cdot \mathbb{E}[\zeta],$$

we conclude that  $\zeta$  is uncorrelated with  $X$ . □

The Bayes estimator  $m_a: \mathcal{S} \rightarrow \mathbb{R}$  to predict  $Y$  with  $X$  satisfies

$$\begin{aligned} m_a(x) &:= \mathbb{E}[Y|X = x] \\ &= \mathbb{E}[Q^{\pi_k}(X, a) + \zeta|X = x] \\ &= Q^{\pi_k}(x, a). \end{aligned}$$

As a result, we have

$$\mathbb{E}_X [|Q_{w_k}(X, a) - m_a(X)|^2] = \mathbb{E}_{s \sim \nu_\rho^{\pi_k}} [|Q_{w_k}(s, a) - Q^{\pi_k}(s, a)|^2].$$

It follows immediately from (14) that

$$\begin{aligned} \mathbb{E} [\mathcal{L}_{\text{critic}}(w_k; \pi_k)] &= \mathbb{E} \left[ \mathbb{E}_{s \sim \nu_\rho^{\pi_k}} \|Q_{w_k}(s, a) - Q^{\pi_k}(s, a)\|_2^2 \right] \\ &= \mathbb{E} \left[ \mathbb{E}_{s \sim \nu_\rho^{\pi_k}} \sum_{a \in \mathcal{A}} |Q_{w_k}(s, a) - Q^{\pi_k}(s, a)|^2 \right] \\ &\leq |\mathcal{A}| \max_{a \in \mathcal{A}} \mathbb{E} \left[ \mathbb{E}_X [|Q_{w_k}(X, a) - m_a(X)|^2] \right], \end{aligned} \quad (31)$$

where the outer expectation is taken with respect to the estimated  $w_k$ , which depends on the samples used for ERM. Therefore, the critic loss of  $Q_{w_k}$  can be upper bounded as long as we can bound the MSE of  $Q_{w_k}(\cdot, a)$  for every  $a \in \mathcal{A}$ .

### A.3 Actor Loss Translation

The actor loss can also be translated. We already know the exact solution to (17) is given by  $g_{k+1}^*$  defined in Lemma 1. The actor loss is thus translated into the error between the estimated function  $f_{\theta_{k+1}}$  and the ground truth function  $\lambda_{k+1}g_{k+1}$ :

$$\begin{aligned} &\mathbb{E} [\mathcal{L}_{\text{actor}}(\theta_{k+1}; \theta_k, w_k)] \\ &= \mathbb{E} \left[ \mathbb{E}_{s \sim \nu_\rho^{\pi_k}} \left\| \lambda_{k+1}^{-1} f_{\theta_{k+1}}(s, \cdot) - (1 - \eta_k \tau_k) \lambda_k^{-1} f_\theta(s, \cdot) + \eta_k Q_{w_k}(s, \cdot) \right\|_2^2 \right] \\ &= \mathbb{E} \left[ \mathbb{E}_{s \sim \nu_\rho^{\pi_k}} \sum_{a \in \mathcal{A}} \left| \lambda_{k+1}^{-1} f_{\theta_{k+1}}(s, a) - (1 - \eta_k \tau_k) \lambda_k^{-1} f_\theta(s, a) + \eta_k Q_{w_k}(s, a) \right|^2 \right] \\ &\leq \frac{|\mathcal{A}|}{\lambda_{k+1}^2} \max_{a \in \mathcal{A}} \mathbb{E} \left[ \mathbb{E}_{s \sim \nu_\rho^{\pi_k}} \left| f_{\theta_{k+1}}(s, a) - \frac{\lambda_{k+1}}{\lambda_k} (1 - \eta_k \tau_k) f_\theta(s, a) + \lambda_{k+1} \eta_k Q_{w_k}(s, a) \right|^2 \right], \end{aligned} \quad (32)$$

where the outer expectation is taken with respect to  $\theta_{k+1}$ , which depends on the samples used for empirical risk minimization. Once we derive an upper bound for the expected error of  $f_{\theta_{k+1}}$ , an upper bound for the actor update loss follows immediately.

## B Missing Proofs in Section 3

### B.1 Proof of Lemma 1

*Proof.* For any  $s \in \mathcal{S}$ , the Karush-Kuhn-Tucker condition of (17) yields

$$Q_{w_k}(s, \cdot) + \left( \tau_k - \frac{1}{\eta_k} \right) \log \pi_k(s, \cdot) + \frac{1}{\eta_k} \log \pi_{k+1}^*(s, \cdot) + (\mu_s^* + \tau_k) \mathbf{1} = 0$$

for some  $\mu_s^* \in \mathbb{R}$ , where we denote  $\pi_{k+1}^*$  as the solution. This means for any  $s \in \mathcal{S}$ ,

$$\pi_{k+1}^*(a|s) \propto \exp((1 - \eta_k \tau_k) \log \pi_k(a|s) - \eta_k Q_{w_k}(s, a)).$$

By definition (18), we have

$$\log \pi_k(a|s) = \lambda_k^{-1} f_{\theta_k}(s, a) - \log \sum_{a' \in \mathcal{A}} \exp(\lambda_k^{-1} f_{\theta_k}(s, a')).$$

Since  $\pi_{k+1}^*(\cdot|s)$  is shift-invariant with  $g_{k+1}^*(s, \cdot)$  for any  $s$ , that is,

$$\pi_{k+1}^*(a|s) = \frac{\exp(g_{k+1}^*(s, a)) \exp(p(s))}{\sum_{a' \in \mathcal{A}} \exp(g_{k+1}^*(s, a')) \exp(p(s))} = \frac{\exp(g_{k+1}^*(s, a) + p(s))}{\sum_{a' \in \mathcal{A}} \exp(g_{k+1}^*(s, a') + p(s))}$$

for any  $p(s)$  invariant to  $a$ , choosing  $g_{k+1}^* = (1 - \eta_k \tau_k) \lambda_k^{-1} f_{\theta_k} - \eta_k Q_{w_k}$  suffices.  $\square$

## C Missing Proofs for Iteration Complexity

In this section, we present the missing proofs in Section 4.1 and auxiliary lemmas for them.

### C.1 Supporting Lemmas for Iteration Complexity

We first introduce the performance difference lemma for the value function, which measures the difference between value functions under different policies.

**Lemma 8** (Performance difference lemma). *For any pair of policies  $\pi$  and  $\pi'$  and any state  $s$ , we have*

$$V^{\pi'}(\rho) - V^\pi(\rho) = \frac{1}{1 - \gamma} \mathbb{E}_{s \sim \nu_{\rho}^{\pi'}} [\langle Q^\pi(s, \cdot), \pi'(\cdot|s) - \pi(\cdot|s) \rangle ].$$

*Proof.* The performance difference is between  $\pi'$  and  $\pi$  is given by

$$\begin{aligned}
& V^{\pi'}(\rho) - V^\pi(\rho) \\
&= V^{\pi'}(\mathcal{P}_0^{\pi'}) - V^\pi(\mathcal{P}_0^{\pi'}) \\
&= \mathbb{E}_{s \sim \mathcal{P}_0^{\pi'}} \sum_{a \in \mathcal{A}} \left( c(s, a) (\pi'(a|s) - \pi(a|s)) + \gamma \int_{\mathcal{S}} \left( V^{\pi'}(s') \pi'(a|s) - V^\pi(s') \pi(a|s) \right) d\mathcal{P}(s'|s, a) \right) \\
&= \mathbb{E}_{s \sim \mathcal{P}_0^{\pi'}} \sum_{a \in \mathcal{A}} \left( c(s, a) + \gamma \int_{\mathcal{S}} V^\pi(s') d\mathcal{P}(s'|s, a) \right) (\pi'(a|s) - \pi(a|s)) \\
&\quad + \gamma \mathbb{E}_{s \sim \mathcal{P}_0^{\pi'}} \sum_{a \in \mathcal{A}} \pi'(a|s) \int_{\mathcal{S}} \left( V^{\pi'}(s') - V^\pi(s') \right) d\mathcal{P}(s'|s, a) \\
&= \mathbb{E}_{s \sim \mathcal{P}_0^{\pi'}} \langle Q^\pi(s, \cdot), \pi'(\cdot|s) - \pi(\cdot|s) \rangle + \gamma \mathbb{E}_{s \sim \mathcal{P}_0^{\pi'}, a \sim \pi'(\cdot|s)} \int_{\mathcal{S}} \left( V^{\pi'}(s') - V^\pi(s') \right) d\mathcal{P}(s'|s, a) \\
&= \mathbb{E}_{s \sim \mathcal{P}_0^{\pi'}} \langle Q^\pi(s, \cdot), \pi'(\cdot|s) - \pi(\cdot|s) \rangle + \gamma \left( V^{\pi'}(\mathcal{P}_1^{\pi'}) - V^\pi(\mathcal{P}_1^{\pi'}) \right) \\
&= \sum_{t=0}^{\infty} \gamma^t \mathbb{E}_{s \sim \mathcal{P}_t^{\pi'}} \langle Q^\pi(s, \cdot), \pi'(\cdot|s) - \pi(\cdot|s) \rangle.
\end{aligned}$$

The first equality uses  $\mathcal{P}_0^{\pi'} \equiv \rho$ . The second equality is from (3) and (4). The fourth equality is from the opposite direction of (4). The last two lines are from the recursion (5) and the sequence converges because the value functions are bounded by (2). Plugging in the definition of visitation distribution completes the proof.  $\square$

Next, we derive an approximate variational inequality (VI) to establish iteration complexity for Algorithm 1 with assumptions on the approximation error. We write it in the form of an equation with a bounded error term.

**Lemma 9.** *If  $1 - \eta_k \tau_k \geq 0$ , then Algorithm 1 yields  $\pi_k$  and  $\pi_{k+1}$  such that for any policy  $\pi$ ,*

$$\begin{aligned}
V^\pi(\rho) - V^{\pi_k}(\rho) &= \frac{\tau_k}{1 - \gamma} \mathbb{E}_{s \sim \nu_\rho^\pi} [h^{\pi_k}(s) - h^\pi(s)] + \frac{2}{(1 - \gamma)\eta_k} \zeta_k \\
&\quad + \frac{1}{(1 - \gamma)\eta_k} \mathbb{E}_{s \sim \nu_\rho^\pi} \left[ \left( D_{\pi_{k+1}}^\pi(s) - D_{\pi_{k+1}}^{\pi_k}(s) \right) - (1 - \eta_k \tau_k) D_{\pi_k}^\pi(s) \right],
\end{aligned}$$

where  $\zeta_k$  is a remainder satisfying

$$|\zeta_k| \leq \mathbb{E}_{s \sim \nu_\rho^\pi} \left\| \lambda_{k+1}^{-1} f_{\theta_{k+1}}(s, \cdot) - (1 - \eta_k \tau_k) \lambda_k^{-1} f_{\theta_k}(s, \cdot) + \eta_k Q^{\pi_k}(s, \cdot) \right\|_\infty.$$

*Proof.* By Lemma 8, we have

$$V^\pi(\rho) - V^{\pi_k}(\rho) = \frac{1}{1 - \gamma} \mathbb{E}_{s \sim \nu_\rho^\pi} [\langle Q^{\pi_k}(s, \cdot), \pi(\cdot|s) - \pi_k(\cdot|s) \rangle].$$

By definition of  $\pi_k$  and  $\pi_{k+1}$ , we have

$$\begin{aligned}
& \langle Q^{\pi_k}(s, \cdot), \pi(\cdot|s) - \pi_k(\cdot|s) \rangle \\
&= \frac{1}{\eta_k} \underbrace{\langle (1 - \eta_k \tau_k) \log \pi_k(s, \cdot) - \log \pi_{k+1}(s, \cdot), \pi(\cdot|s) - \pi_k(\cdot|s) \rangle}_{T_1(s)} \\
&\quad + \frac{1}{\eta_k} \underbrace{\langle \lambda_{k+1}^{-1} f_{\theta_{k+1}}(s, \cdot) - (1 - \eta_k \tau_k) \lambda_k^{-1} f_{\theta_k}(s, \cdot) + \eta_k Q^{\pi_k}(s, \cdot), \pi(\cdot|s) - \pi_k(\cdot|s) \rangle}_{T_2(s)},
\end{aligned}$$

where the equality comes from that  $\log \sum_{a \in \mathcal{A}} \exp(\lambda_k^{-1} f_{\theta_k}(s, a))$  only depends on  $s$  and  $\langle \mathbf{1}, \pi(\cdot|s) - \pi_k(\cdot|s) \rangle = 1 - 1 = 0$ .

By the three-point lemma of KL divergence, we have

$$\begin{aligned}
T_1(s) &= \frac{1}{\eta_k} \langle \log \pi_k(s, \cdot) - \log \pi_{k+1}(s, \cdot), \pi(\cdot|s) - \pi_k(\cdot|s) \rangle \\
&\quad + \tau_k \langle -\log \pi_k(s, \cdot), \pi(\cdot|s) - \pi_k(\cdot|s) \rangle \\
&= \frac{1}{\eta_k} \left( D_{\pi_{k+1}}^{\pi}(s) - D_{\pi_k}^{\pi}(s) - D_{\pi_{k+1}}^{\pi_k}(s) \right) \\
&\quad + \tau_k \left( D_{\pi_k}^{\pi}(s) + h^{\pi_k}(s) - h^{\pi}(s) \right) \\
&= \tau_k \left( h^{\pi_k}(s) - h^{\pi}(s) \right) + \frac{1}{\eta_k} \left( D_{\pi_{k+1}}^{\pi}(s) - D_{\pi_{k+1}}^{\pi_k}(s) \right) - \frac{1 - \eta_k \tau_k}{\eta_k} D_{\pi_k}^{\pi}(s).
\end{aligned}$$

Denote  $\delta_k = \lambda_{k+1}^{-1} f_{\theta_{k+1}} - (1 - \eta_k \tau_k) \lambda_k^{-1} f_{\theta_k} + \eta_k Q^{\pi_k}$ . By Cauchy-Schwarz inequality, we have

$$\begin{aligned}
\left| \mathbb{E}_{s \sim \nu_{\rho}^{\pi}} [T_2(s)] \right| &\leq \frac{1}{\eta_k} \mathbb{E}_{s \sim \nu_{\rho}^{\pi}} |\langle \delta_k(s, \cdot), \pi(\cdot|s) - \pi_k(\cdot|s) \rangle| \\
&\leq \frac{1}{\eta_k} \mathbb{E}_{s \sim \nu_{\rho}^{\pi}} \|\delta_k(s, \cdot)\|_{\infty} \|\pi(\cdot|s) - \pi_k(\cdot|s)\|_1 \\
&\leq \frac{2}{\eta_k} \mathbb{E}_{s \sim \nu_{\rho}^{\pi}} \|\delta_k(s, \cdot)\|_{\infty}.
\end{aligned}$$

Combining the equality for  $T_1(s)$  and the inequality for  $T_2(s)$ , we obtain the result.  $\square$

With the approximate VI established, the one-step error bound for NPMD (Lemma 2) follows immediately.

## C.2 Proof of Lemma 2

*Proof.* Let  $\delta_k = \lambda_{k+1}^{-1} f_{\theta_{k+1}} - (1 - \eta_k \tau_k) \lambda_k^{-1} f_{\theta_k} + \eta_k Q^{\pi_k}$ . By plugging  $\pi = \pi_{k+1}$  in Lemma 9, we obtain

$$\begin{aligned}
& V^{\pi_{k+1}}(\rho) - V^{\pi_k}(\rho) \\
& \leq \frac{\tau_k}{1 - \gamma} \mathbb{E}_{s \sim \nu_\rho^{\pi_{k+1}}} [h^{\pi_k}(s) - h^{\pi_{k+1}}(s)] + \frac{2}{(1 - \gamma)\eta_k} \mathbb{E}_{s \sim \nu_\rho^{\pi_{k+1}}} \|\delta_k(s, \cdot)\|_\infty \\
& \quad - \frac{1 - \eta_k \tau_k}{(1 - \gamma)\eta_k} \mathbb{E}_{s \sim \nu_\rho^{\pi_{k+1}}} [D_{\pi_k}^{\pi_{k+1}}(s)] - \frac{1}{(1 - \gamma)\eta_k} \mathbb{E}_{s \sim \rho} \left[ D_{\pi_{k+1}}^{\pi_k}(s) \frac{d\nu_\rho^{\pi_{k+1}}(s)}{d\rho(s)} \right] \\
& \leq \frac{\tau_k}{1 - \gamma} \log |\mathcal{A}| + \frac{2}{(1 - \gamma)\eta_k} \mathbb{E}_{s \sim \nu_\rho^{\pi_{k+1}}} \|\delta_k(s, \cdot)\|_\infty - \frac{1}{\eta_k} D_{\pi_{k+1}}^{\pi_k}(\rho).
\end{aligned}$$

The change of measure in the first inequality is safe because of Assumption 2. The second inequality uses  $-\log |\mathcal{A}| \leq h^\pi(s) \leq 0$  for any  $\pi$ , the non-negative of KL divergence and (8).

On the other hand, by plugging in  $\pi = \pi^*$ , we obtain

$$\begin{aligned}
& V^{\pi_k}(\rho) - V^*(\rho) \\
& \leq -\frac{\tau_k}{1 - \gamma} \mathbb{E}_{s \sim \nu_\rho^{\pi^*}} [h^{\pi_k}(s) - h^{\pi^*}(s)] + \frac{2}{(1 - \gamma)\eta_k} \mathbb{E}_{s \sim \nu_\rho^{\pi^*}} \|\delta_k(s, \cdot)\|_\infty \\
& \quad - \frac{1}{(1 - \gamma)\eta_k} \mathbb{E}_{s \sim \nu_\rho^{\pi^*}} [D_{\pi_{k+1}}^{\pi^*}(s) - (1 - \eta_k \tau_k) D_{\pi_k}^{\pi^*}(s)] + \frac{1}{(1 - \gamma)\eta_k} \mathbb{E}_{s \sim \rho} \left[ D_{\pi_{k+1}}^{\pi_k}(s) \frac{d\nu_\rho^{\pi^*}(s)}{d\rho(s)} \right] \\
& \leq \frac{\tau_k}{1 - \gamma} \log |\mathcal{A}| + \frac{2}{(1 - \gamma)\eta_k} \mathbb{E}_{s \sim \nu_\rho^{\pi^*}} \|\delta_k(s, \cdot)\|_\infty \\
& \quad - \frac{1}{(1 - \gamma)\eta_k} \mathbb{E}_{s \sim \nu_\rho^{\pi^*}} [D_{\pi_{k+1}}^{\pi^*}(s) - (1 - \eta_k \tau_k) D_{\pi_k}^{\pi^*}(s)] + \frac{\kappa}{(1 - \gamma)\eta_k} D_{\pi_{k+1}}^{\pi_k}(\rho).
\end{aligned}$$

Again, the change of measure in the first inequality is safe under Assumption 2. The second inequality uses  $-\log |\mathcal{A}| \leq h^\pi(s) \leq 0$ , the non-negative of KL divergence and (23).

Combining the inequalities with  $\gamma_\rho = 1 - (1 - \gamma)/\kappa$ , we get

$$\begin{aligned}
& V^{\pi_{k+1}}(\rho) - V^*(\rho) - \gamma_\rho (V^{\pi_k}(\rho) - V^*(\rho)) \\
& = V^{\pi_{k+1}}(\rho) - V^{\pi_k}(\rho) + \frac{1 - \gamma}{\kappa} (V^{\pi_k}(\rho) - V^*(\rho)) \\
& \leq \frac{2\tau_k}{\kappa(1 - \gamma_\rho)} \log |\mathcal{A}| + \frac{2}{\kappa(1 - \gamma_\rho)\eta_k} \mathbb{E}_{s \sim \nu_\rho^{\pi_{k+1}}} \|\delta_k(s, \cdot)\|_\infty + \frac{2}{\kappa(1 - \gamma_\rho)\eta_k} \mathbb{E}_{s \sim \nu_\rho^{\pi^*}} \|\delta_k(s, \cdot)\|_\infty \\
& \quad - \frac{1}{\kappa\eta_k} \mathbb{E}_{s \sim \nu_\rho^{\pi^*}} [D_{\pi_{k+1}}^{\pi^*}(s) - (1 - \eta_k \tau_k) D_{\pi_k}^{\pi^*}(s)],
\end{aligned}$$

where the inequality uses  $\gamma_\rho > 0$ .

Let  $\delta_k^Q = \eta_k (Q^{\pi_k} - Q_{w_k})$  and  $\delta_k^\Pi = \lambda_{k+1}^{-1} f_{\theta_{k+1}} - (1 - \eta_k \tau_k) \lambda_k^{-1} f_{\theta_k} + \eta_k Q_{w_k}$ . Then we have

$$\mathbb{E}_{s \sim \nu_\rho^{\pi_{k+1}}} \|\delta_k(s, \cdot)\|_\infty \leq \mathbb{E}_{s \sim \nu_\rho^{\pi_{k+1}}} \left[ \left\| \delta_k^Q(s, \cdot) \right\|_\infty + \left\| \delta_k^\Pi(s, \cdot) \right\|_\infty \right],$$

Using Cauchy-Schwarz inequality and Assumption 3, we can replace the error measure  $\nu_\rho^{\pi_{k+1}}$  by  $\nu_\rho^{\pi_k}$ :

$$\begin{aligned}
& \mathbb{E}_{s \sim \nu_\rho^{\pi_{k+1}}} \left\| \delta_k^Q(s, \cdot) \right\|_\infty \\
& \leq \sqrt{\mathbb{E}_{s \sim \nu_\rho^{\pi_{k+1}}} \left[ \frac{d\nu_\rho^{\pi_{k+1}}(s)}{d\nu_\rho^{\pi_k}(s)} \right] \mathbb{E}_{s \sim \nu_\rho^{\pi_{k+1}}} \left[ \frac{d\nu_\rho^{\pi_k}(s)}{d\nu_\rho^{\pi_{k+1}}(s)} \right] \left\| \delta_k^Q(s, \cdot) \right\|_\infty^2} \\
& = \sqrt{(\chi^2(\nu_\rho^{\pi_{k+1}}, \nu_\rho^{\pi_k}) + 1) \left( \mathbb{E}_{s \sim \nu_\rho^{\pi_k}} \left\| \delta_k^Q(s, \cdot) \right\|_\infty^2 \right)} \\
& \leq \eta_k \sqrt{C_\nu \mathcal{L}_{\text{critic}}(w_k; \pi_k)}.
\end{aligned}$$

Similarly, we have

$$\begin{aligned}
& \mathbb{E}_{s \sim \nu_\rho^{\pi_{k+1}}} \left\| \delta_k^\Pi(s, \cdot) \right\|_\infty \\
& \leq \sqrt{\mathbb{E}_{s \sim \nu_\rho^{\pi_{k+1}}} \left[ \frac{d\nu_\rho^{\pi_{k+1}}(s)}{d\nu_\rho^{\pi_k}(s)} \right] \mathbb{E}_{s \sim \nu_\rho^{\pi_{k+1}}} \left[ \frac{d\nu_\rho^{\pi_k}(s)}{d\nu_\rho^{\pi_{k+1}}(s)} \right] \left\| \delta_k^\Pi(s, \cdot) \right\|_\infty^2} \\
& = \sqrt{(\chi^2(\nu_\rho^{\pi_{k+1}}, \nu_\rho^{\pi_k}) + 1) \left( \mathbb{E}_{s \sim \nu_\rho^{\pi_k}} \left\| \delta_k^\Pi(s, \cdot) \right\|_\infty^2 \right)} \\
& \leq \sqrt{C_\nu \mathcal{L}_{\text{actor}}(\theta_{k+1}; \theta_k, w_k)}.
\end{aligned}$$

Thus we get

$$\mathbb{E}_{s \sim \nu_\rho^{\pi_{k+1}}} \left\| \delta_k(s, \cdot) \right\|_\infty \leq \sqrt{C_\nu} \left( \eta_k \sqrt{\mathcal{L}_{\text{critic}}(w_k; \pi_k)} + \sqrt{\mathcal{L}_{\text{actor}}(\theta_{k+1}; \theta_k, w_k)} \right).$$

Applying the same argument, we can replace the error measure  $\nu_\rho^{\pi_{k+1}}$  by  $\nu_\rho^{\pi_k}$  and obtain

$$\mathbb{E}_{s \sim \nu_\rho^{\pi_k}} \left\| \delta_k(s, \cdot) \right\|_\infty \leq \sqrt{C_\nu} \left( \eta_k \sqrt{\mathcal{L}_{\text{critic}}(w_k; \pi_k)} + \sqrt{\mathcal{L}_{\text{actor}}(\theta_{k+1}; \theta_k, w_k)} \right).$$

We complete the proof by plugging in the above inequalities and rearranging terms.  $\square$

### C.3 Proof of Theorem 1

*Proof.* For  $k = 0$ , we have  $V^{\pi_0}(\rho) - V^*(\rho) \leq \frac{C}{1-\gamma}$  from (2). Since  $\theta_0 = 0$ , we have  $f_{\theta_0}(s, a)$  be constant for any  $s$  and  $a$ , thus  $D_{\pi_0}^*(s) = \log |\mathcal{A}|$ .

By Lemma 2 and concavity of the square root function, taking the expectation with respect to the

samples  $\Xi_k^Q$  and  $\Xi_k^\Pi$  conditioned on previous samples yields

$$\begin{aligned}
& \mathbb{E}[V^{\pi_{k+1}}(\rho) - V^*(\rho)] \\
& \leq \mathbb{E}\left(V^{\pi_{k+1}}(\rho) - V^*(\rho) + \frac{\tau_{k+1}}{\kappa(1-\gamma\rho)}\mathbb{E}_{s\sim\nu_{\rho}^{\pi^*}}[D_{\pi_{k+1}}^{\pi^*}(s)]\right) \\
& = \mathbb{E}\left(V^{\pi_{k+1}}(\rho) - V^*(\rho) + \frac{\gamma\rho\tau_k}{\kappa(1-\gamma\rho)}\mathbb{E}_{s\sim\nu_{\rho}^{\pi^*}}[D_{\pi_{k+1}}^{\pi^*}(s)]\right) \\
& \leq \gamma\rho\left(V^{\pi_k}(\rho) - V^*(\rho) + \frac{\tau_k}{\kappa(1-\gamma\rho)}\mathbb{E}_{s\sim\nu_{\rho}^{\pi^*}}[D_{\pi_k}^{\pi^*}(s)]\right) \\
& \quad + \frac{4\sqrt{C_\nu}}{\kappa(1-\gamma\rho)}\left(\sqrt{\mathbb{E}[\mathcal{L}_{\text{critic}}(w_k; \pi_k)]} + \frac{\tau_k}{1-\gamma\rho}\sqrt{\mathbb{E}[\mathcal{L}_{\text{actor}}(\theta_{k+1}; \theta_k, w_k)]}\right) + \frac{2\tau_k \log |\mathcal{A}|}{\kappa(1-\gamma\rho)} \\
& \leq \gamma\rho\left(V^{\pi_k}(\rho) - V^*(\rho) + \frac{\tau_k}{\kappa(1-\gamma\rho)}\mathbb{E}_{s\sim\nu_{\rho}^{\pi^*}}[D_{\pi_k}^{\pi^*}(s)]\right) + \frac{(8\sqrt{C_\nu}+2\log |\mathcal{A}|)C}{\kappa(1-\gamma\rho)}\gamma\rho^{k+1}.
\end{aligned}$$

Dividing both sides by  $\gamma\rho^{k+1}$ , telescoping from 0 to  $k$  and rearranging terms, we obtain

$$\begin{aligned}
& \mathbb{E}[V^{\pi_{k+1}}(\rho) - V^*(\rho)] \\
& \leq \frac{C}{1-\gamma} \cdot \gamma\rho^{k+1} \left( (1 + \log |\mathcal{A}|) + (k+1)(8\sqrt{C_\nu} + 2\log |\mathcal{A}|) \right),
\end{aligned}$$

where the expectation is taken with respect to all samples from zeroth to  $k$ -th iteration.

Let  $C_1 = 1 + \log |\mathcal{A}|$ ,  $C_2 = 8\sqrt{C_\nu} + 2\log |\mathcal{A}|$ . For any  $\epsilon > 0$ , it suffices to choose  $k = \lceil a(\log \frac{b}{\epsilon} + \log \log \frac{b}{\epsilon}) \rceil$  with  $a = \frac{1}{\log \frac{1}{\gamma\rho}}$  and  $b = \frac{2C(C_1+C_2)}{(1-\gamma)\log \frac{1}{\gamma\rho}}$ , since

$$\begin{aligned}
\mathbb{E}[V^{\pi_k}(\rho) - V^*(\rho)] & \leq (C_1 + C_2)k\gamma\rho^k \cdot \frac{C}{1-\gamma} \\
& \leq \frac{(C_1 + C_2)a(\log \frac{b}{\epsilon} + \log \log \frac{b}{\epsilon})}{\frac{b}{\epsilon} \log \frac{b}{\epsilon}} \cdot \frac{C}{1-\gamma} \\
& \leq \frac{2(C_1 + C_2)a \log \frac{b}{\epsilon}}{b \log \frac{b}{\epsilon}} \cdot \frac{C\epsilon}{1-\gamma} = \epsilon.
\end{aligned}$$

In view of  $\log x \geq 1 - \frac{1}{x}$ , we obtain

$$\begin{aligned}
k & \leq \log_{\frac{1}{\gamma\rho}} \left( \frac{2C(C_1 + C_2)}{(1-\gamma)\epsilon \log \frac{1}{\gamma\rho}} \log \left( \frac{2C(C_1 + C_2)}{(1-\gamma)\epsilon \log \frac{1}{\gamma\rho}} \right) \right) + 1 \\
& \leq \log_{\frac{1}{\gamma\rho}} \left( \frac{2C(C_1 + C_2)}{(1-\gamma\rho)(1-\gamma)\epsilon} \log \left( \frac{2C(C_1 + C_2)}{(1-\gamma\rho)(1-\gamma)\epsilon} \right) \right) + 1 \\
& = \tilde{O} \left( \log_{\frac{1}{\gamma\rho}} \left( \frac{C(\sqrt{C_\nu} + \log |\mathcal{A}|)}{\kappa(1-\gamma\rho)^2\epsilon} \right) \right),
\end{aligned}$$

where  $\tilde{O}(\cdot)$  hides the logarithm terms. □



## D Missing Proofs for Sample Complexity

In this section, we provide missing proofs for Theorems 4 and 5. The proofs are based on the statistical recovery result (Lemma 20) for CNN in Appendix G.

### D.1 Proof of Theorem 4

*Proof.* From (2) and Lemma 3 we know  $Q^{\pi_k}(\cdot, a)$  is  $\frac{C}{1-\gamma}$ -bounded and  $(L_Q, \alpha)$ -Lipschitz on  $\mathcal{S}$  for all  $a \in \mathcal{A}$ . From (31) in Appendix A.2 we have

$$\mathbb{E}[\mathcal{L}_{\text{critic}}(w_k; \pi_k)] \leq |\mathcal{A}| \max_{a \in \mathcal{A}} \mathbb{E} \left[ \mathbb{E}_{s \sim \nu_{\rho}^{\pi_k}} |Q_{w_k}(s, a) - Q^{\pi_k}(s, a)|^2 \right],$$

Thus to ensure  $\mathbb{E}[\mathcal{L}_{\text{critic}}(w_k; \pi_k)] \leq C^2 \gamma_{\rho}^{2(k+1)}$ , it suffices to use a sample size  $N$  such that for all  $a \in \mathcal{A}$ ,

$$\mathbb{E}_{\Xi_k} \mathbb{E}_{s \sim \nu_{\rho}^{\pi_k}} |Q_{w_k}(s, a) - Q^{\pi_k}(s, a)|^2 \leq \frac{C^2 \gamma_{\rho}^{2(k+1)}}{|\mathcal{A}|}. \quad (33)$$

We set the following for  $\mathcal{W}_k = \mathcal{W}_{\text{Lip}}(\frac{C}{1-\gamma}, L_Q, \alpha, \epsilon_Q)$ :

$$\begin{aligned} M &= O(N^{\frac{d}{d+2\alpha}}), \quad L = O(\log N + D + \log D), \quad J = O(D), \quad I \in [2, D], \quad R_1 = O(1), \\ \log R_2 &= O(\log^2 N + D \log N), \quad \epsilon_Q = (L_Q^2 + \frac{C^2}{(1-\gamma)^2}) D^{\frac{3\alpha}{2\alpha+d}} N^{-\frac{\alpha}{2\alpha+d}}, \end{aligned}$$

where  $O(\cdot)$  hides some constant depending on  $\log L_Q$ ,  $\log \frac{C}{1-\gamma}$ ,  $d$ ,  $\alpha$ ,  $\omega$ ,  $B$ , and the surface area  $\text{Area}(\mathcal{S})$ . Then by Lemma 7 in Appendix A.2 and Lemma 20 in Appendix G, the following bound on the regression error holds:

$$\begin{aligned} &\mathbb{E}_{\Xi_k} \mathbb{E}_{s \sim \nu_{\rho}^{\pi_k}} |Q_{w_k}(s, a) - Q^{\pi_k}(s, a)|^2 \\ &\leq C' \left( (\bar{L}_Q + 1)^2 \frac{C^2}{(1-\gamma)^2} + \sigma^2 \right) N^{-\frac{2\alpha}{2\alpha+d}} \log^6 N, \end{aligned} \quad (34)$$

where  $\bar{L}_Q$  is defined as in (26),  $\sigma^2 = \frac{\gamma^2 C^2}{4(1-\gamma)^2} \leq \frac{C^2}{4(1-\gamma)^2}$  is the variance proxy derived in Lemma 7 and  $C'$  is a constant depending on  $D^{\frac{6\alpha}{2\alpha+d}}$ ,  $\log L_Q$ ,  $\log \frac{C}{1-\gamma}$ ,  $d$ ,  $\alpha$ ,  $\omega$ ,  $B$ , and the surface area  $\text{Area}(\mathcal{S})$ .

By choosing  $N = \left(\frac{1}{\delta} \log^3 \frac{1}{\delta}\right)^{\frac{d}{\alpha}+2}$  where  $\delta = \sqrt{\frac{1}{4096((\bar{L}_Q+1)^2+\frac{1}{4})C'|\mathcal{A}|(\frac{d}{\alpha}+2)^6}}(1-\gamma)\gamma_\rho^{k+1}$ , we have

$$\begin{aligned} N^{-\frac{2\alpha}{2\alpha+d}} \log^6 N &= \frac{\left(\left(\frac{d}{\alpha}+2\right) \log\left(\frac{1}{\delta} \log^3 \frac{1}{\delta}\right)\right)^6}{\frac{1}{\delta^2} \log^6 \frac{1}{\delta}} \\ &\leq \frac{\left(\frac{d}{\alpha}+2\right)^6 \left(4 \log \frac{1}{\delta}\right)^6}{\frac{1}{\delta^2} \log^6 \frac{1}{\delta}} \\ &= \frac{(1-\gamma)^2 \gamma_\rho^{2(k+1)}}{\left((\bar{L}_Q+1)^2+\frac{1}{4}\right)C'|\mathcal{A}|}. \end{aligned}$$

Plugging the result into (34), we obtain (33).

Denoting  $C_3 = \sqrt{4096((\bar{L}_Q+1)^2+\frac{1}{4})C'|\mathcal{A}|(\frac{d}{\alpha}+2)^6} = O(\sqrt{|\mathcal{A}|})$ , we have the sample size  $N = \tilde{O}\left(\frac{C_3}{1-\gamma}\gamma_\rho^{-(k+1)}\right)^{\frac{d}{\alpha}+2} = \tilde{O}\left(\frac{\sqrt{|\mathcal{A}|}}{1-\gamma}\gamma_\rho^{-(k+1)}\right)^{\frac{d}{\alpha}+2}$ . When Assumptions 2 and 3 hold, we know from Theorem 1 that the total iteration number  $K$  satisfies

$$\gamma_\rho^{-K} = \tilde{O}\left(\frac{C(\sqrt{C_\nu} + \log |\mathcal{A}|)}{\kappa(1-\gamma_\rho)^2\epsilon}\right).$$

Plugging  $K$  into our choice of  $N$  yields the result.  $\square$

## D.2 Proof of Theorem 5

*Proof.* By (32), it suffices to specify the architecture  $\mathcal{F}$  and restrictions so that for all  $a \in \mathcal{A}$  and all  $k \leq K$ ,

$$\mathbb{E}_{\Xi_k} \mathbb{E}_{s \sim \nu_\rho^{\pi_k}} |f_{\theta_{k+1}}(s, a) - \gamma_\rho^2 f_{\theta_k}(s, a) + Q_{w_k}(s, a)|^2 \leq \frac{C^2 \gamma_\rho^{2(k+1)}}{|\mathcal{A}|}. \quad (35)$$

By Lemma 5, our choice of  $\eta_k, \tau_k, \lambda_k, \mathcal{W}_k$  and  $\Theta_k$  ensures that  $\lambda_{k+1} g_{k+1}^*(\cdot, a) = \gamma_\rho^2 f_{\theta_k}(\cdot, a) - Q_{w_k}(\cdot, a)$  is  $(\frac{L_Q}{1-\gamma_\rho^2}, \alpha, \frac{\epsilon_Q}{1-\gamma_\rho^2})$ -approximately Lipschitz and is uniformly bounded by  $\frac{C}{(1-\gamma_\rho^2)(1-\gamma)}$ . Following the same lines of proof in Appendix D.1, we set the following for the underlying CNN architecture  $\mathcal{F}$  and the restricted parameter spaces  $\mathcal{W}_k$  and  $\Theta_k$ :

$$\begin{aligned} M &= O(N^{\frac{d}{d+2\alpha}}), \quad L = O(\log N + D + \log D), \quad J = O(D), \quad I \in [2, D], \quad R_1 = O(1), \\ \log R_2 &= O(\log^2 N + D \log N), \quad \epsilon_Q^{(k)} = (L_Q^2 + \frac{C^2}{(1-\gamma_\rho)^2}) D^{\frac{3\alpha}{2\alpha+d}} N^{-\frac{\alpha}{2\alpha+d}}, \end{aligned}$$

where  $O(\cdot)$  hides some constant depending on  $\log L_Q, \log \frac{C}{1-\gamma}, d, \alpha, \omega, B$ , and the surface area  $\text{Area}(\mathcal{S})$ . We let  $N = \left(\frac{1}{\delta} \log^3 \frac{1}{\delta}\right)^{\frac{d}{\alpha}+2}$  with  $\delta = \sqrt{\frac{1}{C''|\mathcal{A}|(\frac{d}{\alpha}+2)^6}}(1-\gamma)(1-\gamma_\rho^2)\gamma_\rho^{K+1}$ , where  $C''$  is a constant depending on  $D^{\frac{6\alpha}{2\alpha+d}}, \bar{L}_Q, \log L_Q, \log \frac{C}{1-\gamma}, d, \alpha, \omega, B$ , and the surface area  $\text{Area}(\mathcal{S})$ , and then we have (35) sat-

ified. Denoting  $C_4 = \sqrt{C''|\mathcal{A}|(\frac{d}{\alpha} + 2)^6} = O(\sqrt{|\mathcal{A}|})$ , we can write  $N = \tilde{O}\left(\frac{C_4}{(1-\gamma_\rho^2)(1-\gamma)}\gamma_\rho^{-(K+1)}\right)^{\frac{d}{\alpha}+2}$ .

For  $\epsilon > 0$ , the total iteration number  $K$  satisfies

$$\gamma_\rho^{-K} = \tilde{O}\left(\frac{C(\sqrt{C_\nu} + \log|\mathcal{A}|)}{\kappa(1-\gamma_\rho)^2\epsilon}\right).$$

Plugging  $K$  into our choice of  $N$  yields the result.  $\square$

## E Approximation Theory for CNN

In this section, we introduce the approximation theory for CNN. We first consider the case when target function  $f_0 = Q^\pi(\cdot, a)$  is  $(L_Q, \alpha)$ -Lipschitz for any  $a \in \mathcal{A}$  (Theorem 2), and then proceed to the case when  $f_0$  is a general  $(L_f, \alpha, \epsilon_f)$ -approximately Lipschitz function (Theorem 3). Corollary 1 follows immediately from Theorem 3.

Let us define a class of single-block CNNs in the form of

$$f(x) = W \cdot \text{Conv}_{\mathcal{W}, \mathcal{B}}(P(x)) \tag{36}$$

as

$$\begin{aligned} \mathcal{F}^{\text{SCNN}}(L, J, I, R_1, R_2) = \{f \mid f(x) \text{ in the form (36) with } L \text{ layers; the filter size} \\ \text{is bounded by } I; \text{ the number of channels is bounded by } J; \\ \max_l \|\mathcal{W}^{(l)}\|_\infty \vee \|\mathcal{B}^{(l)}\|_\infty \leq R_1, \|W\|_\infty \leq R_2\}. \end{aligned} \tag{37}$$

We will use this class of single-block CNNs as the building blocks of our final CNN approximation for the ground truth Lipschitz function.

### E.1 Proof of Theorem 2 Overview

Theorem 2 establishes the relation between network architecture and approximation error for  $f_0 = Q^\pi$ . We prove Theorem 2 for  $(L_f, \alpha)$ -Lipschitz  $f_0$  in the following steps:

**Step 1: Decompose  $f_0$  as a sum of locally supported functions over the manifold.** Since manifold  $\mathcal{S}$  is assumed compact (Assumption 1), we can cover it with a finite set of  $D$ -dimensional open Euclidean balls  $\{B_\beta(\mathbf{c}_i)\}_{i=1}^{C_\mathcal{S}}$ , where  $\mathbf{c}_i$  denotes the center of the  $i$ -th ball and  $\beta$  is the radius. We choose  $\beta < \frac{\varpi}{4}$  and define  $U_i = B_\beta(\mathbf{c}_i) \cap \mathcal{S}$ . Note that each  $U_i$  is diffeomorphic to an open subset of  $\mathbb{R}^d$  (Niyogi et al., 2008, Lemma 5.4). Moreover, the set  $\{U_i\}_{i=1}^{C_\mathcal{S}}$  forms an open cover for  $\mathcal{S}$ . There exists a carefully designed open cover with cardinality  $C_\mathcal{S} \leq \left\lceil \frac{\text{Area}(\mathcal{S})}{\beta^d} T_d \right\rceil$ , where  $\text{Area}(\mathcal{S})$  denotes the surface area of  $\mathcal{S}$  and  $T_d$  denotes the thickness of  $U_i$ 's, that is, the average number of  $U_i$ 's that contain a given point on  $\mathcal{S}$ . It has been shown that  $T_d = O(d \log d)$  (Conway and Sloane, 1988).

Moreover, for each  $U_i$ , we can define a linear transformation

$$\phi_i(x) = a_i V_i^\top (x - \mathbf{c}_i) + b_i, \quad (38)$$

where  $a_i \in (0, 1]$  is a scaling factor and  $b_i \in \mathbb{R}^d$  is the translation vector, both of which are chosen to ensure  $\phi(U_i) \subset [0, 1]^d$ , and the columns of  $V_i \in \mathbb{R}^{D \times d}$  form an orthonormal basis for the tangent space  $T_{\mathbf{c}_i}(\mathcal{S})$  at  $\mathbf{c}_i$ . Overall, the atlas  $\{(\phi_i, U_i)\}_{i=1}^{C_S}$  transforms each local neighborhood on the manifold to a  $d$ -dimensional cube.

Thus, we can decompose  $f_0$  using this atlas as

$$f_0 = \sum_{i=1}^{C_S} f_i, \quad \text{with} \quad f_i = f_0 \times \rho_i, \quad (39)$$

because there exists such a  $C^\infty$  partition of unity  $\{\rho_i\}_{i=1}^{C_S}$  with  $\text{supp}(\rho_i) \subset U_i$  (Liu et al., 2021, Proposition 1). Since each  $f_i$  is only supported on a subset of  $U_i$ , we can further write

$$f_0 = \sum_{i=1}^{C_S} (f_i \circ \phi_i^{-1}) \circ \phi_i \times \mathbf{1}_{U_i}, \quad (40)$$

where  $\mathbf{1}_{U_i}$  is the indicator function of  $U_i$ .

Lastly, we extend  $f_i \circ \phi_i^{-1}$  to the entire cube  $[0, 1]^d$  with 0:

$$\bar{f}_i(x) = \begin{cases} f_i \circ \phi_i^{-1}(x), & x \in \text{supp}(f_i \circ \phi_i^{-1}), \\ 0, & x \in [0, 1]^d \setminus \text{supp}(f_i \circ \phi_i^{-1}). \end{cases} \quad (41)$$

By Lemma 12 in Appendix E.5,  $\bar{f}_i$  is a Lipschitz function with Lipschitz constant at most  $L_i := C_i(L_f + \|f_0\|_\infty)$ , where  $C_i$  is a constant depending on  $\alpha, \omega, \phi_i$  and  $\rho_i$ . This extended function will be approximated with first-order B-splines in the next step.

**Step 2: Approximate each local function with first-order B-splines.** Since each local function  $\bar{f}_i$  is Lipschitz on  $d$ -dimensional unit cube, a weighted sum of first-order B-splines can approximate it. The number of splines depends exponentially on the intrinsic dimension  $d$ , rather than the ambient dimension  $D$ . To be more precise, we partition the unit cube into  $N = 2^{pd}$  small cubes with side lengths  $2^{-p}$ , where  $p \in \mathbb{N}$  is positive. We denote  $J(p) = \{0, 1, \dots, 2^p - 1\}^d$  as a vector index set. The first-order B-spline  $M_{p,j}$  with shift vector  $j \in J(p)$  is defined as

$$M_{p,j}(x) = \prod_{k=1}^d \psi(2^p x_k - j_k), \quad (42)$$

where  $\psi: [0, 2] \rightarrow \mathbb{R}$  is a sawtooth function:

$$\psi(x) = \begin{cases} x, & 0 \leq x \leq 1, \\ 2 - x, & 1 < x \leq 2, \\ 0, & \text{otherwise.} \end{cases}$$

Each B-spline  $M_{p,j}$  is supported on the small cube  $B_j = \{x \in \mathbb{R}^d \mid j_k \leq x_k \leq j_k + 2, \forall k \in [d]\}$ . Then by Lemma 13, there exists a function  $\tilde{f}_i$  in the form

$$\tilde{f}_i = \sum_{j \in J(p)} c_{i,j} M_{p,j},$$

such that

$$\|\tilde{f}_i - \bar{f}_i\|_\infty \leq 2L_i d N^{-\alpha/d}. \quad (43)$$

By (40) and (43), we now have a sum of first-order B-splines

$$\tilde{f} := \sum_{i=1}^{C_S} \tilde{f}_i \circ \phi_i \times \mathbf{1}_{U_i} = \sum_{i=1}^{C_S} \sum_{j \in J(p)} c_{i,j} M_{p,j} \circ \phi_i \times \mathbf{1}_{U_i}, \quad (44)$$

which can approximate the target Lipschitz function  $f_0$  with error

$$\|\tilde{f} - f_0\|_\infty \leq 2C_S d \max_{i=1, \dots, C_S} C_i (L_f + \|f_0\|_\infty) N^{-\alpha/d}. \quad (45)$$

**Step 3: Approximate each first-order B-spline with a composition of CNNs.** We now turn to approximate  $\tilde{f}$  defined in (44) with a composition of CNNs. We first approximate some building blocks with single-block CNNs defined as in (37) and then ensemble them together. The building blocks include the multiplication operator  $\times$ , chart mappings  $\{\phi_i\}_{i=1}^{C_S}$ , indicator functions  $\{\mathbf{1}_{U_i}\}_{i=1}^{C_S}$ , and first-order B-splines  $\{M_{p,j}\}_{j \in J(p)}$ .

The multiplication operator  $\times$  can be approximated by a single-block CNN  $\hat{\times}$  with at most  $\eta$  error in the  $L^\infty$  sense (Proposition 3), which needs  $O(\log \frac{1}{\eta})$  layers and 6 channels. All weight parameters are bounded by  $(c_0^2 \vee 1)$ , where  $c_0$  is the uniform upper bound of the input functions to be multiplied.

The chart mapping  $\phi_i$ , according to (38), is a linear transformation. Thus, it can be expressed with a single-layer perceptron  $\hat{\phi}_i$ , which can be equivalently expressed by a CNN.

The indicator function  $\mathbf{1}_{U_i}$  is equal to 1 if  $d_i^2(x) = \|x - \mathbf{c}_i\|_2^2 \leq \beta^2$  and equal to 0 otherwise. By this definition, we can write  $\mathbf{1}_{U_i}$  as a composition of a univariate indicator  $\mathbf{1}_{[0, \beta^2]}$  and the distance function  $d_i^2$ :

$$\mathbf{1}_{U_i}(x) = \mathbf{1}_{[0, \beta^2]} \circ d_i^2(x). \quad (46)$$

Given  $\theta \in (0, 1)$  and  $\Delta \geq 8DB^2\theta$ , it turns out that  $\mathbf{1}_{[0, \beta^2]}$  and  $d_i^2$  can be approximated with two

single-block CNNs  $\widehat{\mathbf{1}}_\Delta$  and  $\widehat{d}_i^2$  respectively (Proposition 4) such that

$$\left\| \widehat{d}_i^2 - d_i^2 \right\|_\infty \leq 4B^2 D \theta \quad (47)$$

and

$$\widehat{\mathbf{1}}_\Delta \circ \widehat{d}_i^2(x) = \begin{cases} 1, & \text{if } x \in U_i, d_i^2(x) \leq \beta^2 - \Delta, \\ 0, & \text{if } x \notin U_i, \\ \text{between 0 and 1,} & \text{otherwise.} \end{cases}$$

The architecture and size of  $\widehat{\mathbf{1}}_\Delta$  and  $\widehat{d}_i^2$  are characterized in Proposition 4 as functions of  $\theta$  and  $\Delta$ .

The first-order B-spline  $M_{p,j}$  can be approximated by a single-block CNN  $\widehat{M}_{p,j}$  up to arbitrarily chosen  $\epsilon_1$  error (Proposition 1). We can find a proper  $\epsilon_1$  a set of single-block CNNs  $\{\widehat{f}_{i,j}\}_{j \in J(p)}$  such that the error matches (43):

$$\left\| \sum_{j \in J(p)} \widehat{f}_{i,j}^{\text{SCNN}} - \widetilde{f}_i \right\|_\infty \leq 2L_i d N^{-\alpha/d}. \quad (48)$$

The architecture and size of  $\widehat{f}_{i,j}^{\text{SCNN}}$  are characterized in Proposition 2 as functions of  $N$ .

Putting the above results together, we can develop a composition of single-block CNNs, which can be further expressed by a single-block CNN (Lemma 14):

$$\widehat{g}_{i,j}^{\text{SCNN}} = \widehat{\times} \left( \widehat{f}_{i,j}^{\text{SCNN}} \circ \widehat{\phi}_i, \widehat{\mathbf{1}}_\Delta \circ \widehat{d}_i^2 \right). \quad (49)$$

Details are provided in Appendix E.2.

**Step 4: Express the sum of CNN compositions with a CNN** Finally, we can assemble everything into  $\widehat{f}$  as

$$\widehat{f} = \sum_{i=1}^{C_S} \sum_{j \in J(p)} \widehat{g}_{i,j}^{\text{SCNN}}, \quad (50)$$

which serves as an approximation of  $f_0$ . By choosing the appropriate network size in Lemma 10, we can ensure that

$$\left\| \widehat{f} - f_0 \right\|_\infty \leq c_0 (L_f + \|f_0\|_\infty) N^{-\alpha/d}$$

for some constant  $c_0$  depending on  $d$ ,  $\alpha$ ,  $\omega$ ,  $B$ , and the surface area  $\text{Area}(\mathcal{S})$ .

By Lemma 15, for  $\widetilde{M}, \widetilde{J} > 0$ , we can write this sum of  $C_S \cdot |J(p)| = C_S \cdot N$  single-block CNNs as a sum of  $\widetilde{M}$  single-block CNNs with the same architecture, whose channel number upper bound  $J$  depends on  $\widetilde{J}$ . This allows Theorem 2 to be more flexible with network architecture. By Lemma 17, this sum of  $\widetilde{M}$  single-block CNNs can be further expressed as one CNN in the CNN class (13). Finally,  $N$  (or equivalently,  $p$ ) will be chosen appropriately as a function of network architecture parameters,

and the approximation theory of CNN is proven by plugging in  $f_0 = Q^\pi$ ,  $L_f = L_Q$  in Lemma 3.

In the following, we provide the proof details for Theorem 2.

## E.2 Proof of Theorem 2

*Proof.* We start from the decomposition of the approximation error of  $\widehat{f}$ , which is based on the decomposition of the approximation error of  $\widehat{g}_{i,j}^{\text{SCNN}}$  in (49).

**Lemma 10.** *Let  $\eta > 0$  be the approximation error of the multiplication operator  $\widehat{\times}(\cdot, \cdot)$  as defined in Step 3 of Appendix E.1 and Proposition 3,  $\Delta$  and  $\theta$  be defined as in Step 3 of Appendix E.1 and Proposition 4. Assume  $N = 2^{pd}$  is chosen according to Proposition 2. For any  $i = 1, \dots, C_S$ , we have  $\|\widehat{f} - f_0\|_\infty \leq \sum_{i=1}^{C_S} (A_{i,1} + A_{i,2} + A_{i,3})$  with*

$$\begin{aligned} A_{i,1} &= \sum_{j \in J(p)} \left\| \widehat{\times} \left( \widehat{f}_{i,j}^{\text{SCNN}} \circ \widehat{\phi}_i, \widehat{\mathbf{1}}_\Delta \circ \widehat{d}_i^2 \right) - \widehat{f}_{i,j}^{\text{SCNN}} \circ \widehat{\phi}_i \times (\widehat{\mathbf{1}}_\Delta \circ \widehat{d}_i^2) \right\|_\infty \leq N\eta, \\ A_{i,2} &= \left\| \left( \sum_{j \in J(p)} \left( \widehat{f}_{i,j}^{\text{SCNN}} \circ \widehat{\phi}_i \right) \right) \times (\widehat{\mathbf{1}}_\Delta \circ \widehat{d}_i^2) - f_i \times (\widehat{\mathbf{1}}_\Delta \circ \widehat{d}_i^2) \right\|_\infty \leq 4L_i d N^{-\alpha/d}, \\ A_{i,3} &= \left\| f_i \times (\widehat{\mathbf{1}}_\Delta \circ \widehat{d}_i^2) - f_i \times \mathbf{1}_{U_i} \right\|_\infty \leq \frac{C'(\pi + 1)}{\beta(1 - \beta/\omega)} \Delta \end{aligned}$$

for some constant  $C'$  depending on  $\rho_i$  and  $\phi_i$ . Furthermore, for any  $\epsilon \in (0, 1)$ , setting

$$\eta = L_i d N^{-1-\alpha/d}, \quad \Delta = \frac{L_i d \beta (1 - \beta/\omega) N^{-\alpha/d}}{C'(\pi + 1)}, \quad \theta = \frac{\Delta}{16B^2 D} \quad (51)$$

yields

$$\|\widehat{f} - f_0\|_\infty \leq C''(L_f + \|f_0\|_\infty) N^{-\frac{\alpha}{d}},$$

where  $C''$  is a constant depending on  $d$ ,  $\alpha$ ,  $\omega$ ,  $\rho_i$  and  $\phi_i$ . The choice in (51) satisfies the condition  $\Delta > 8B^2 D \theta$  in Proposition 4.

*Proof. of Lemma 10* As in Proposition 3,  $A_{i,1}$  measures the approximation error from  $\widehat{\times}$ :

$$A_{i,1} = \sum_{j \in J(p)} \left\| \widehat{\times} \left( \widehat{f}_{i,j}^{\text{SCNN}} \circ \widehat{\phi}_i, \widehat{\mathbf{1}}_\Delta \circ \widehat{d}_i^2 \right) - \widehat{f}_{i,j}^{\text{SCNN}} \circ \widehat{\phi}_i \times (\widehat{\mathbf{1}}_\Delta \circ \widehat{d}_i^2) \right\|_\infty \leq N\eta.$$

The term  $A_{i,2}$  measures the error from CNN approximation of local Lipschitz functions. As in Proposition 2,  $A_{i,2} \leq 4L_i d N^{-\alpha/d}$ .

The term  $A_{i,3}$  measures the error from the CNN approximation of the chart determination function. The bound of  $A_{i,3}$  can be derived using Proposition 4 and the proof of Lemma 4 in (Chen et al., 2022), since  $\bar{f}_i$  is a Lipschitz function on  $[0, 1]^d$ .

Finally, by Lemma 12, we have  $L_i = O(L_f + \|f\|_\infty)$ , and the proof is complete.  $\square$

In order to attain the error desired in Lemma 10, we need each network in (49) with appropriate size. The network size of the components can be analyzed as follows:

- $\widehat{\mathbb{1}}_i$ : The chart determination network  $\widehat{\mathbb{1}}_i := \widehat{d}_i^2 \circ \widehat{\mathbb{1}}_\Delta$  is the composition of  $\widehat{d}_i^2$  and  $\widehat{\mathbb{1}}_\Delta$ . By Proposition 4,  $\widehat{d}_i^2$  is a single-block CNN with  $O(\log \frac{1}{\theta} + D) = O(\frac{\alpha}{d} \log N + D + \log D)$  layers and  $6D$  channels;  $\widehat{\mathbb{1}}_\Delta$  is a single-block CNN with  $O(\log(\beta^2/\Delta)) = O(\frac{\alpha}{d} \log N)$  layers and 2 channels. In both subnetworks, all parameters are bounded by  $O(1)$ . By Lemma 14, the chart determination network  $\widehat{\mathbb{1}}_i$  is a single-block CNN with  $O(\frac{\alpha}{d} \log N + D + \log D)$  layers,  $6D + 2$  channels and all weight parameters bounded by  $O(1)$ .
- $\widehat{\times}$ : By Proposition 3, the multiplication network is a single-block CNN with  $O(\log \frac{1}{\eta}) = O((1 + \frac{\alpha}{d}) \log N)$  layers and  $O(1)$  channels. By construction of  $\widehat{f}_{i,j}^{\text{SCNN}}$  and  $\widehat{\mathbb{1}}_\Delta$ , all weight parameters are bounded by  $(\|f\|_\infty^2 \vee 1)$ .
- $\widehat{\phi}_i$ : The projection  $\phi_i$  is a linear mapping, so it can be expressed with a single-layer perceptron. By Lemma 8 in Liu et al. (2021), this single-layer perceptron can be expressed with a single-block CNN with  $D + 2$  layers and width  $d$ . All parameters are of order  $O(1)$ .
- $\widehat{f}_{i,j}^{\text{SCNN}}$ : By Proposition 2, each  $\widehat{f}_{i,j}^{\text{SCNN}}$  is a single-block CNN with  $O(\log N)$  layers and  $80d$  channels. All weight parameters are in the order of  $O(N^{\frac{1}{d}})$ .

Next, we show that the composition  $\widehat{\times} \left( \widehat{f}_{i,j}^{\text{SCNN}} \circ \widehat{\phi}_i, \widehat{\mathbb{1}}_\Delta \circ \widehat{d}_i^2 \right)$  can be simply expressed as a single-block CNN. By Lemma 14, there exists a single-block CNN  $g_{i,j}$  with  $O(\log N + D)$  layers and  $80d$  channels realizing  $\widehat{f}_{i,j}^{\text{SCNN}} \circ \widehat{\phi}_i$ . All parameters in  $g_{i,j}$  are in the order of  $O(N^{\frac{1}{d}})$ . Moreover, recall that the chart determination network  $\widehat{\mathbb{1}}_i$  is a single-block CNN with  $O(\log N + D + \log D)$  layers and  $6D + 2$  channels, whose parameters are of  $O(1)$ . By Lemma 14 in Liu et al. (2021), one can construct a convolutional block, denoted by  $\bar{g}_{i,j}$ , such that

$$\bar{g}_{i,j}(x) = \begin{bmatrix} (g_{i,j}(x))_+ & (g_{i,j}(x))_- & (\widehat{\mathbb{1}}_i(x))_+ & (\widehat{\mathbb{1}}_i(x))_- \\ \star & \star & \star & \star \end{bmatrix}. \quad (52)$$

Here  $\bar{g}_{i,j}$  has  $80d + 6D + 2$  channels.

Since the input of  $\widehat{\times}$  is  $\begin{bmatrix} g_{i,j} \\ \widehat{\mathbb{1}}_i \end{bmatrix}$ , by Lemma 15 in Liu et al. (2021), there exists a CNN  $\mathring{g}_{i,j}$  which takes (52) as the input and outputs  $\widehat{\times}(g_{i,j}, \widehat{\mathbb{1}}_i)$ .

Since  $\bar{g}_{i,j}$  only contains convolutional layers, the composition  $\mathring{g}_{i,j} \circ \bar{g}_{i,j}$ , denoted by  $\mathring{g}_{i,j}^{\text{SCNN}}$ , is a single-block CNN and for any  $x \in \mathcal{S}$ ,  $\widehat{g}_{i,j}^{\text{SCNN}}(x) = \widehat{\times} \left( \widehat{f}_{i,j}^{\text{SCNN}} \circ \widehat{\phi}_i(x), \widehat{\mathbb{1}}_\Delta \circ \widehat{d}_i^2(x) \right)$ . We have  $\widehat{g}_{i,j}^{\text{SCNN}} \in \mathcal{F}^{\text{SCNN}}(L, J, I, R, R)$  with

$$L = O(\log N + D + \log D), \quad J = 160d + 12D + O(1), \quad R = O(N^{\frac{1}{d}}),$$



and  $I$  can be any integer in  $[2, D]$ . Therefore, we have shown that  $\widehat{g}_{i,j}^{\text{SCNN}}$  is a single-block CNN that expresses the composition (49), as we desired.

Furthermore, recall that  $\widehat{f}$  can be written as a sum of  $C_S N$  such single-block CNNs. By Lemma 15, for any  $\widetilde{M}$  and  $\widetilde{J}$  satisfying  $\widetilde{M}\widetilde{J} = O(C_S N)$  and  $\widetilde{J} \geq 160d + 12D + O(1)$ , there exists a CNN architecture  $\mathcal{F}^{\text{SCNN}}(L, J, I, R, R)$  that gives rise to a set of single-block CNNs  $\{\widehat{g}_i\}_{i=1}^{\widetilde{M}} \subset \mathcal{F}^{\text{SCNN}}(L, J, I, R, R)$  with

$$\widehat{f} = \sum_{i=1}^{\widetilde{M}} \widehat{g}_i \quad (53)$$

and

$$L = O(\log N + D + \log D), \quad J = O(D), \quad R = O(N^{\frac{1}{a}}).$$

By Lemma 16, we slightly adjust the CNN architecture by re-balancing the weight parameters of the convolutional blocks and that of the final fully connected layer. In particular, we rescale all parameters in convolutional layers of  $\widehat{g}_i$  to be no larger than 1. This procedure preserves the approximation power of the CNN while reducing the covering number (see Appendix F) of the CNN class. We set  $\lambda = c' N^{\frac{1}{a}} (8ID) \widetilde{M}^{-\frac{1}{L}}$ , where  $c'$  is a constant such that  $R \leq c' N^{\frac{1}{a}}$ . With this  $\lambda$ , we have  $\widehat{f}_i \in \mathcal{F}^{\text{SCNN}}(L, J, I, R_1, R_2)$  with

$$\begin{aligned} L &= O(\log N + D + \log D), \quad J = O(D), \quad R_1 = O((8ID)^{-1} \widetilde{M}^{-\frac{1}{L}}) = O(1), \\ \log R_2 &= O(\log \widetilde{M} + \log^2 N + D \log N) \end{aligned} \quad (54)$$

such that  $\widehat{g}_i \equiv \widehat{f}_i$ .

Finally, we prove that it suffices to use one CNN to realize the sum of single-block CNNs in (53). By Lemma 17, there exists a CNN that can express the sum of  $\widetilde{M}$  single-block CNNs with architecture  $\mathcal{F}(M, L, J, I, R_1, R_2)$ , where

$$\begin{aligned} M &= O(\widetilde{M}), \quad L = O(\log N + D + \log D), \quad J = O(D\widetilde{J}), \\ R_1 &= O((8ID)^{-1} \widetilde{M}^{-\frac{1}{L}}) = O(1), \quad \log R_2 = O(\log \widetilde{M} + \log^2 N + D \log N). \end{aligned}$$

Here,  $\widetilde{M}, \widetilde{J}$  satisfy

$$\widetilde{M}\widetilde{J} = O(N),$$

which is a requirement inherited from Lemma 15. This CNN is our final approximation of  $f_0$ .

Applying this relation  $N = O(\widetilde{M}\widetilde{J})$  to (54) gives

$$\|\widehat{f} - f_0\| \leq (L_f + \|f_0\|_\infty) (\widetilde{M}\widetilde{J})^{-\frac{\alpha}{a}}$$

and the network size

$$\begin{aligned} M &= O(\widetilde{M}), \quad L = O(\log(\widetilde{M}\widetilde{J}) + D + \log D), \quad J = O(D\widetilde{J}), \\ R_1 &= O((8ID)^{-1}\widetilde{M}^{-\frac{1}{L}}) = O(1), \quad \log R_2 = O(\log \widetilde{M} + \log^2(\widetilde{M}\widetilde{J}) + D \log(\widetilde{M}\widetilde{J})). \end{aligned}$$

By (2) and Lemma 3, we have  $L_f = L_Q = \frac{C}{1-\gamma}\bar{L}_Q$  and  $\|f_0\|_\infty = \frac{C}{1-\gamma}$ , which completes the proof of Theorem 2.  $\square$

### E.3 Proof of Lemma 3

*Proof.* Let us recall a useful characterization for total variation distance between probability measures  $\mu, \nu$  on any measurable space  $\mathcal{X}$ :

$$d_{\text{TV}}(\mu, \nu) = \frac{1}{2} \sup_{f: \mathcal{X} \rightarrow [-1,1]} \left| \int_{\mathcal{X}} f \, d\mu - \int_{\mathcal{X}} f \, d\nu \right|. \quad (55)$$

Define

$$f(s) = \frac{2(1-\gamma)}{C} \cdot V^\pi(s) - 1.$$

By (2) we have  $-1 \leq f(s) \leq 1$  for any  $s \in \mathcal{S}$ . In view of (4), (55) and that  $\mathcal{M}$  is  $(L_{\mathcal{P}}, L_c)$ -Lipschitz, we have

$$\begin{aligned} |Q^\pi(s, a) - Q^\pi(s', a)| &\leq |c(s, a) - c(s', a)| + \gamma \left| \int_{\mathcal{S}} V^\pi(s'') \, d(\mathcal{P}(s''|s, a) - \mathcal{P}(s''|s', a)) \right| \\ &= |c(s, a) - c(s', a)| + \frac{\gamma C}{2(1-\gamma)} \left| \int_{\mathcal{S}} f(s'') \, d(\mathcal{P}(s''|s, a) - \mathcal{P}(s''|s', a)) \right| \\ &\leq |c(s, a) - c(s', a)| + \frac{\gamma C}{(1-\gamma)} d_{\text{TV}}(\mathcal{P}(\cdot|s, a), \mathcal{P}(\cdot|s', a)) \\ &\leq L_c \cdot d_{\mathcal{S}}^\alpha(s, s') + \frac{\gamma C}{1-\gamma} L_{\mathcal{P}} \cdot d_{\mathcal{S}}^\alpha(s, s') \\ &= L_Q \cdot d_{\mathcal{S}}^\alpha(s, s'). \end{aligned}$$

The first line is from (4) and the triangle inequality. The second line is from the definition of  $f$  and that  $\mathcal{P}(\cdot|s, a)$  is a distribution. The third line is from (55), and the fourth line is from the Lipschitz assumption.  $\square$

### E.4 Proof of Theorem 3

*Proof.* We first show in Lemma 11 that for any approximately Lipschitz function  $f_0$ , there exists a Lipschitz ‘‘reference function’’ that is not far from  $f_0$  in the  $L^\infty$  sense and has the same Lipschitz constant.

**Lemma 11.** *Suppose Assumption 1 holds. If a function  $f_0: \mathcal{S} \rightarrow \mathbb{R}$  is  $(L, \alpha, \epsilon)$ -approximately Lips-*

chitz, then there exists an  $(L, \alpha)$ -Lipschitz function  $\bar{f}_0$  such that  $\|\bar{f}_0\|_\infty \leq \|f_0\|_\infty$  and  $\|f_0 - \bar{f}_0\|_\infty \leq 2\epsilon$ .

*Proof. of Lemma 11* Define an envelope function  $f_L(x) := \inf_{y \in \mathcal{S}} \{f_0(y) + L \cdot d_{\mathcal{S}}^\alpha(y, x)\}$ . It follows immediately from the  $(L, \alpha, \epsilon)$ -approximate Lipschitzness of  $f$  that for any  $x \in \mathcal{S}$ ,

$$\begin{aligned} f_L(x) &\leq f_0(x) + L \cdot d_{\mathcal{S}}^\alpha(x, x) = f_0(x), \\ f_L(x) &\geq \inf_{y \in \mathcal{S}} \{f_0(x) - L \cdot d_{\mathcal{S}}^\alpha(y, x) - 2\epsilon + L \cdot d_{\mathcal{S}}^\alpha(y, x)\} = f_0(x) - 2\epsilon, \end{aligned}$$

hence  $\|f_L - f_0\|_\infty \leq 2\epsilon$ . Furthermore, for any  $x, y \in \mathcal{S}$ ,

$$\begin{aligned} f_L(x) - f_L(y) &= \inf_{z \in \mathcal{S}} \{f_0(z) + L \cdot d_{\mathcal{S}}^\alpha(z, x)\} - \inf_{z \in \mathcal{S}} \{f_0(z) + L \cdot d_{\mathcal{S}}^\alpha(z, y)\} \\ &= \inf_{z \in \mathcal{S}} \{f_0(z) + L \cdot d_{\mathcal{S}}^\alpha(z, x)\} + \sup_{z \in \mathcal{S}} \{-f_0(z) - L \cdot d_{\mathcal{S}}^\alpha(z, y)\} \\ &\leq \sup_{z \in \mathcal{S}} \{L \cdot d_{\mathcal{S}}^\alpha(z, x) - L \cdot d_{\mathcal{S}}^\alpha(z, y)\} \\ &\leq \sup_{z \in \mathcal{S}} \{L \cdot (d_{\mathcal{S}}^\alpha(z, y) + d_{\mathcal{S}}^\alpha(y, x)) - L \cdot d_{\mathcal{S}}^\alpha(z, y)\} \\ &\leq L \cdot d_{\mathcal{S}}^\alpha(x, y). \end{aligned}$$

The first inequality is from that  $\inf_{z \in \mathcal{S}} \{f_0(z) + L \cdot d_{\mathcal{S}}^\alpha(z, x)\} \leq f_0(z') + L \cdot d_{\mathcal{S}}^\alpha(z', x)$  for any  $z' \in \mathcal{S}$  and thus we can move it into the supremum and set  $z' = z$ . The second inequality is from the triangle inequality of  $d_{\mathcal{S}}(\cdot, \cdot)$  and the subadditivity of  $h(x) = x^\alpha$ . Similarly we have  $f_L(y) - f_L(x) \leq L \cdot d_{\mathcal{S}}^\alpha(y, x)$  and hence  $f_L$  is  $L$ -Lipschitz. By truncating the negative part of  $f_L$  by  $-\|f_0\|_\infty$ , we obtain  $\bar{f}_0$  such that

$$\bar{f}_0(x) = \begin{cases} f_L(x), & f_L(x) \geq -\|f_0\|_\infty, \\ -\|f_0\|_\infty, & f_L(x) < -\|f_0\|_\infty. \end{cases}$$

We can easily verify that  $\bar{f}_0$  is  $L$ -Lipschitz,  $\|\bar{f}_0\|_\infty \leq \|f_0\|_\infty$  and  $\|f_0 - \bar{f}_0\|_\infty \leq 2\epsilon$ .  $\square$

By Lemma 11, there exists a  $(L_f, \alpha)$ -Lipschitz function  $\bar{f}_0$  such that  $\|\bar{f}_0\|_\infty \leq \|f_0\|_\infty$  and

$$\|\bar{f}_0 - f_0\|_\infty \leq 2\epsilon_f.$$

Therefore, similar to Theorem 2, for any integers  $I \in [2, D]$ ,  $\widetilde{M}, \widetilde{J} > 0$ ,

$$\begin{aligned} M &= O(\widetilde{M}), \quad L = O(\log(\widetilde{M}\widetilde{J}) + D + \log D), \quad J = O(D\widetilde{J}), \\ \log R_2 &= O(\log^2(\widetilde{M}\widetilde{J}) + D \log(\widetilde{M}\widetilde{J})), \quad R_1 = (8ID)^{-1} \widetilde{M}^{-\frac{1}{I}} = O(1), \end{aligned}$$

there exists a CNN  $f \in \mathcal{F}(M, L, J, I, R_1, R_2)$  such that

$$\|f - f_0\|_\infty \leq \|f - \bar{f}_0\|_\infty + \|\bar{f}_0 - f_0\|_\infty \leq (L_f + \|f_0\|_\infty)(\widetilde{M}\widetilde{J})^{-\frac{\alpha}{d}} + 2\epsilon_f.$$

where  $O(\cdot)$  hides a constant depending on  $\log L_f$ ,  $\log \|f_0\|_\infty$ ,  $d$ ,  $\alpha$ ,  $\omega$ ,  $B$ , and the surface area  $\text{Area}(\mathcal{S})$ .

The rest of the proof is to show that  $f$  is uniformly bounded by  $\|f_0\|_\infty$  and is  $(L_f, \alpha, \widehat{\epsilon}_f)$ -approximately Lipschitz with  $\widehat{\epsilon}_f = (L_f + \|f_0\|_\infty)(\widetilde{M}\widetilde{J})^{-\frac{\alpha}{d}}$ . To show the uniform upper bound, we can apply a truncation layer to the components of  $\widehat{f}$  so that every output will not exceed the range  $[-\|f_0\|_\infty, \|f_0\|_\infty]$ . This can be realized by adding a two-layer ReLU network  $g: \mathbb{R} \rightarrow \mathbb{R}$ ,

$$g(x) = \text{ReLU}(2\|f_0\|_\infty - \text{ReLU}(\|f_0\|_\infty - x)) - \|f_0\|_\infty.$$

By Theorem 1 in [Oono and Suzuki \(2019\)](#), such a ReLU network can be expressed by a CNN  $\widehat{g}$  with constant parameters. By Lemma 14, applying this CNN to the output of  $f$  results in a new CNN with the same order of size. In this case, we simply replace  $\widehat{f}$  with this new CNN. By Lemma 11,  $\|\bar{f}_0\|_\infty \leq \|f_0\|_\infty$ , so the truncation layer would not affect the approximation error, and we complete the proof for the uniform upper bound.

By Lemma 4, we conclude that  $f$  is  $(L_f, \alpha, \widehat{\epsilon}_f)$ -approximately Lipschitz with  $\widehat{\epsilon}_f = (L_f + \|f_0\|_\infty)(\widetilde{M}\widetilde{J})^{-\frac{\alpha}{d}}$ . □

## E.5 Supporting Lemmas for CNN Approximation

In this section, we provide some auxiliary lemmas for CNN approximation. Lemma 12 shows that each local function  $\bar{f}_i$  defined in (41) is Lipschitz on the low-dimensional Euclidean unit cube  $[0, 1]^d$ . The Lipschitz constant  $L_i$  is controlled by the  $L^\infty$  norm and the Lipschitz constant of the original function  $L_f$

**Lemma 12.** *Let  $\bar{f}_i$  be defined as in (41). Then each function  $\bar{f}_i$  is uniformly bounded by  $\|f\|_\infty$  and is  $(L_i, \alpha)$ -Lipschitz on  $[0, 1]^d$  with  $L_i = O(L_f + \|f\|_\infty)$ , where  $O(\cdot)$  hides some constant depending on  $\alpha, \omega, \phi_i$  and  $\rho_i$ .*

*Proof.* We only need to show the Lipschitz continuity on the support of  $f_i \circ \phi_i^{-1}$ . Otherwise, the Lipschitz condition holds trivially since  $f_i \circ \phi_i^{-1}$  is bounded and extended to the whole unit cube with 0.

Suppose  $x, y \in \text{supp}(f_i \circ \phi_i^{-1})$  are two points in the support, then there exist  $u, v \in \text{supp}(\rho_i) \subset U_i$  such that  $u = \phi_i^{-1}(x), v = \phi_i^{-1}(y)$ . By definition of the chart  $(U_i, \phi_i)$ , we have  $\|u - v\|_2 \leq 2\beta < \frac{\omega}{2}$  and that

$$\|x - y\|_2 = \left\| a_i V_i^\top (u - v) \right\|_2 \leq \|u - v\|_2 < \frac{\omega}{2},$$

since  $a_i \leq 1$  and  $V_i$  is orthonormal. According to Proposition 6.3 in [Niyogi et al. \(2008\)](#), the geodesic

distance between  $u$  and  $v$  is upper bounded by the Euclidean distance in  $\mathbb{R}^D$  up to a constant factor:

$$d_{\mathcal{S}}(u, v) \leq \omega - \omega \sqrt{1 - \frac{2\|u - v\|_2}{\omega}} \leq 2\|u - v\|_2.$$

By Lemma 2 in [Chen et al. \(2022\)](#),  $\phi_i$  is a diffeomorphism as long as the Euclidean ball radius satisfies  $\beta \leq \frac{\omega}{4}$ . By our construction,  $\beta < \frac{\omega}{4}$ , thus  $\phi_i^{-1}$  is differentiable with its Jacobian bounded. Therefore, there exists a constant  $L_{i,1}$  such that

$$L_{i,1} := \sup_{z \in [0,1]^d} \|\nabla \phi_i^{-1}(z)\|_{\text{op}} < +\infty.$$

where  $\nabla \phi_i^{-1}(z)$  is the Jacobian of  $\phi_i^{-1}$  at  $z$  and  $\|\cdot\|_{\text{op}}$  denotes the operator norm. Also notice that  $\rho_i$  is  $C^\infty$ , thus we conclude that there exist another constant  $L_{i,2}$  such that

$$L_{i,2} := \sup_{z \in [0,1]^d} \|\nabla(\rho_i \circ \phi_i^{-1})(z)\|_2 < +\infty.$$

Combine the results together, we have

$$\begin{aligned} & |f_i \circ \phi_i^{-1}(x) - f_i \circ \phi_i^{-1}(y)| \\ &= |f_i(u) - f_i(v)| \\ &= |f(u)\rho_i(u) - f(v)\rho_i(v)| \\ &\leq |f(u)\rho_i(u) - f(u)\rho_i(v)| + |f(u)\rho_i(v) - f(v)\rho_i(v)| \\ &\leq \|f\|_\infty |\rho_i \circ \phi_i^{-1}(x) - \rho_i \circ \phi_i^{-1}(y)| + |f(u) - f(v)| \\ &\leq \|f\|_\infty \sup_{z \in [0,1]^d} \|\nabla(\rho_i \circ \phi_i^{-1})(z)\|_2 \|x - y\|_2 + L_f \cdot d_{\mathcal{S}}^\alpha(u, v) \\ &\leq \|f\|_\infty \left(\frac{\omega}{2}\right)^{1-\alpha} L_{i,2} \cdot \|x - y\|_2^\alpha + L_f 2^\alpha L_{i,1}^\alpha \cdot \|x - y\|_2^\alpha \\ &\leq C_i (\|f\|_\infty + L_f) \|x - y\|_2^\alpha \end{aligned}$$

where  $C_i = \max(2^\alpha L_{i,1}^\alpha, (\frac{\omega}{2})^{1-\alpha} L_{i,2})$  is a constant depending on  $\alpha, \omega, \phi_i$  and  $\rho_i$ . Denote  $L_i := C_i (\|f\|_\infty + L_f)$ , we conclude that  $f_i \circ \phi_i^{-1}$  is  $(L_i, \alpha)$ -Lipschitz.  $\square$

Lemma 13 further shows that Lipschitz functions on the unit cube  $[0, 1]^d$  can be arbitrarily approximated by first-order B-splines. The approximation error is  $O(N^{-\alpha/d})$ .

**Lemma 13.** *Let  $f$  be an  $(L, \alpha)$ -Lipschitz function on the unit cube  $[0, 1]^d$  and take nonzero value only in the interior of the cube. For any  $p \in \mathbb{N}$ ,  $p \geq 1$ ,  $N = 2^{pd}$ , there exists a function  $\tilde{f}_N$  in the form*

$$\tilde{f}_N = \sum_{j \in J(p)} c_j M_{p,j}$$

such that

$$\left\| \tilde{f}_N - f \right\|_\infty \leq 2LdN^{-\alpha/d},$$

where  $\max_{j \in J(p)} c_j = \|f\|_\infty$ .

*Proof.* For any  $p \in \mathbb{N}$ ,  $p \geq 1$ , the index set  $J(p) = \{0, 1, \dots, 2^p - 2\}^d$  as defined in Step 2 of Appendix E.1. We denote  $G(p) = \{2^{-k}y \mid y \in \mathbb{N}^d, 0 \leq y_k \leq 2^p, \forall k \in [d]\}$  as the set of all grid points. Let

$$\tilde{f}_N = \sum_{j \in J(p)} c_j M_{p,j},$$

where  $c_j = f(2^{-p}(j_1 + 1), \dots, 2^{-p}(j_d + 1))$  for all  $j \in J(p)$ . By definition of the first-order B-spline and that  $f$  takes nonzero value only in the interior of the cube, we have  $\tilde{f}_N(x) = 0$  if  $x_k \in \{0, 1\}$  for some  $k \in [d]$  and thus  $\tilde{f}_N(x) = f(x)$  for all  $x \in G(p)$ . Moreover,  $\tilde{f}_N$  is a coordinate-wise  $(L, \alpha)$ -Lipschitz linear function.

For any point  $x \in [0, 1]^d$ , there exists a grid point  $y \in G(p)$  such that  $\|x - y\|_\infty \leq 2^{-p-1}$ . Define a sequence of points  $\{y^{(t)}\}_{t=0}^d$  as

$$y_k^{(t)} = \begin{cases} y_k, & k \leq t, \\ x_k, & k > t. \end{cases}$$

We have  $y^{(0)} = x$  and  $y^{(d)} = y$ . We can move the point  $x$  to  $y$  by changing one coordinate at a time following the sequence  $\{y^{(t)}\}$ . Thus we have

$$\begin{aligned} \left| \tilde{f}_N(x) - f(x) \right| &= \left| \tilde{f}_N(y) - f(y) + f(y) - f(x) + \sum_{t=0}^{d-1} \left( \tilde{f}_N(y^{(t)}) - \tilde{f}_N(y^{(t+1)}) \right) \right| \\ &\stackrel{(a)}{\leq} |f(y) - f(x)| + \sum_{t=0}^{d-1} \left| \tilde{f}_N(y^{(t)}) - \tilde{f}_N(y^{(t+1)}) \right| \\ &\stackrel{(b)}{\leq} L \|x - y\|_2^\alpha + L \sum_{t=0}^{d-1} \left\| y^{(t)} - y^{(t+1)} \right\|_2^\alpha \\ &\stackrel{(c)}{\leq} 2^{1-(p+1)\alpha} Ld, \end{aligned}$$

where (a) uses  $\tilde{f}_N(y) = f(y)$  and the triangle inequality, (b) uses the Lipschitz continuity, and (c) is from the upper bound for norms. Since  $x$  is arbitrarily chosen from the unit cube, we have

$$\left\| \tilde{f}_N - f \right\|_\infty \leq 2^{1-(p+1)\alpha} Ld.$$

Plugging in  $N = 2^{pd}$  yields the result. □

Proposition 1 is a special case of Lemma 10 in Liu et al. (2021) for first-order splines (first-order cardinal B-splines). It shows that a single-block CNN can approximate each first-order B-spline to arbitrary accuracy.

**Proposition 1** (Liu et al. (2021, Lemma 10)). *Let  $p \in \mathbb{N}$  and  $j \in \mathbb{N}^d$ . There exists a constant  $C$  depending only on  $d$  such that for any  $\epsilon \in (0, 1)$  and any  $2 \leq I \leq d$ , there exists a single-block CNN  $\widehat{M}_{p,j} \in \mathcal{F}^{\text{SCNN}}(L, J, I, R, R)$  with  $L = 3 + 2\lceil \log_2(\frac{3}{C\epsilon}) + 5 \rceil \lceil \log_2 d \rceil$ ,  $J = 80d$  and  $R = 4 \vee 2^p$  that satisfies*

$$\left\| M_{p,j} - \widehat{M}_{p,j} \right\|_{L^\infty([0,1]^d)} \leq \epsilon,$$

and  $\widehat{M}_{p,j}(x) = 0$  for all  $x \notin B_{p,j} := \{x \in \mathbb{R}^d \mid 2^{-p}j_k \leq x_k \leq 2^{-p}(j_k + 2)\}$ .

As a result, we show in Proposition 2 that CNNs can approximate local functions.

**Proposition 2.** *Let  $\bar{f}_i$  be defined as in (41). For  $N = 2^{pd}$  and any  $2 \leq I \leq D$ , there exists a set of single-block CNNs  $\{\widehat{f}_{i,j}^{\text{SCNN}}\}_{j \in J(p)}$  such that*

$$\left\| \sum_{j \in J(p)} \widehat{f}_{i,j}^{\text{SCNN}} - \bar{f}_i \right\|_{L^\infty([0,1]^d)} \leq 4L_i d N^{-\alpha/d}.$$

Each single-block CNN  $\widehat{f}_{i,j}^{\text{SCNN}}$  is in  $\mathcal{F}^{\text{SCNN}}(L, J, I, R, R)$  with

$$L = O(\log N), \quad J = 80d, \quad R = O(N^{\frac{1}{d}}),$$

where  $O(\cdot)$  hides some constant depending on  $d$  and  $\alpha$ .

*Proof.* By Lemma 13 and the  $(L_i, \alpha)$ -Lipschitzness of  $\bar{f}_i$ , for  $p \geq 1$ ,  $N = 2^{pd}$ , there exists a function  $\widetilde{f}_i$  in the form

$$\widetilde{f}_i = \sum_{j \in J(p)} c_{i,j} M_{p,j}$$

such that

$$\left\| \widetilde{f}_i - \bar{f}_i \right\|_\infty \leq 2L_i d N^{-\alpha/d}.$$

By Proposition 1, there exists a collection of single-block CNNs  $\{\widehat{M}_{p,j}\}_{j \in J(p)}$  that approximates the first-order B-splines  $\{M_{p,j}\}_{j \in J(p)}$ . Suppose  $\left\| \widehat{M}_{p,j} - M_{p,j} \right\|_{L^\infty} \leq \epsilon_1$  for all  $j \in J(p)$  and some  $\epsilon_1 \in (0, 1)$ ,

we have

$$\begin{aligned} \left\| \sum_{j \in J(p)} c_{i,j} \widehat{M}_{p,j} - \bar{f}_i \right\|_{\infty} &\leq |J(p)| \|\bar{f}_i\|_{\infty} \epsilon_1 + 2L_i d N^{-\alpha/d} \\ &\leq N L_i \epsilon_1 + 2L_i d N^{-\alpha/d}, \end{aligned}$$

where the second inequality is from  $\|\bar{f}_i\|_{\infty} = \|f\|_{\infty} \leq L_i$  in Lemma 12. By letting  $\epsilon_1 = 2dN^{-\frac{d+\alpha}{d}}$ , we obtain

$$\left\| \sum_{j \in J(p)} c_{i,j} \widehat{M}_{p,j} - \bar{f}_i \right\|_{\infty} \leq 4L_i d N^{-\alpha/d}.$$

According to Proposition 1, for any  $j \in J(p)$ , the single-block CNN  $\widehat{M}_{p,j} \in \mathcal{F}^{\text{SCNN}}(L, J, I, R, R)$  with

$$\begin{aligned} L &= 3 + 2 \left\lceil \frac{d + \alpha}{d} \log_2 \frac{3^{\frac{d}{d+\alpha}} N}{2C_0 d} \right\rceil \lceil \log_2 d \rceil, \quad J = 80d, \\ 2 &\leq I \leq d, \quad R = 4 \vee N^{\frac{1}{d}}. \end{aligned}$$

By letting  $\widehat{f}_{i,j}^{\text{SCNN}} = c_{i,j} \widehat{M}_{p,j}$  we prove the proposition.  $\square$

The rest is to show that the multiplication operator and the indicator function can be approximated by CNNs. Proposition 3 shows that CNN can approximate the multiplication of scalars.

**Proposition 3.** *Let  $\times$  be the scalar multiplication operator. For any  $\eta \in (0, 1)$ , there exists a single-block CNN  $\widehat{\times}$  such that*

$$\|a \times b - \widehat{\times}(a, b)\|_{\infty} \leq \eta,$$

where  $a, b$  are functions uniformly bounded by  $c_0$ . The approximated single-block CNN  $\widehat{\times}$  is in  $\mathcal{F}^{\text{SCNN}}(L, J, I, R, R)$  with  $L = O(\log \frac{1}{\eta}) + D$  layers,  $J = 24$  channels and any filter size  $I$  such that  $2 \leq I \leq D$ . All parameters are bounded by  $R = (c_0^2 \vee 1)$ . Furthermore, the weight matrix in the fully connected layer of  $\widehat{\times}$  has nonzero entries only in the first row.

*Proof.* By Proposition 3 in Yarotsky (2017), there exists a feed-forward ReLU network that can approximate the multiplication operator between values with magnitude bounded by  $c_0$  with  $\eta$  error. Such a feed-forward network has  $O(\log \frac{1}{\eta})$  layers, each layer has its width bounded by 6, and all parameters are bounded by  $c_0^2$ . Therefore, such a feed-forward neural network is sufficient to approximate  $\times$  with  $\eta$  error in  $L^{\infty}$ -norm, since the function  $a, b$  are uniformly bounded by  $c_0$ .

Furthermore, by Lemma 8 in Liu et al. (2021), we can express the aforementioned feed-forward network with a single-block CNN in  $\mathcal{F}^{\text{SCNN}}(L, J, I, R, R)$ , where  $L, J, I, R$  are specified in the statement of the proposition.  $\square$



The indicator function  $\mathbb{1}_{U_i}$  can be written as the composition of the indicator function of the closed interval  $[0, \beta^2]$  and the squared Euclidean distance function  $d_i: \mathcal{S} \rightarrow \mathbb{R}_+$  to the ball center  $\mathbf{c}_i$ :

$$\mathbb{1}_{U_i}(x) = \mathbb{1}_{[0, \beta^2]} \circ d_i(x), \quad (56)$$

where  $d_i(x) = \|x - \mathbf{c}_i\|_2^2$ . As Proposition 4 shows, these components can be approximated by CNNs.

**Proposition 4** (Liu et al. (2021, Lemma 9)). *Let  $d_i$  and  $\mathbb{1}_{[0, \beta^2]}$  be defined as in (56). For any  $\theta \in (0, 1)$  and  $\Delta \geq 8B^2D\theta$ , there exists a single-block CNN  $\widehat{d}_i$  approximating  $d_i$  such that*

$$\left\| \widehat{d}_i - d_i \right\|_{\infty} \leq 4B^2D\theta,$$

and a single-block CNN  $\widehat{\mathbb{1}}_{\Delta}$  approximating  $\mathbb{1}_{[0, \beta^2]}$  with

$$\widehat{\mathbb{1}}_{\Delta}(x) = \begin{cases} 1, & \text{if } x \leq (1 - 2^{-k})(\beta^2 - 4B^2D\theta), \\ 0, & \text{if } x \geq \beta^2 - 4B^2D\theta, \\ 2^k((\beta^2 - 4B^2D\theta)^{-1}x - 1), & \text{otherwise,} \end{cases}$$

for  $x \in \mathcal{S}$ . The single-block CNN for  $\widehat{d}_i$  has  $O(\log(1/\theta) + D)$  layers,  $6D$  channels and all weight parameters are bounded by  $4B^2$ . The single-block CNN  $\widehat{\mathbb{1}}_{\Delta}$  has  $\lceil \log(\beta^2/\Delta) \rceil$  layers, 2 channels and all weight parameters are bounded by  $\max(2, |\beta^2 - 4B^2D\theta|)$ .

As a result, for any  $x \in \mathcal{S}$ ,  $\widehat{\mathbb{1}}_{\Delta} \circ \widehat{d}_i(x)$  gives an approximation of  $\mathbb{1}_{U_i}$  satisfying

$$\widehat{\mathbb{1}}_{\Delta} \circ \widehat{d}_i(x) = \begin{cases} 1, & \text{if } x \in U_i \text{ and } d_i(x) \leq \beta^2 - \Delta, \\ 0, & \text{if } x \notin U_i, \\ \text{between 0 and 1,} & \text{otherwise.} \end{cases}$$

## E.6 Supporting Lemmas for CNN Architecture

In this section, we introduce several lemmas for (single-block) CNN architecture. Lemma 14 states that the composition of two single-block CNNs can be expressed as one single-block CNN with augmented architecture.

**Lemma 14** (Liu et al. (2021, Lemma 13)). *Let  $\mathcal{F}_1 = \mathcal{F}^{\text{SCNN}}(L_1, J_1, I_1, R_1, R_1)$  be a CNN architecture from  $\mathbb{R}^D \rightarrow \mathbb{R}$  and  $\mathcal{F}_2 = \mathcal{F}^{\text{SCNN}}(L_2, J_2, I_2, R_2, R_2)$  be a CNN architecture from  $\mathbb{R} \rightarrow \mathbb{R}$ . Assume the weight matrix in the fully connected layer of  $\mathcal{F}_1$  and  $\mathcal{F}_2$  has nonzero entries only in the first row. Then there exists a CNN architecture  $\mathcal{F}_3 = \mathcal{F}^{\text{SCNN}}(L, J, I, R, R)$  from  $\mathbb{R}^D \rightarrow \mathbb{R}$  with*

$$L = L_1 + L_2, \quad J = \max(J_1, J_2), \quad I = \max(I_1, I_2), \quad R = \max(R_1, R_2)$$

such that for any  $f_1 \in \mathcal{F}_1$  and  $f_2 \in \mathcal{F}_2$ , there exists  $f \in \mathcal{F}_3$  such that  $f(x) = f_2 \circ f_1(x)$ . Furthermore,

the weight matrix in the fully connected layer of  $\mathcal{F}_3$  has nonzero entries only in the first row.

Lemma 15 states that the sum of  $n_0$  single-block CNNs with the same architecture can be expressed as the sum of  $n_1$  single-block CNNs with modified width.

**Lemma 15** (Liu et al. (2022, Lemma 7)). *Let  $\{f_i\}_{i=1}^{n_0}$  be a set of single-block CNNs with architecture  $\mathcal{F}^{\text{SCNN}}(L_0, J_0, I_0, R_0, R_0)$ . For any integers  $n$  and  $\tilde{J}$  satisfying  $1 \leq n \leq n_0$ ,  $n\tilde{J} = O(n_0J_0)$  and  $\tilde{J} \geq J_0$ , there exists an architecture  $\mathcal{F}^{\text{SCNN}}(L, J, I, R, R)$  that gives a set of single-block CNNs  $\{g_i\}_{i=1}^n$  such that*

$$\sum_{i=1}^n g_i(x) = \sum_{i=1}^{n_0} f_i(x).$$

Such an architecture has

$$L = O(L_0), \quad J = O(\tilde{J}), \quad I = I_0, \quad R = R_0.$$

Furthermore, the fully connected layer of  $f$  has nonzero elements only in the first row.

Lemma 16 implies that one can slightly adjust the CNN architecture by re-balancing the weight parameter boundary of the convolutional blocks and that of the final fully connected layer. While re-balancing the weight would not affect the approximation power of the CNN, it will change the covering number of the CNN class, which is conducive to a different variance.

**Lemma 16** (Liu et al. (2021, Lemma 16)). *Let  $\lambda \geq 1$ . For any  $g \in \mathcal{F}^{\text{SCNN}}(L, J, I, R_1, R_2)$ , there exists  $f \in \mathcal{F}^{\text{SCNN}}(L, J, I, \lambda^{-1}R_1, \lambda^L R_2)$  such that  $g(x) \equiv f(x)$ .*

Finally, we prove Lemma 17, which states that the sum of single-block CNNs can be realized by a CNN of the form (13).

**Lemma 17.** *Let  $\mathcal{F}^{\text{SCNN}}(L, J, I, R_1, R_2)$  be any CNN architecture from  $\mathbb{R}^D \rightarrow \mathbb{R}$ . Assume the weight matrix in the fully connected layer of  $\mathcal{F}^{\text{SCNN}}(L, J, I, R_1, R_2)$  has nonzero entries only in the first row. For any positive integer  $M$ , there exists a CNN architecture  $\mathcal{F}(M, L, J + 4, I, R_1, R_2(1 \vee R_1^{-1}))$  such that for any  $\{\hat{f}_i(x)\}_{i=1}^M \subset \mathcal{F}^{\text{SCNN}}(L, J, I, R_1, R_2)$ , there exists  $\hat{f} \in \mathcal{F}(M, L, J + 4, I, R_1, R_2(1 \vee R_1^{-1}))$  with*

$$\hat{f}(x) = \sum_{m=1}^M \hat{f}_m(x).$$

*Proof.* Denote the architecture of  $\hat{f}_m$  with

$$\hat{f}_m(x) = W_m \cdot \text{Conv}_{\mathcal{W}_m, \mathcal{B}_m}(x),$$

where  $\mathcal{W}_m = \{\mathcal{W}_m^{(l)}\}_{l=1}^L$ ,  $\mathcal{B}_m = \{\mathcal{B}_m^{(l)}\}_{l=1}^L$ . Furthermore, denote the weight matrix and bias in the fully connected layer of  $\hat{f}$  with  $\widehat{W}$ ,  $\widehat{b}$  and the set of filters and biases in the  $m$ -th block of  $\hat{f}$  with  $\widehat{\mathcal{W}}_m$  and  $\widehat{\mathcal{B}}_m$  respectively. The padding layer  $\widehat{P}$  in  $\hat{f}$  pads the input  $x$  from  $\mathbb{R}^D$  to  $\mathbb{R}^{D \times 4}$  with zeros. Each column denotes a channel.

Let us first show that for each  $m$ , there exists some  $\text{Conv}_{\widehat{\mathcal{W}}_m, \widehat{\mathcal{B}}_m} : \mathbb{R}^{D \times 4} \rightarrow \mathbb{R}^{D \times 4}$  such that for any  $Z \in \mathbb{R}^{D \times 4}$  with the form

$$Z = \begin{bmatrix} (x)_+ & (x)_- & \star & \star \end{bmatrix}, \quad (57)$$

where  $(x)_+$  means applying  $(\cdot \vee 0)$  to every entry of  $x$  and  $(x)_-$  means applying  $-(\cdot \wedge 0)$  to every entry of  $x$ , so all entries in  $Z$  are non-negative. We have

$$\text{Conv}_{\widehat{\mathcal{W}}_m, \widehat{\mathcal{B}}_m}(Z) = \begin{bmatrix} \frac{R_1}{R_2}(f_m(\mathbf{x}) \vee 0) & -\frac{R_1}{R_2}(f_m(\mathbf{x}) \wedge 0) \\ \mathbf{0} & \mathbf{0} & \star & \star \\ & & \vdots & \vdots \\ & & \star & \star \end{bmatrix} + Z \quad (58)$$

where  $\star$ 's denotes entries that do not affect this result and may take any different value.

For any  $m$ , the first layer of  $f_m$  takes input in  $\mathbb{R}^D$ . Thus, the filters in  $\mathcal{W}_m^{(1)}$  are in  $\mathbb{R}^D$ . Again, we pad these filters with zeros to get filters in  $\mathbb{R}^{D \times 4}$  and construct  $\widehat{\mathcal{W}}_m^{(1)}$  such that

$$\begin{aligned} (\widehat{\mathcal{W}}_m^{(1)})_{1,:} &= \begin{bmatrix} \mathbf{e}_1 & \mathbf{0} & \mathbf{0} & \mathbf{0} \end{bmatrix}, \\ (\widehat{\mathcal{W}}_m^{(1)})_{2,:} &= \begin{bmatrix} \mathbf{0} & \mathbf{e}_1 & \mathbf{0} & \mathbf{0} \end{bmatrix}, \\ (\widehat{\mathcal{W}}_m^{(1)})_{3,:} &= \begin{bmatrix} \mathbf{0} & \mathbf{0} & \mathbf{e}_1 & \mathbf{0} \end{bmatrix}, \\ (\widehat{\mathcal{W}}_m^{(1)})_{4,:} &= \begin{bmatrix} \mathbf{0} & \mathbf{0} & \mathbf{0} & \mathbf{e}_1 \end{bmatrix}, \\ (\widehat{\mathcal{W}}_m^{(1)})_{4+j,:} &= \begin{bmatrix} (\mathcal{W}_m^{(1)})_{j,:} & (-\mathcal{W}_m^{(1)})_{j,:} & \mathbf{0} & \mathbf{0} \end{bmatrix}, \end{aligned}$$

where we use the fact that  $\mathcal{W}_m^{(1)} * (x)_+ - \mathcal{W}_m^{(1)} * (x)_- = \mathcal{W}_m^{(1)} * x$ . The first four output channels at the end of this first layer are copies of  $Z$ . For the filters in later layers of  $\widehat{f}_m$  and all biases, we simply set

$$\begin{aligned} (\widehat{\mathcal{W}}_m^{(l)})_{1,:} &= \begin{bmatrix} \mathbf{e}_1 & \mathbf{0} & \mathbf{0} & \mathbf{0} & \cdots & \mathbf{0} \end{bmatrix} && \text{for } l = 2, \dots, L, \\ (\widehat{\mathcal{W}}_m^{(l)})_{2,:} &= \begin{bmatrix} \mathbf{0} & \mathbf{e}_1 & \mathbf{0} & \mathbf{0} & \cdots & \mathbf{0} \end{bmatrix} && \text{for } l = 2, \dots, L, \\ (\widehat{\mathcal{W}}_m^{(l)})_{3,:} &= \begin{bmatrix} \mathbf{0} & \mathbf{0} & \mathbf{e}_1 & \mathbf{0} & \cdots & \mathbf{0} \end{bmatrix} && \text{for } l = 2, \dots, L-1, \\ (\widehat{\mathcal{W}}_m^{(l)})_{4,:} &= \begin{bmatrix} \mathbf{0} & \mathbf{0} & \mathbf{0} & \mathbf{e}_1 & \cdots & \mathbf{0} \end{bmatrix} && \text{for } l = 2, \dots, L-1, \\ (\widehat{\mathcal{W}}_m^{(l)})_{4+j,:} &= \begin{bmatrix} \mathbf{0} & \mathbf{0} & \mathbf{0} & \mathbf{0} & (\mathcal{W}_m^{(l)})_{j,:} \end{bmatrix} && \text{for } l = 2, \dots, L-1, \\ (\widehat{\mathcal{B}}_m^{(l)})_{j,:} &= \begin{bmatrix} \mathbf{0} & \mathbf{0} & \mathbf{0} & \mathbf{0} & (\mathcal{B}_m^{(l)})_{j,:} \end{bmatrix} && \text{for } l = 1, \dots, L-1. \end{aligned}$$

In  $\text{Conv}_{\widehat{\mathcal{W}}_m, \widehat{\mathcal{B}}_m}$ , an additional convolutional layer is constructed to realize the fully connected layer in  $\widehat{f}_m$ . By our assumption, only the first row of  $W_m$  is nonzero. Furthermore, we set  $\widehat{\mathcal{B}}_m^{(L)} = \mathbf{0}$  and  $\widehat{\mathcal{W}}_m^L$

as size-one filters with three output channels in the form of

$$\begin{aligned} (\widehat{\mathcal{W}}_m^{(L)})_{3,:} &= \left[ \mathbf{0} \quad \mathbf{0} \quad \mathbf{e}_1 \quad \mathbf{0} \quad \frac{R_1}{R_2}(W_m)_{1,:} \right], \\ (\widehat{\mathcal{W}}_m^{(L)})_{4,:} &= \left[ \mathbf{0} \quad \mathbf{0} \quad \mathbf{0} \quad \mathbf{e}_1 \quad -\frac{R_1}{R_2}(W_m)_{1,:} \right]. \end{aligned}$$

Under such choices, (58) is proved, and all parameters in  $\widehat{\mathcal{W}}_m, \widehat{\mathcal{B}}_m$  are bounded by  $R_1$ .

By composing all convolutional blocks, we have

$$\begin{aligned} & (\text{Conv}_{\widehat{\mathcal{W}}_M, \widehat{\mathcal{B}}_M}) \circ \cdots \circ (\text{Conv}_{\widehat{\mathcal{W}}_1, \widehat{\mathcal{B}}_1}) \circ P(x) \\ &= \begin{bmatrix} & \frac{R_1}{R_2} \sum_{m=1}^M (\widehat{f}_m \vee 0) & -\frac{R_1}{R_2} \sum_{m=1}^M (\widehat{f}_m \wedge 0) \\ (x)_+ & (x)_- & \star & \star \\ & & \vdots & \vdots \\ & & \star & \star \end{bmatrix}. \end{aligned}$$

Lastly, the fully connected layer can be set as

$$\widetilde{W} = \begin{bmatrix} 0 & 0 & \frac{R_2}{R_1} & -\frac{R_2}{R_1} \\ \mathbf{0} & \mathbf{0} & \mathbf{0} & \mathbf{0} \end{bmatrix}, \quad \widetilde{b} = 0.$$

Note that the weights in the fully connected layer are bounded by  $R_2(1 \vee R_1^{-1})$ .

The above construction gives

$$\widehat{f}(x) = \sum_{m=1}^M (\widehat{f}_m(x) \vee 0) + \sum_{m=1}^M (\widehat{f}_m(x) \wedge 0) = \sum_{m=1}^M \widehat{f}_m(x).$$

□

## F CNN Class Covering Number

In this section, we prove a bound on the covering number of the convolutional neural network class used in Algorithm 1. The supporting lemmas and their proofs are provided in Appendix F.1

**Lemma 18.** *Given  $\delta > 0$ , the  $\delta$ -covering number of the CNN class  $\mathcal{F}(M, L, J, I, R_1, R_2)$  satisfies*

$$\mathcal{N}(\delta, \mathcal{F}(M, L, J, I, R_1, R_2), \|\cdot\|_\infty) \leq (2(R_1 \vee R_2)\Lambda_1\delta^{-1})^{\Lambda_2},$$

where

$$\Lambda_1 = (M + 3)JD(1 \vee R_2)(1 \vee R_1)\widetilde{\rho}\widetilde{\rho}^+, \quad \Lambda_2 = ML(J^2I + J) + JD + 1$$

with  $\widetilde{\rho} = \rho^M, \widetilde{\rho}^+ = 1 + ML\rho^+, \rho = (JIR_1)^L$  and  $\rho^+ = (1 \vee JIR_1)^L$ .

With a network architecture as stated in Theorems 2 and 3, we have

$$\log \mathcal{N}(\delta, \mathcal{F}(M, L, J, I, R_1, R_2), \|\cdot\|_\infty) = O\left(\widetilde{M}\widetilde{J}^2 D^3 \log^5(\widetilde{M}\widetilde{J}) \log \frac{1}{\delta}\right),$$

where  $O(\cdot)$  hides a constant depending on  $d, \alpha, \omega, B$ , and the surface area  $\text{Area}(\mathcal{S})$ .

To show Lemma 18, we first prove a supporting lemma (Lemma 19) that relates the distance in the function space of CNNs (in the  $L^\infty$  sense) to the distance in the parameter space. In this way, we transform the covering of the CNN class into the covering of the parameter space, which is simpler to deal with. We then give a proof of Lemma 18 in Appendix F.2.

### F.1 Supporting Lemmas for Lemma 18

Proposition 5 below provides an upper bound on the  $L^\infty$ -norm of a series of convolutional neural network blocks in terms of its architecture parameters, e.g. number of layers, number of channels, etc.

Let  $J_m^{(i)}$  be the number of channels in  $i$ -th layer of the  $m$ -th block, and let  $I_m^{(i)}$  be the filter size of  $i$ -th layer in the  $m$ -th block. We define  $Q_{[i,j]}$  as

$$Q_{[i,j]}(x) = (\text{Conv}_{\mathcal{W}_j, \mathcal{B}_j}) \circ \cdots \circ (\text{Conv}_{\mathcal{W}_i, \mathcal{B}_i})(x).$$

**Proposition 5.** For  $m = 1, 2, \dots, M$  and  $x \in [-1, 1]^D$ , we have

$$\|Q_{[1,m]}(x)\|_\infty \leq (1 \vee R_1) \left( \prod_{j=1}^m \prod_{i=1}^{L_j} J_j^{(i-1)} I_j^{(i)} R_1 \right) \left( 1 + \sum_{k=1}^m L_k \prod_{i=1}^{L_k} (1 \vee J_k^{(i-1)} I_k^{(i)} R_1) \right).$$

*Proof.*

$$\begin{aligned} & \|Q_{[1,m]}(x)\|_\infty \\ &= \|\text{Conv}_{\mathcal{W}_m, \mathcal{B}_m}(Q_{[1,m-1]}(x))\|_\infty \\ &\leq \prod_{i=1}^{L_m} J_m^{(i-1)} I_m^{(i)} R_1 \|Q_{[1,m-1]}(x)\|_\infty + R_1 L_m \prod_{i=1}^{L_m} (1 \vee J_m^{(i-1)} I_m^{(i)} R_1) \\ &\leq \|P(x)\|_\infty \prod_{j=1}^m \prod_{i=1}^{L_j} J_j^{(i-1)} I_j^{(i)} R_1 + R_1 \sum_{k=1}^m L_k \prod_{i=1}^{L_k} (1 \vee J_k^{(i-1)} I_k^{(i)} R_1) \prod_{l=j+1}^m \prod_{i=1}^{L_l} J_l^{(i-1)} I_l^{(i)} R_1 \\ &\leq \|x\|_\infty \prod_{j=1}^m \prod_{i=1}^{L_j} J_j^{(i-1)} I_j^{(i)} R_1 + R_1 \sum_{k=1}^m L_k \prod_{i=1}^{L_k} (1 \vee J_k^{(i-1)} I_k^{(i)} R_1) \prod_{l=j+1}^m \prod_{i=1}^{L_l} J_l^{(i-1)} I_l^{(i)} R_1 \\ &\leq (1 \vee R_1) \left( \prod_{j=1}^m \prod_{i=1}^{L_j} J_j^{(i-1)} I_j^{(i)} R_1 \right) \left( 1 + \sum_{k=1}^m L_k \prod_{i=1}^{L_k} (1 \vee J_k^{(i-1)} I_k^{(i)} R_1) \right), \end{aligned}$$

where the first two inequalities are obtained by applying Proposition 9 from Oono and Suzuki (2019)

recursively.  $\square$

Lemma 19 quantifies the sensitivity of a CNN with respect to small changes in its weight parameters. This will be used to create a discrete covering for the CNN class.

**Lemma 19.** *Let  $\epsilon > 0$ . For any  $f, f' \in \mathcal{F}(M, L, J, I, R_1, R_2)$  such that  $\|W - W'\|_\infty \leq \epsilon$ ,  $\|b - b'\|_\infty \leq \epsilon$ ,  $\|\mathcal{W}_m^{(l)} - \mathcal{W}_m^{(l)'}\|_\infty \leq \epsilon$  and  $\|\mathcal{B}_m^{(l)} - \mathcal{B}_m^{(l)'}\|_\infty \leq \epsilon$  for all  $m$  and  $l$ , where  $(W, b, \{(\mathcal{W}_m^{(l)}, \mathcal{B}_m^{(l)})\}_{l=1}^{L_m}\}_{m=1}^M)$  and  $(W', b', \{(\mathcal{W}_m^{(l)'}, \mathcal{B}_m^{(l)'})\}_{l=1}^{L_m}\}_{m=1}^M)$  are the parameters of  $f$  and  $f'$  respectively, we have*

$$\|f - f'\|_\infty \leq \Lambda_1 \epsilon,$$

where  $\Lambda_1$  is defined in Lemma 18.

*Proof.* For any  $x \in [-1, 1]^D$ ,

$$\begin{aligned} & |f(x) - f'(x)| \\ &= |W \otimes Q(x) + b - W' \otimes Q'(x) - b'| \\ &= |(W - W') \otimes Q(x) + b - b' + W' \otimes (Q(x) - Q'(x))| \\ &= |(W - W') \otimes Q(x) + b - b' + W' \otimes (Q(x) - \text{Conv}_{\mathcal{W}_M, \mathcal{B}_M}(Q'(x)) + \text{Conv}_{\mathcal{W}_M, \mathcal{B}_M}(Q'(x)) - Q'(x))| \\ &= \left| (W - W') \otimes Q(x) + b - b' + \sum_{m=1}^M W' \otimes Q_{[m+1, M]} \circ (\text{Conv}_{\mathcal{W}_m, \mathcal{B}_m} - \text{Conv}_{\mathcal{W}'_m, \mathcal{B}'_m}) \circ Q'_{[0, m-1]} \right| \\ &\leq |(W - W') \otimes Q(x; \theta) + b - b'| + \sum_{m=1}^M \left| W' \otimes Q_{[m+1, M]} \circ (\text{Conv}_{\mathcal{W}_m, \mathcal{B}_m} - \text{Conv}_{\mathcal{W}'_m, \mathcal{B}'_m}) \circ Q'_{[0, m-1]} \right| \\ &\stackrel{(a)}{\leq} (3 + M)JD(1 \vee R_1)(1 \vee R_2) \left( \prod_{j=1}^M \prod_{i=1}^{L_j} J_j^{(i-1)} I_j^{(i)} R_1 \right) \left( 1 + \sum_{k=1}^M L_k \prod_{i=1}^{L_k} (1 \vee J_k^{(i-1)} I_k^{(i)} R_1) \right) \epsilon, \end{aligned}$$

where (a) is obtained through the following reasoning.

The first term in (a) can be bounded as

$$\begin{aligned} & |(W - W') \otimes Q(x) + b - b'| \\ &\leq (\|W\|_0 + \|W'\|_0) \|W - W'\|_\infty \|Q(x)\|_\infty + \|b - b'\|_\infty \\ &\leq 2JD\epsilon \|Q(x)\|_\infty + \epsilon \\ &\leq 3JD\epsilon \|Q(x)\|_\infty \\ &\leq 3JD \max\{1, R_1\} \left( \prod_{j=1}^M \prod_{i=1}^{L_j} J_j^{(i-1)} I_j^{(i)} R_1 \right) \left( 1 + \sum_{k=1}^M L_k \prod_{i=1}^{L_k} (1 \vee J_k^{(i-1)} I_k^{(i)} R_1) \right) \epsilon, \end{aligned}$$

where the first inequality uses Proposition 8 from Oono and Suzuki (2019) and the last inequality is obtained by invoking Proposition 5.

For the second term in (a), it is true that for any  $m = 1, \dots, M$ , we have

$$\begin{aligned}
& \left| W' \otimes Q_{[m+1, M]} \circ (\text{Conv}_{\mathcal{W}_m, \mathcal{B}_m} - \text{Conv}_{\mathcal{W}'_m, \mathcal{B}'_m}) \circ Q'_{[1, m-1]} \right| \\
& \stackrel{(b)}{\leq} \|W'\|_0 R_2 \left\| Q_{[m+1, M]} \circ (\text{Conv}_{\mathcal{W}_m, \mathcal{B}_m} - \text{Conv}_{\mathcal{W}'_m, \mathcal{B}'_m}) \circ Q'_{[1, m-1]} \right\|_\infty \\
& \stackrel{(c)}{\leq} JDR_2 \left( \prod_{j=m+1}^M \prod_{i=1}^{L_j} J_j^{(i-1)} I_j^{(i)} R_1 \right) \left\| (\text{Conv}_{\mathcal{W}_m, \mathcal{B}_m} - \text{Conv}_{\mathcal{W}'_m, \mathcal{B}'_m}) \circ Q'_{[1, m-1]} \right\|_\infty \\
& \stackrel{(d)}{\leq} JDR_2 \left( \prod_{j=m+1}^M \prod_{i=1}^{L_j} J_j^{(i-1)} I_j^{(i)} R_1 \right) \left( \prod_{i=1}^{L_m} J_m^{(i-1)} I_m^{(i)} R_1 \left\| Q'_{[1, m-1]} \right\|_\infty \epsilon \right) \\
& \stackrel{(e)}{\leq} JDR_2 \left( \prod_{j=m+1}^M \prod_{i=1}^{L_j} J_j^{(i-1)} I_j^{(i)} R_1 \right) \left( \prod_{i=1}^{L_m} J_m^{(i-1)} I_m^{(i)} R_1 \right) \\
& \quad (1 \vee R_1) \left( \prod_{j=1}^m \prod_{i=1}^{L_j} J_j^{(i-1)} I_j^{(i)} R_1 \right) \left( 1 + \sum_{k=1}^m L_k \prod_{i=1}^{L_k} (1 \vee J_k^{(i-1)} I_k^{(i)} R_1) \right) \epsilon \\
& \leq JDR_2 \left( \prod_{j=1}^M \prod_{i=1}^{L_j} J_j^{(i-1)} I_j^{(i)} R_1 \right) (1 \vee R_1) \left( 1 + \sum_{k=1}^M L_k \prod_{i=1}^{L_k} (1 \vee J_k^{(i-1)} I_k^{(i)} R_1) \right) \epsilon,
\end{aligned}$$

where (b) is by Proposition 7 from [Oono and Suzuki \(2019\)](#), (c) is by Proposition 2 and 4 from [Oono and Suzuki \(2019\)](#), (d) is by Proposition 2 and 5 from [Oono and Suzuki \(2019\)](#), and (e) is obtained by invoking Proposition 5.  $\square$

## F.2 Proof of Lemma 18

*Proof.* We grid the range of each parameter into subsets with width  $\Lambda_1^{-1}\delta$ , so there are at most  $2(R_1 \vee R_2)\Lambda_1\delta^{-1}$  different subsets for each parameter. In total, there are  $(2(R_1 \vee R_2)\Lambda_1\delta^{-1})^{\Lambda_2}$  bins in the grid. For any  $f, f' \in \mathcal{F}(M, L, J, I, R_1, R_2)$  within the same grid, by Lemma 19, we have  $\|f - f'\|_\infty \leq \delta$ . We can construct an  $\epsilon$ -covering with cardinality  $(2(R_1 \vee R_2)\Lambda_1\delta^{-1})^{\Lambda_2}$  by selecting one neural network from each bin in the grid.

Taking log and plugging in the network architecture parameters in Theorems 2 and 3, we have

$$\begin{aligned}
\log \mathcal{N}(\delta, \mathcal{F}(M, L, J, I, R_1, R_2), \|\cdot\|_\infty) &= O(\Lambda_2 \log((R_1 \vee R_2) \Lambda_1 \delta^{-1})) \\
&\leq O\left(\widetilde{M} D D^2 \widetilde{J}^2 \log(\widetilde{M} \widetilde{J}) \log^2(\widetilde{M} \widetilde{J}) \log^2(\widetilde{M} \widetilde{J}) \log \frac{1}{\delta}\right) \\
&= O\left(\widetilde{M} \widetilde{J}^2 D^3 \log^5(\widetilde{M} \widetilde{J}) \log \frac{1}{\delta}\right),
\end{aligned}$$

where the inequality is due to  $\Lambda_2 = O(\widetilde{M} D D^2 \widetilde{J}^2 \log(\widetilde{M} \widetilde{J}))$ . By plugging in the choice of  $R_1$  with sufficiently small integer  $\widetilde{J}$ , we have  $\rho = (1/2)^L M^{-1} \leq M^{-1}$  and thus  $\tilde{\rho} \leq (1 + M^{-1})^M \leq e$ . Moreover,

we have  $\tilde{\rho}^+ = 1 + ML$ . □

## G Statistical Result of CNN Approximation

In this section, we derive the statistical estimation error for using a CNN empirical MSE minimizer to estimate an approximately Lipschitz ground truth function over an i.i.d. dataset. We need to choose the appropriate CNN architecture and size in order to balance the approximation error from Theorem 3 and the variance. This statistical estimation error can be decomposed into the error of using CNN to approximate the target function (Theorem 3), terms that grow with the covering number of our CNN class, and the error of using the discrete covering to approximate our CNN class.

**Lemma 20.** *Suppose Assumption 1 holds,  $f_0: \mathcal{S} \rightarrow \mathbb{R}$  is a bounded  $(L_f, \alpha, \epsilon_f)$ -approximately Lipschitz function. We are given samples  $\Xi_N = \{x_i, y_i\}_{i=1}^N$  where  $x_i$ 's are i.i.d. sampled from a distribution  $\mathcal{D}_x$  on  $\mathcal{S}$  and  $y_i = f_0(x_i) + \zeta_i$ .  $\zeta_i$ 's are i.i.d. sub-Gaussian random noise with variance proxy  $\sigma^2$  and are uncorrelated with  $x_i$ 's. If  $\epsilon_f = \mu D^{\frac{3\alpha}{2\alpha+d}} N^{-\frac{\alpha}{2\alpha+d}}$  for some constant  $\mu = O(L_f + \|f_0\|_\infty)$  and the estimator*

$$\hat{f}_N = \operatorname{argmin}_{f \in \mathcal{F}_0} \frac{1}{N} \sum_{i=1}^N (f(x_i) - y_i)^2$$

is computed with neural network function class  $\mathcal{F}_0 = \mathcal{F}_{\text{Lip}}(A, L_0, \alpha, \epsilon_0)$  such that

$$\begin{aligned} M &= O(N^{\frac{d}{d+2\alpha}}), \quad L = O(\log N + D + \log D), \quad J = O(D), \quad I \in [2, D], \quad A = \|f_0\|_\infty, \\ R_1 &= O(1), \quad \log R_2 = O(\log^2 N + D \log N), \quad L_0 = L_f, \quad \epsilon_0 = D^{\frac{3\alpha}{2\alpha+d}} N^{-\frac{\alpha}{2\alpha+d}}, \end{aligned}$$

then we have

$$\mathbb{E}_{\Xi_N} \left[ \int_{\mathcal{S}} \left( \hat{f}_N(x) - f_0(x) \right)^2 d\mathcal{D}_x(x) \right] \leq c_0 ((L_f + A)^2 + \sigma^2) N^{-\frac{2\alpha}{2\alpha+d}} \log^6 N,$$

where  $c_0$  is some constant depending on  $D^{\frac{6\alpha}{2\alpha+d}}$ ,  $\log L_f$ ,  $\log \|f_0\|_\infty$ ,  $d$ ,  $\alpha$ ,  $\omega$ ,  $B$ , and the surface area  $\text{Area}(\mathcal{S})$ .  $O(\cdot)$  hides some constant depending on  $\log L_f$ ,  $\log \|f_0\|_\infty$ ,  $d$ ,  $\alpha$ ,  $\omega$ ,  $B$ , and the surface area  $\text{Area}(\mathcal{S})$ .



First, note that the nonparametric regression error can be decomposed into two terms:

$$\begin{aligned}
& \mathbb{E}_{\Xi_N} \left[ \int_{\mathcal{S}} \left( \widehat{f}_N(x) - f_0(x) \right)^2 d\mathcal{D}_x(x) \right] \\
&= \underbrace{2\mathbb{E}_{\Xi_N} \left[ \frac{1}{N} \sum_{i=1}^N \left( \widehat{f}_N(x_i) - f_0(x_i) \right)^2 \right]}_{T_1} \\
&\quad + \underbrace{\mathbb{E}_{\Xi_N} \left[ \int_{\mathcal{S}} \left( \widehat{f}_N(x) - f_0(x) \right)^2 d\mathcal{D}_x(x) \right] - 2\mathbb{E}_{\Xi_N} \left[ \frac{1}{N} \sum_{i=1}^N \left( \widehat{f}_N(x_i) - f_0(x_i) \right)^2 \right]}_{T_2},
\end{aligned}$$

where  $T_1$  reflects the squared bias of using CNN to approximate  $f_0$ , and  $T_2$  is the variance term.

### G.1 Supporting Lemmas for Lemma 20

We introduce two supporting lemmas from [Chen et al. \(2022\)](#) that show upper bounds for  $T_1$  and  $T_2$  in terms of the approximation error and covering number.

**Lemma 21** ([Chen et al. \(2022, Lemma 5\)](#)). *Fix the neural network class  $\mathcal{F}_{\text{Lip}}(A, L_0, \alpha, \epsilon_0)$ . For any constant  $\delta \in (0, 2A)$ , we have*

$$\begin{aligned}
T_1 \leq & 4 \inf_{f \in \mathcal{F}_{\text{Lip}}(A, L_0, \alpha, \epsilon_0)} \int_{\mathcal{S}} (f(x) - f_0(x))^2 d\mathcal{D}_x(x) \\
& + 48\sigma^2 \frac{\log \mathcal{N}(\delta, \mathcal{F}_{\text{Lip}}(A, L_0, \alpha, \epsilon_0), \|\cdot\|_{\infty}) + 2}{N} \\
& + \left( 8\sqrt{6} \sqrt{\frac{\log \mathcal{N}(\delta, \mathcal{F}_{\text{Lip}}(A, L_0, \alpha, \epsilon_0), \|\cdot\|_{\infty}) + 2}{N}} + 8 \right) \sigma \delta,
\end{aligned}$$

where  $\mathcal{N}(\delta, \mathcal{F}_{\text{Lip}}(A, L_0, \alpha, \epsilon_0), \|\cdot\|_{\infty})$  denotes the  $\delta$ -covering number of  $\mathcal{F}_{\text{Lip}}(A, L_0, \alpha, \epsilon_0)$  with respect to the  $L^{\infty}$  norm, that is, there exists a discretization of the class  $\mathcal{F}_{\text{Lip}}(A, L_0, \alpha, \epsilon_0)$  with  $\mathcal{N}(\delta, \mathcal{F}_{\text{Lip}}(A, L_0, \alpha, \epsilon_0), \|\cdot\|_{\infty})$  distinct elements such that for any  $f \in \mathcal{F}$ , there is a  $\bar{f}$  in the discretization satisfying  $\|\bar{f} - f\|_{\infty} \leq \delta$ .

**Lemma 22** ([Chen et al. \(2022, Lemma 6\)](#)). *Fix the neural network class  $\mathcal{F}_{\text{Lip}}(A, L_0, \alpha, \epsilon_0)$ . For any constant  $\delta \in (0, 2A)$ , we have*

$$T_2 \leq \frac{104A^2}{3N} \log \mathcal{N}(\delta/4A, \mathcal{F}_{\text{Lip}}(A, L_0, \alpha, \epsilon_0), \|\cdot\|_{\infty}) + \left( 4 + \frac{1}{2A} \right) \delta.$$

With Lemmas 21 and 22, we can immediately prove Lemma 20.

## G.2 Proof of Lemma 20

*Proof.* Applying Lemmas 21 and 22 to the bias and variance decomposition, we derive

$$\begin{aligned}
\mathbb{E}_{\Xi_N} \left[ \int_{\mathcal{S}} \left( \widehat{f}_N(x) - f_0(x) \right)^2 d\mathcal{D}_x(x) \right] &\leq 4 \inf_{f \in \mathcal{F}_{\text{Lip}}(A, L_0, \alpha, \epsilon_0)} \int_{\mathcal{S}} (f(x) - f_0(x))^2 d\mathcal{D}_x(x) \\
&\quad + 48\sigma^2 \frac{\log \mathcal{N}(\delta, \mathcal{F}_{\text{Lip}}(A, L_0, \alpha, \epsilon_0), \|\cdot\|_{\infty}) + 2}{N} \\
&\quad + 8\sqrt{6} \sqrt{\frac{\log \mathcal{N}(\delta, \mathcal{F}_{\text{Lip}}(A, L_0, \alpha, \epsilon_0), \|\cdot\|_{\infty}) + 2}{N}} \sigma \delta \\
&\quad + \frac{104A^2}{3N} \log \mathcal{N}(\delta/4A, \mathcal{F}_{\text{Lip}}(A, L_0, \alpha, \epsilon_0), \|\cdot\|_{\infty}) \\
&\quad + \left( 4 + \frac{1}{2A} + 8 \right) \delta. \tag{59}
\end{aligned}$$

By Theorem 3, if we set  $\widetilde{M}\widetilde{J} = \epsilon^{-\frac{d}{\alpha}}$  and choose  $M, L, J, I, R_1, R_2, A$  such that

$$\begin{aligned}
M &= O(\epsilon^{-\frac{d}{\alpha}}), \quad L = O(\log(\epsilon^{-\frac{d}{\alpha}}) + D + \log D), \quad J = O(D), \quad I \in [2, D], \\
R_1 &= O(1), \quad \log R_2 = O(\log^2(\epsilon^{-\frac{d}{\alpha}}) + D \log(\epsilon^{-\frac{d}{\alpha}})), \quad A = \|f_0\|_{\infty},
\end{aligned}$$

for some  $\epsilon \in (0, 1)$ , then there exists an  $f \in \mathcal{F}_{\text{Lip}}(A, L_f, \alpha, \epsilon)$  such that

$$\|f - f_0\|_{\infty} \leq (L_f + A)\epsilon + 2\epsilon_f.$$

Since  $\mathcal{F}_{\text{Lip}}(A, L_f, \alpha, \epsilon) \subseteq \mathcal{F}(M, L, J, I, R_1, R_2)$ , we have

$$\mathcal{M}(\delta, \mathcal{F}_{\text{Lip}}(A, L_f, \alpha, \epsilon), \|\cdot\|_{\infty}) \leq \mathcal{M}(\delta, \mathcal{F}(M, L, J, I, R_1, R_2), \|\cdot\|_{\infty}),$$

where  $\mathcal{M}$  denotes the packing number. Combining the relation between covering and packing numbers that  $\mathcal{N}(\delta, \mathcal{F}) \leq \mathcal{M}(\delta, \mathcal{F}) \leq \mathcal{N}(\delta/2, \mathcal{F})$ , we have

$$\mathcal{N}(\delta, \mathcal{F}_{\text{Lip}}(A, L_f, \alpha, \epsilon), \|\cdot\|_{\infty}) \leq \mathcal{N}(\delta/2, \mathcal{F}(M, L, J, I, R_1, R_2), \|\cdot\|_{\infty}).$$

By Lemma 18, we have

$$\begin{aligned}
\log \mathcal{N}(\delta', \mathcal{F}(M, L, J, I, R_1, R_2)) &= O\left(\widetilde{M}\widetilde{J}^2 D^3 \log^5(\widetilde{M}\widetilde{J}) \log \frac{1}{\delta'}\right) \\
&= O\left(\epsilon^{-\frac{d}{\alpha}} D^3 \log^5(\epsilon^{-\frac{d}{\alpha}}) \log \frac{1}{\delta'}\right).
\end{aligned}$$

Plugging the results back in (59), we get

$$\begin{aligned} \mathbb{E}_{\Xi_N} \left[ \int_{\mathcal{S}} \left( \widehat{f}_N(x) - f_0(x) \right)^2 d\mathcal{D}_x(x) \right] \\ \leq \widetilde{O} \left( ((L_f + A)\epsilon + 2\epsilon_f)^2 + \frac{A^2 + \sigma^2}{N} \epsilon^{-\frac{d}{\alpha}} D^3 \log^5(\epsilon^{-\frac{d}{\alpha}}) \log \frac{1}{\delta} \right. \\ \left. + \sqrt{\frac{\epsilon^{-\frac{d}{\alpha}} D^3 \log^5(\epsilon^{-\frac{d}{\alpha}}) \log \frac{1}{\delta}}{N}} \sigma \delta + \sigma \delta + \frac{\sigma^2}{N} \right). \quad (60) \end{aligned}$$

Finally we choose  $\epsilon$  to satisfy  $\epsilon^2 = D^3 N^{-1} \epsilon^{-\frac{d}{\alpha}}$ , which gives  $\epsilon = D^{\frac{3\alpha}{2\alpha+d}} N^{-\frac{\alpha}{2\alpha+d}}$ . It suffices to pick  $\delta = \frac{1}{N}$ . Since  $\epsilon_f = \mu D^{\frac{3\alpha}{2\alpha+d}} N^{-\frac{\alpha}{2\alpha+d}}$  with  $\mu = O(L_f + \|f_0\|_\infty)$ , we have  $T_1 = O(T_2)$ , that is, the bias term is dominated by the variance term. Therefore, by substituting both  $\epsilon$  and  $\delta$  in (60), we get the estimation error bound

$$\mathbb{E}_{\Xi_N} \left[ \int_{\mathcal{S}} \left( \widehat{f}_N(x) - f_0(x) \right)^2 d\mathcal{D}_x(x) \right] \leq c_0 ((L_f + A)^2 + \sigma^2) N^{-\frac{2\alpha}{2\alpha+d}} \log^6 N,$$

where  $c_0$  is a constant depending on  $D^{\frac{6\alpha}{2\alpha+d}}$ ,  $\log L_f$ ,  $\log \|f_0\|_\infty$ ,  $d$ ,  $\alpha$ ,  $\omega$ ,  $B$ , and the surface area  $\text{Area}(\mathcal{S})$ .  $\square$